



APJESS

Journal of Engineering  
and **Smart Systems**

Volume : 11

Issue : 2

Year : 2023

## Volume 11 / Issue 2

*Academic Platform Journal of Engineering and Smart Systems*

### Editor in Chief (Owned By Academic Perspective)

Dr. Mehmet SARIBIYIK, Sakarya University of Applied Sciences, Turkey

### Editors

Dr. Caner ERDEN, Sakarya University of Applied Sciences, Turkey

Dr. John YOO, Bradley University, USA

### Editorial Board

Dr. Abdullah Hulusi KÖKÇAM, Sakarya University, Turkey

Dr. Ali Tahir KARAŞAHİN, Karabuk University, Turkey

Dr. Aydın MÜHÜRÇÜ, Kırklareli University, Turkey

Dr. Ayşe Nur AY, Sakarya University of Applied Sciences, Turkey

Dr. Cengiz KAHRAMAN, Istanbul Technical University, Turkey

Dr. Elif Elçin GÜNAY, Sakarya University, Turkey

Dr. Erkan ÇELİK, Istanbul University, Turkey

Dr. Fatih VARÇIN, Sakarya University of Applied Sciences, Turkey

Dr. Gürcan YILDIRIM, Abant İzzet Baysal University, Turkey

Dr. Hacı Mehmet ALAKAŞ, Kirikkale University, Turkey

Dr. Huseyin SEKER, Birmingham City University, Birmingham, United Kingdom

Dr. Kerem Küçük, Kocaeli University, Turkey

Dr. Marco A. ACEVES-FERNÁNDEZ, Universidad Autónoma De Queréta, Mexico

Dr. Mazin MOHAMMED, University Of Anbar, Iraq

Dr. Mehmet Emin AYDIN, University of The West Of England, United Kingdom

Dr. Muhammet KURULAY, Yıldız Technical University, Turkey

Dr. Muhammed Maruf ÖZTÜRK, Suleyman Demirel University, Turkey

Dr. Ömer AYDIN, Celal Bayar University, Turkey

Dr. Rakesh PHANDEN, Amity University Uttar Pradesh, India

Dr. Uğur Erkin KOCAMAZ, Bursa Uludağ University, Turkey

Dr. Tuğba TUNACAN, Abant İzzet Baysal University, Turkey

Dr. Tülay YILDIRIM, Yıldız Technical University, Turkey

Dr. Valentina E. BALAS, Aurel Vlaicu University of Arad, Romania

### Language Editor

Dr. Hakan ASLAN, Sakarya University, Turkey

### Editorial Assistants

Selim İLHAN, Sakarya University, Turkey

İbrahim MUCUK, Sakarya University, Turkey

### Correspondence Address

Academic Platform Journal of Engineering and Smart Systems

Akademik Perspektif Derneği, Tığcılar Mahallesi Kadir Sokak No:12

Kat:1 Adapazarı SAKARYA

+90 551 628 9477 (WhatsApp only)

<https://dergipark.org.tr/tr/pub/apjess>

**Issue Link:** <https://dergipark.org.tr/tr/pub/apjess/issue/77290>

## Aim and Scope

Academic Platform Journal of Engineering and Smart Systems (APJESS) is a peer reviewed open-access journal which focuses on the research and applications related to smart systems and artificial intelligence. APJESS accepts both **original research papers** and **review articles** written in **English**. It is essential that the information created in scientific study needs to be new, suggest new method or give a new dimension to an existing information. Articles submitted for publication are evaluated by at least two referees in case the editor finds potential scientific merit, and final acceptance and rejection decision are taken by editorial board. The authors are not informed about the name of referees who evaluate the papers. In similar way, the referees are not allowed to see the names of authors. The papers which do not satisfy the scientific level of the journal can be refused with unexplained reason.

There are two key principles that APJESS was founded on: Firstly, to publish the most exciting, novel, technically sound, and clearly presented researches with respect to the subjects of smart systems and artificial intelligence. Secondly, to provide a rapid turn-around time possible for reviewing and publishing, and to disseminate the articles freely for research, teaching and reference purposes.

Any information about a submitted manuscript cannot be disclosed by the editor and any other editorial staff to anyone other than the corresponding author, reviewers, potential reviewers, other editorial advisers, and the publisher. No confidential information or ideas obtained through peer review can be used for personal advantage.

## Journal History

The journal was published between 2013-2021 with the title of "Academic Platform - Journal of Engineering and Science". It will be published under its new title "Academic Platform Journal of Engineering and Smart Systems" after 2022.

**Former Title:** Academic Platform - Journal of Engineering and Science

**Years:** 2013-2021

## Scope

APJESS aims to publish research and review papers dealing with, but not limited to, the following research fields:

- Knowledge Representation and Reasoning,
- Data Mining & Data Science,
- Supervised, Semi-Supervised and Unsupervised Learning,
- Machine Learning (ML) and Neural Computing,
- Evolutionary Computation,
- Natural Language Processing, Internet of Things, Big Data
- Fuzzy Systems,
- Intelligent Information Processing,
- AI Powered Robotic Systems,
- Multi-agent Systems and Programming for Smart Systems

## Author Guidelines

### Article Types

Manuscripts submitted to APJESS should neither be published previously nor be under consideration for publication in another journal.

The main article types are as follows:

**Research Articles:** Original research manuscripts. The journal considers all original research manuscripts provided that the work reports scientifically sound experiments and provides a substantial amount of new information.

**Review Articles:** These provide concise and precise updates on the latest progress made in a given area of research.

### Checklist for Submissions

Please,

- read the [Aims & Scope](#) to see if your manuscript is suitable for the journal,
- use the [Microsoft Word template](#) to prepare your manuscript;
- Download [Copyright Transfer Form](#) and signed by all authors.
- make sure that issues about [Ethical Principles and Publication Policy](#), [Copyright and Licensing](#), [Archiving Policy](#), [Repository Policy](#) have been appropriately considered;
- Ensure that all authors have approved the content of the submitted manuscript.

The main text should be formed in the following order:

**Manuscript:** The article should start with an introduction written in scientific language, putting thoughts together from diverse disciplines combining evidence-based knowledge and logical arguments, conveying views about the aim and purpose of the article. It must address all readers in general. The technical terms, symbols, abbreviations must be defined at the first time when they are used in the article. The manuscript should be formed in the following order:

Introduction,

Material and Method,

Findings,

Discussion and Conclusion.

**References:** At the end of the paper provide full details of all references cited in-text. The reference list should be arranged in the order of appearance of the in-text citations, not in an alphabetical order, beginning with [1], and continuing in an ascending numerical order, from the lowest number to the highest. In the reference list, only one resource per reference number is acceptable.

References must be numbered in order of appearance in the text (including citations in tables and legends) and listed individually at the end of the manuscript. We recommend preparing the references with a bibliography software package, such as EndNote, Reference Manager or Zotero to avoid typing mistakes and duplicated references. Include the digital object identifier (DOI) for all references where available. Please use IEEE style.

IEEE Sample Reference List

[1] R. E. Ziemer and W. H. Tranter, Principles of Communications: Systems, Modulation, and Noise, 7th ed. Hoboken, NJ: Wiley, 2015.

[2] J. D. Bellamy et al., Computer Telephony Integration, New York: Wiley, 2010.

- [3] C. Jacks, High Rupturing Capacity (HRC) Fuses, New York: Penguin Random House, 2013, pp. 175–225.
- [4] N. B. Vargafik, J. A. Wiebelt, and J. F. Malloy, "Radiative transfer," in *Convective Heat*. Melbourne: Engineering Education Australia, 2011, ch. 9, pp. 379–398.
- [5] H. C. Hottel and R. Siegel, "Film condensation," in *Handbook of Heat Transfer*, 2nd ed. W. C. McAdams, Ed. New York: McGraw-Hill, 2011, ch. 9, pp. 78–99.
- [6] H. H. Gaynor, *Leading and Managing Engineering and Technology, Book 2: Developing Managers and Leaders*. IEEE-USA, 2011. Accessed on: Oct. 15, 2016. [Online]. Available: <http://www.ieeeusa.org/communications/ebooks/files/sep14/n2n802/Leading-and-Managing-Engineering-and-Technology-Book-2.pdf>
- [7] G. H. Gaynor, "Dealing with the manager leader dichotomy," in *Leading and Managing Engineering and Technology, Book 2, Developing Leaders and Mangers*. IEEE-USA, 2011, pp. 27–28. Accessed on: Jan. 23, 2017. [Online]. Available: <http://www.ieeeusa.org/communications/ebooks/files/sep14/n2n802/Leading-and-Managing-Engineering-and-Technology-Book-2.pdf>
- [8] M. Cvijetic, "Optical transport system engineering," in *Wiley Encyclopedia of Telecommunications*, vol. 4, J. G. Proakis, Ed. New York: John Wiley & Sons, 2003, pp. 1840–1849. Accessed on: Feb. 5, 2017. [Online]. Available: <http://ebscohost.com>
- [9] T. Kaczorek, "Minimum energy control of fractional positive electrical circuits", *Archives of Electrical Engineering*, vol. 65, no. 2, pp.191–201, 2016.
- [10] P. Harsha and M. Dahleh, "Optimal management and sizing of energy storage under dynamic pricing for the efficient integration of renewable energy", *IEEE Trans. Power Sys.*, vol. 30, no. 3, pp. 1164–1181, May 2015.
- [11] A. Vaskuri, H. Baumgartner, P. Kärhä, G. Andor, and E. Ikonen, "Modeling the spectral shape of InGaAlP-based red light-emitting diodes," *Journal of Applied Physics*, vol. 118, no. 20, pp. 203103-1–203103-7, Jul. 2015. Accessed on: Feb. 9, 2017. [Online]. Available: doi: 10.1063/1.4936322
- [12] K. J. Krishnan, "Implementation of renewable energy to reduce carbon consumption and fuel cell as a back-up power for national broadband network (NBN) in Australia," Ph.D dissertation, College of Eng. and Sc., Victoria Univ., Melbourne, 2013.
- [13] C. R. Ozansoy, "Design and implementation of a Universal Communications Processor for substation integration, automation and protection," Ph.D. dissertation, College of Eng. and Sc., Victoria Univ., Melbourne, 2006. [Online]. Accessed on: June 22, 2017. [Online]. Available: <http://vuir.vu.edu.au/527/>
- [14] M. T. Long, "On the statistical correlation between the heave, pitch and roll motion of road transport vehicles," Research Master thesis, College of Eng. and Sc., Victoria Univ., Melb., Vic., 2016.
- [15] *Safe Working on or Near Low-voltage Electrical Installations and Equipment*, AS/NZS 4836:2011, 2011.

## Ethical Principles and Publication Policy

### Peer Review Policy

Academic Platform Journal of Engineering and Smart Systems (APJESS) applies double blind peer-review process in which both the reviewer and the author are anonymous. Reviewer selection for each submitted article is up to area editors, and reviewers are selected based on the reviewer's expertise, competence, and previous experience in reviewing papers for APJES.

Every submitted article is evaluated by area editor, at least, for an initial review. If the paper reaches minimum quality criteria, fulfills the aims, scope and policies of APJES, it is sent to at least two reviewers for evaluation.

The reviewers evaluate the paper according to the Review guidelines set by editorial board members and return it to the area editor, who conveys the reviewers' anonymous comments back to the author. Anonymity is strictly maintained.

The double-blind peer-review process is managed using “ULAKBİM Dergi Sistemleri”, namely Dergipark platform.

## **Open Access Policy**

APJESS provides immediate open access for all users to its content on the principle that making research freely available to the public, supporting a greater global exchange of knowledge.

## **Archiving Policy**

APJESS is accessed by Dergipark platform which utilizes the LOCKSS system to create a distributed archiving system among participating libraries and permits those libraries to create permanent archives of the journal for purposes of preservation and restoration.

## **Originality and Plagiarism Policy**

Authors by submitting their manuscript to APJESS declare that their work is original and authored by them; has not been previously published nor submitted for evaluation; original ideas, data, findings and materials taken from other sources (including their own) are properly documented and cited; their work does not violate any rights of others, including privacy rights and intellectual property rights; provided data is their own data, true and not manipulated. Plagiarism in whole or in part without proper citation is not tolerated by APJESS. Manuscripts submitted to the journal will be checked for originality using anti-plagiarism software.

## **Journal Ethics and Malpractice Statement**

For all parties involved in the publishing process (the author(s), the journal editor(s), the peer reviewers, the society, and the publisher) it is necessary to agree upon standards of expected ethical behavior. The ethics statements for APJESS are based on the Committee on Publication Ethics (COPE) Code of Conduct guidelines available at [www.publicationethics.org](http://www.publicationethics.org).

### **1. Editor Responsibilities**

#### **Publication Decisions & Accountability**

The editor of APJESS is responsible for deciding which articles submitted to the journal should be published, and, moreover, is accountable for everything published in the journal. In making these decisions, the editor may be guided by the journal's editorial board and/or area editors, and considers the policies of the journal. The editor should maintain the integrity of the academic record, preclude business needs from compromising intellectual and ethical standards, and always be willing to publish corrections, clarifications, retractions, and apologies when needed.

#### **Fair play**

The editor should evaluate manuscripts for their intellectual content without regard to race, gender, sexual orientation, religious belief, ethnic origin, citizenship, or political philosophy of the author(s).

### **Confidentiality**

The editor and any editorial staff must not disclose any information about a submitted manuscript to anyone other than the corresponding author, reviewers, potential reviewers, other editorial advisers, and the publisher, as appropriate.

### **Disclosure, conflicts of interest, and other issues**

The editor will be guided by COPE's Guidelines for Retracting Articles when considering retracting, issuing expressions of concern about, and issuing corrections pertaining to articles that have been published in APJES.

Unpublished materials disclosed in a submitted manuscript must not be used in an editor's own research without the explicit written consent of the author(s). Privileged information or ideas obtained through peer review must be kept confidential and not used for personal advantage.

The editor should seek so ensure a fair and appropriate peer-review process. The editor should recuse himself/herself from handling manuscripts (i.e. should ask a co-editor, associate editor, or other member of the editorial board instead to review and consider) in which they have conflicts of interest resulting from competitive, collaborative, or other relationships or connections with any of the authors, companies, or (possibly) institutions connected to the papers. The editor should require all contributors to disclose relevant competing interests and publish corrections if competing interests are revealed after publication. If needed, other appropriate action should be taken, such as the publication of a retraction or expression of concern.

## **2. Reviewer Responsibilities**

### **Contribution to editorial decisions**

Peer review assists the editor in making editorial decisions and, through the editorial communication with the author, may also assist the author in improving the manuscript.

### **Promptness**

Any invited referee who feels unqualified to review the research reported in a manuscript or knows that its timely review will be impossible should immediately notify the editor so that alternative reviewers can be contacted.

### **Confidentiality**

Any manuscripts received for review must be treated as confidential documents. They must not be shown to or discussed with others except if authorized by the editor.

### **Standards of objectivity**

Reviews should be conducted objectively. Personal criticism of the author(s) is unacceptable. Referees should express their views clearly with appropriate supporting arguments.

### **Acknowledgement of sources**

Reviewers should identify relevant published work that has not been cited by the author(s). Any statement that an observation, derivation, or argument had been previously reported should be accompanied by the relevant citation. Reviewers should also call to the editor's attention any substantial similarity or overlap between the manuscript under consideration and any other published data of which they have personal knowledge.

### **Disclosure and conflict of interest**

Privileged information or ideas obtained through peer review must be kept confidential and not used for personal advantage. Reviewers should not consider evaluating manuscripts in which they have

conflicts of interest resulting from competitive, collaborative, or other relationships or connections with any of the authors, companies, or institutions connected to the submission.

### **3. Author Responsibilities**

#### **Reporting standards**

Authors reporting results of original research should present an accurate account of the work performed as well as an objective discussion of its significance. Underlying data should be represented accurately in the manuscript. A paper should contain sufficient detail and references to permit others to replicate the work. Fraudulent or knowingly inaccurate statements constitute unethical behavior and are unacceptable.

#### **Originality and plagiarism**

The authors should ensure that they have written entirely original works, and if the authors have used the work and/or words of others that this has been appropriately cited or quoted.

#### **Multiple, redundant, or concurrent publication**

An author should not in general publish manuscripts describing essentially the same research in more than one journal or primary publication. Parallel submission of the same manuscript to more than one journal constitutes unethical publishing behavior and is unacceptable.

#### **Acknowledgement of sources**

Proper acknowledgment of the work of others must always be given. Authors should also cite publications that have been influential in determining the nature of the reported work.

#### **Authorship of a manuscript**

Authorship should be limited to those who have made a significant contribution to the conception, design, execution, or interpretation of the reported study. All those who have made significant contributions should be listed as co-authors. Where there are others who have participated in certain substantive aspects of the research project, they should be named in an Acknowledgement section. The corresponding author should ensure that all appropriate co-authors are included in the author list of the manuscript, and that all co-authors have seen and approved the final version of the paper and have agreed to its submission for publication. All co-authors must be clearly indicated at the time of manuscript submission. Request to add co-authors, after a manuscript has been accepted will require approval of the editor.

#### **Hazards and human or animal subjects**

If the work involves chemicals, procedures, or equipment that has any unusual hazards inherent in their use, the authors must clearly identify these in the manuscript. Additionally, manuscripts should adhere to the principles of the World Medical Association (WMA) Declaration of Helsinki regarding research study involving human or animal subjects.

#### **Disclosure and conflicts of interest**

All authors should disclose in their manuscript any financial or other substantive conflict of interest that might be construed to influence the results or their interpretation in the manuscript. All sources of financial support for the project should be disclosed.

#### **Fundamental errors in published works**

In case an author discovers a significant error or inaccuracy in his/her own published work, it is the author's obligation to promptly notify the journal's editor to either retract the paper or to publish an appropriate correction statement or erratum.



#### **4. Publisher Responsibilities**

##### **Editorial autonomy**

Academic Perspective Foundation is committed to working with editors to define clearly the respective roles of publisher and of editors in order to ensure the autonomy of editorial decisions, without influence from advertisers or other commercial partners.

##### **Intellectual property and copyright**

We protect the intellectual property and copyright of Academic Perspective Foundation, its imprints, authors and publishing partners by promoting and maintaining each article's published version of record. Academic Perspective Foundation ensures the integrity and transparency of each published article with respect to: conflicts of interest, publication and research funding, publication and research ethics, cases of publication and research misconduct, confidentiality, authorship, article corrections, clarifications and retractions, and timely publication of content.

##### **Scientific Misconduct**


In cases of alleged or proven scientific misconduct, fraudulent publication, or plagiarism the publisher, in close collaboration with the editors, will take all appropriate measures to clarify the situation and to amend the article in question. This includes the prompt publication of a correction statement or erratum or, in the most severe cases, the retraction of the affected work.


## Contents


Research Articles		
Title	Authors	Pages
A Novel Method Determining the Size and Angle of an Object Using a Depth Camera Without Reference	Muhammed YILDIZ, Bilal GÜREVİN, Ramazan GÜL, Sema EĞRİ, Furkan GÜLTÜRK, Fatih ÇALIŞKAN, İhsan PEHLİVAN	41-46
Improving the Prediction Accuracy in Deep Learning-based Cryptocurrency Price Prediction	Furkan BALCI	47-61
Estimation of the Daily Production Levels of a Run-of-River Hydropower Plant Using the Artificial Neural Network	Hüseyin ALTINKAYA, Mustafa YILMAZ	62-72
A Proposed Approach to Evaluate Digital Business Model Selection for SuperApps using Interval Valued Spherical Fuzzy AHP	Murat Levent DEMİRCAN	73-86
Prediction of Unconfined Compressive Strength of Microfine Cement Injected Sands Using Fuzzy Logic Method	Eray YILDIRIM, Eyubhan AVCI, Nurten AKGÜN TANBAY	87-94


# A Novel Method Determining the Size and Angle of an Object Using a Depth Camera Without Reference

<sup>1</sup>Bilal GÜREVİN, <sup>2</sup>Ramazan GÜL, <sup>3</sup>Sema EĞRİ, <sup>4</sup>Furkan GÜLTÜRK,  
<sup>\*5</sup>Muhammed YILDIZ, <sup>6</sup>Fatih ÇALIŞKAN, <sup>7</sup>Ihsan PEHLİVAN


<sup>1</sup>Department of Mechatronics Engineering, Sakarya University of Applied Sciences, Sakarya, Türkiye, bilalsau@gmail.com 


<sup>2</sup>OPTİMAK STU, Sakarya, Türkiye, gulramazan180@gmail.com 

<sup>3</sup>OPTİMAK STU, Sakarya, Türkiye, egrisemaa@gmail.com 

<sup>4</sup>Department of Electrical and Electronics Engineering, Sakarya University of Applied Sciences, Sakarya, Türkiye, gulturk58furkan@gmail.com 

<sup>5</sup>Department of Electrical and Electronics Engineering, Sakarya University of Applied Sciences, Sakarya, Türkiye, yldzmuhammet92@gmail.com 

<sup>6</sup>Department of Metallurgical and Materials Engineering, Sakarya University of Applied Sciences, Sakarya, Türkiye, fcaliskan@subu.edu.tr 

<sup>7</sup>Department of Electrical and Electronics Engineering, Sakarya University of Applied Sciences, Sakarya, Türkiye, ipehlivan@subu.edu.tr 

## Abstract

In traditional methods, a fixed object is taken as a reference for size determination. The size of the other object is calculated by comparing the dimensions of this reference object. However, when it is desired to measure objects at different heights, the measurement of the reference object must also be changed. In the study carried out, the size and angle of the products flowing through the line were determined by using a depth camera. The data set was created by taking the measurements of an object of known dimensions from 34 different distances. The mentioned data set consists of the ratio of the number of pixels of the edges of the object to the lengths of the edges. By comparing the correlation between the obtained data set and the distance values, a mathematical equation was extracted with the help of the MATLAB program. With the help of this equation, regardless of the height and color of the object, only the distance to the camera and all 3 dimensions can be calculated. In addition, the angle of the object with the software-generated reference line was calculated by taking the long side of the object as a reference. In this way, the size and angle of the products flowing through the line were determined with a single camera without the need for a reference object and without any color and size discrimination.

**Keywords:** Depth Camera; Dimension Measurement; Angle Measurement; Mathematical Model

## 1. INTRODUCTION

Our sense organs perceive the physical and chemical stimuli in our environment and carry them to the centers in the brain in certain ways and enable them to be interpreted. eyesight; It improves our ability to perceive, comprehend and predict events quickly and manages our intuition at every moment of our lives. For the formation of three-dimensional vision; The same images should fall on the same points (visual center) of both eyes from different angles. When the images taken at these points are sent to our brain, our brain combines these two images taken from different angles into a single image [1]. When there is some difference between the images, our eyes can make the images equal with the fusion (overlap) mechanism. The remaining amount of difference is eliminated by our brain and a three-dimensional image is formed. Although 2D images are used to detect objects in today's robotics studies, they are insufficient because they lack depth sensing features. Depth cameras are needed to detect features such as size, distance and angle. The wide field of view is an essential feature for robotic applications

where it is vital to see as much of the scene as possible. The Intel® RealSense™ D435 camera, which is used in the study and has a range of up to 10 m, can be easily integrated into many studies for this purpose. When we look at the literature studies, many studies with depth cameras are encountered. Some of the work done are listed below. M. S. Ahn et al. analyzed and modeled the aforementioned sensor in a study in the field of robotics. [2].

Lee et al., in their study, examined the systematic or unsystematic depth errors that occur in image processing with a depth camera and studied the methods applied to eliminate this situation [3]. In yet another study, Ji-Ho Cho and colleagues used a single depth camera to represent human figures on three-dimensional televisions, detecting pixels that could not be processed due to variable environmental conditions and conducted studies to solve this situation [4]. Ji-Seong Jeong et al. performed parallel visual processing and visualization in real time [5]. In this application, the image was processed with a depth camera at 30 fps and viewed.

In their study, Adi and Widodo measured the distance of an object with the help of a stereo camera. Based on the center of the object, they obtained the measurement of objects 3-6 meters away with 4% error with the Euclidean distance measurement method. [6]. Kim performed the distance measurement of the leading vehicle in the article study. It measured the distance to the detected vehicle using the AdaBoost algorithm based on ACF-aggregated channel features. In his experiments in different road environments, he estimated vehicle detection with 87.5% accuracy, distance estimation with 92.8% accuracy and the time required for processing as 0.76 seconds per frame [7]. Lin et al. detected guava fruit and branch using RGB-D camera. In this way, they ensured that the fruits could be collected without hitting the branch. A 3D image was obtained by using the central location of the detected fruit and the nearest branch information. The experiment was successful between 94% and 98% and showed that fruit detection can be used in harvesting robots [8].

Parr et al. investigate the performance of five depth cameras in relation to their potential for grape yield prediction. The error performances of the cameras were compared with the data they obtained [9]. Kurtser et al. made vine yield estimation in their study. By using the depth information obtained from the RGB-D camera, they obtained the size data of the grape bunch. With the data they obtained, they made estimations with an error margin of 2.8 to 3.5 cm. [10]. Wang et al. conducted a study on counting mango fruits and measuring product size at the same time [11]. RGB-D camera, stereo camera and ToF (time of flight) sensor were used to measure distance, which is a necessary information for calculating fruit size. They preferred RGB-D camera in terms of cost and performance. However, as a result of the study, they stated that it is not very practical to use the RGB-D camera under direct intense sunlight. Maeda et al. performed an area measurement application using a depth camera to determine the tomato leaf area. [12]. Zheng et al. have studied the non-contact size measurement of vegetables using a 3D depth camera [13]. In this study, the key points are extracted by detecting the vegetable from 6 points. In this study, 4 vegetables were measured from a distance of 60 cm and deep nets were used as a method.

Cuong et al. made object detection and measurement of this object using a 3D depth camera [14]. Before the measurement, they studied preprocessing, object detection, extraction of key points and deep interpolation, respectively. With the application of interpolation, the edges and corners of the shape are created more clearly. The images used in the study were taken from a flat object on a fixed table. Hantong XU and colleagues worked on 3D modeling using the Microsoft Kinect V1 depth camera. In this study, he deduced the shape of the material to be 2-dimensional plane and reflected from a third point behind the plane. In this study, firstly, the two-dimensional position of the material is determined with the image taken from the RGB belt, and then the shape of the product is extracted from the reflection by using the depth feature with a third point according to the position. Thus, it is possible to extract the three-dimensional shape of objects with complex shapes by a different method other than drawing. [15]. Li Wu et al. used a depth camera to follow the growth of a potato plant. By making color

classification with the depth camera, they made an estimate on the development and elongation amount by considering the morphological change on the plant [16]. Ruchay et al. instantly measured the body size of a cattle with the help of a depth camera. While doing this, they used a Microsoft Kinect V2 depth camera and obtained a three-dimensional image by using the depth-reflected measurements from the camera. Such manual animal body measurements have turned into a more functional and practical method with the help of a depth camera [17]. Griffin et al. studied the detection of objects and their distance from the camera by using the depth measurement created by camera movement with the artificial intelligence model they trained [18]. In this study, the calibration of the camera was achieved by using measurements taken from multiple products. The increase in pixels in the image as the object gets closer to the camera and the decrease in the pixels obtained as it moves away is the main obstacle for us to reach the real dimensions of the object in the image. As with other 3D sensing modalities, active stereo systems suffer from this problem. In mass production lines, it is an important problem that the products that pass through the conveyor are stacked and packaged at the end of the line, and that the incoming products arrive at the right angle and know their dimensions. While calculating the spatial and orientational determinations of an object with traditional methods, an RGB camera is usually used and a reference object is placed next to the object to be measured. Calculations of the object to be measured are made based on the pixels of the reference object. However, when measuring objects of different heights, the reference object must be changed continuously. In addition, color detection is also needed as there may be objects of different colors. In another method, dimensions and orientation angles can be measured by taking measurements from different angles with two different 3D cameras. However, this brings with it the cost problem.

In this study, the distance of the object on a plane to the 3D camera is calculated with a mathematical equation, and size, size and orientation (angle) calculations are performed. In this way, the necessary measurements were obtained with a single camera without the need for any reference object and a second camera on the plane. In addition, this process was carried out without the need for color separation. In this article, after the introduction, the main features of the 3D depth camera are mentioned in the second part. In addition, with the mathematical model we obtained, object size determination and angular calculation studies are explained. In the last part, the evaluation of the size and angle determinations of the objects, independent of color and size, is included.

## 2. MATERIALS AND METHODS

In this section, size and angular calculations of the objects flowing from the conveyor line are mentioned. In addition, the hardware features of the depth camera used in the study are expressed.

### 2.1. Intel® RealSense™ D435

3D cameras are imaging devices that allow three-dimensional reproduction of depth perception in images as

experienced by human vision. The depth camera can simultaneously capture the color and geometry information of any object at the video frame rate. Used to capture depth data and color data on real-world objects [19].



**Figure 1.** Intel® RealSense™ D435 Camera

Intel® RealSense™ D435, one of the depth cameras, was used in this study. The general structure of the camera is as shown in Figure 1. This camera is designed for devices to gain the ability to see, understand and interact with their environment, as well as learn from their environment. Ideal for fast-moving applications, this 3D camera; Thanks to the depth sensor, it offers a very wide field of view with a global shutter.

## 2.2. Object Detection

In this section, the image processing steps on the images taken with the 3D depth camera are mentioned. Thresholding is done between the 3D camera and the surface of the object. In this way, as in Figure 2, the area between the surface and the camera is perceived as logic-1, and the area under the surface as logic-0. Figure 3 shows the thresholded picture.

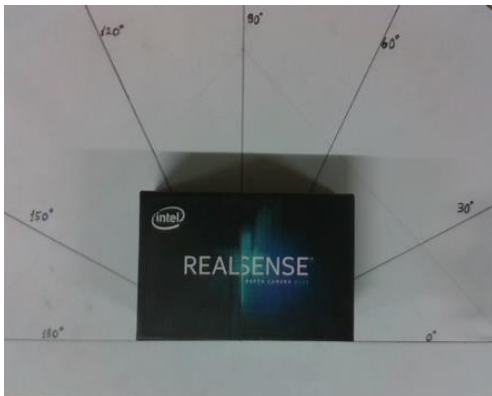


**Figure 2.** The normal image taken from camera



**Figure 3.** The image taken from camera and threshold applied

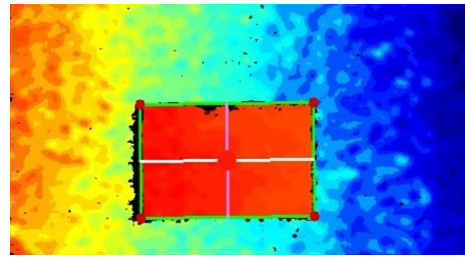


**Figure 4.** Corner point and edge detection product

Morphological processing was applied to remove the noise in the obtained images. Among the objects obtained as white on a black background, the objects were contoured in order to detect the objects of the desired size, and the objects below the determined value were not filtered and processed. Finally, the image of the object to be measured was obtained as in Figure 4 and the corner points were determined.

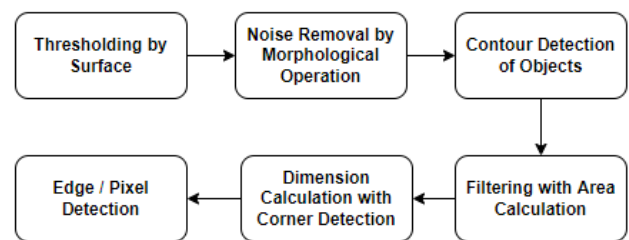


**Figure 5.** Image processing, filtering and size detection flowchart of the object

The edge lengths of the object are extracted using the corner points. The extracted edge lengths were measured as the number of pixels. In Section 2.3, the side lengths of the object, which are measured from different distances, are expressed as pixel edge length ratios in a table. In addition, in Figure 5 you can see the image processing filtering and size detection flowchart of the object.

## 2.3. Mathematical Model Extraction

With the depth camera, the distance of the object from the camera can be found. However, some mathematical operations are required to find the true lengths of the sides of the object. The object whose dimensions are to be measured is expressed with a different number of pixels inversely proportional to its distance from the camera. For example, when an object is close to the camera, it is represented by more pixels than when it is far from the camera. This relationship was expressed with a mathematical equation and the conversion of the pixel number to the length was carried out. In order to create the relationship equation, a rectangular object with known dimensions was viewed at different distances to the camera, and a data set was created. This dataset contains the ratio of the distance of the object to the camera and the number of pixels representing the edges to the actual edge length. Table 1 shows the data set.

The relationship between the distance of the object from the camera and the number of pixels representing the edge length is a non-linear relationship. This non-linear relationship can be observed better when the obtained data set is graphically expressed as shown in Figure 6. The x-axis in the graph represents the distance from the camera (cm) and the y-axis represents the ratio of pixels to the edge length.

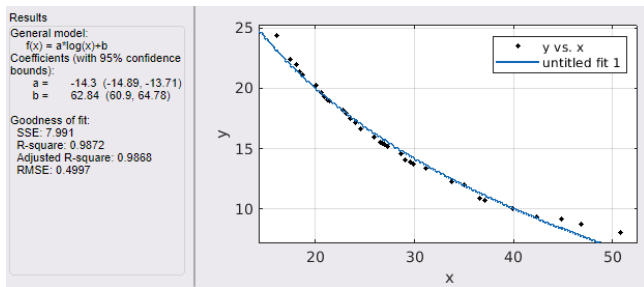


**Figure 6.** Distance logarithmic relation of object

$$ratio = a \cdot \log d_{camToObject} + b \quad (1)$$

$$l_{real} = \frac{l_{pixel}}{ratio} \quad (2)$$

Curve Fitting Toolbox tool provided by MATLAB program was used for curve fitting. By choosing the logarithmic function that best represents the data set (Equation 1), the unknown coefficients of the function were calculated by the program. The x-axis of the graph in Figure 6 represents  $camToObject$  and the y-axis represents  $ratio$ . These values were obtained as  $a = -14.3$  and  $b = 62.84$ . In Equation 1,  $d_{camToObject}$  (cm) is the distance of the object from the camera, and  $rate$  (pixels/cm) is the number of pixels per millimeter on the object. Using Equation 1 as in Equation 2,  $l_{pixel}$  (pixel) and actual length of the object in centimeters  $l_{real}$  (cm) are obtained from the number of pixels representing the edge of the object. With this method used, the edge lengths of rectangular objects of different sizes can be measured without the need for any reference object whose dimensions are known on the image. Thanks to this obtained logarithmic relation, the dimensions of the object can be determined regardless of distance.

#### 2.4. Size Detection with Mathematical Model

With the depth camera, the height of the object is determined by measuring the distance of the camera to the object and the ground where the object is located. The edge lengths obtained from the camera image are in pixels. Using Equation 1 and Equation 2, the edge lengths obtained in pixels are converted to lengths in centimeters. The volume of a rectangular object whose base sides and height are known is calculated in this way. Figure 7 shows a sample whose 3D dimensions were calculated.

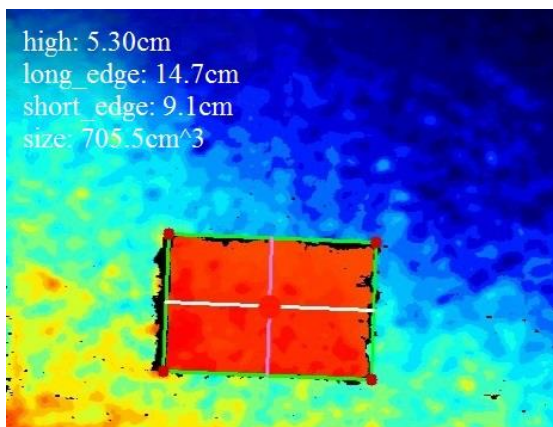


**Figure 7.** Sample product image with 3D dimension calculated

**Table 1.** Distance-dependent edge-to-pixel ratio of object

Distance (cm)	Pixel/Edge_a (pixel/mm)	Pixel/Edge_b (pixel/mm)
16,1	24,35714	24
17,5	22,42857	22,44444
18,1	22	21,77778
18,4	21,35714	21,33333
18,7	21,14286	21,11111
20,1	20,28571	19,77778
20,6	19,64286	19
20,9	19,28571	18,77778
21,2	19,07143	18,55556
21,4	18,92857	18,33333
22,8	18,21429	17,44444
23,1	17,92857	17,11111
23,5	17,5	17
24	17,14286	16,66667
24,6	16,64286	15,88889
25,9	16	15,33333
26,6	15,5	14,94444
26,8	15,42857	14,88889
27	15,35714	14,77778
27,3	15,21429	14,33333
28,6	14,57143	13,88889
29,1	14,07143	13,66667
29,6	13,92857	13,44444
29,9	13,71429	13,11111
31,2	13,35714	13,22222
33,8	12,28571	12,22222
35	12	11,77778
36,6	10,92857	11,22222
37,1	10,71429	11
39,9	10	10
42,3	9,357143	9,444444
44,9	9,142857	9,333333
46,8	8,714286	8,666667
50,8	8,071429	8

#### 2.5. Angle Calculation with Mathematical Model

In this section, the measurement of the orientation angle of the detected rectangular object is explained. A white line in Figure 8 has been added to the camera image for correct mounting of the camera on the conveyor. This line is parallel to the horizontal axis of the image frame. The lower left corner of each frame obtained from the camera is accepted as the origin of the coordinate system, its vertical edge is its ordinate and its horizontal edge is its abscissa. Corner coordinates of the contour representing the object are determined by reference to this coordinate system. The orientation angle of the object is calculated by using the coordinates of the long edge from the side edges obtained in Section 2.2.

$$\theta = \tan^{-1} \left( \frac{y_2 - y_1}{x_2 - x_1} \right) \quad (3)$$

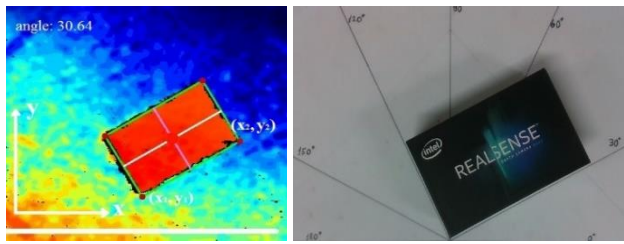


Figure 8. Angle detection object and its normal image

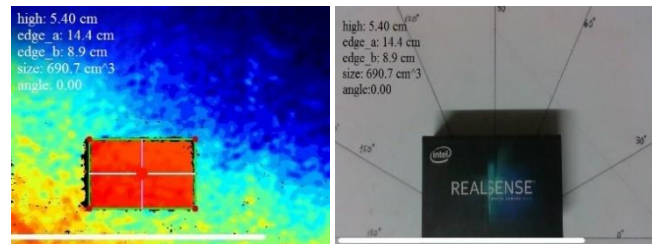


Figure 9. Sample-1 dimension and angle calculation

### 3. EXPERIMENTAL RESULTS

The mathematical model developed for the size and angle detection of objects was tested on 6 different objects. Table 2 shows the actual dimensions of these objects and the dimensions obtained as a result of the developed method. Figure 9, Figure 10, Figure 11, Figure 12, Figure 13, Figure 14 show the objects whose size and angle measurements were made using the depth camera and the developed method. A virtual line was created on the screen where the image is taken. The angle of the object was determined by measuring the angle made by the (+)x side of the long side of the object with the imaginary line. For example, when the sample-1 given in Figure 9 is examined; the long side (edge\_a) is 14.3 cm, the short side (edge\_b) is 9.1 cm, the height is 5.2 cm, and the standing angle on the surface is 0 degrees. When the measurement is carried out with the developed method; It is seen that the long side (edge\_a) is 14.4 cm, the short side (edge\_b) is 8.9 cm, the height is 5.4 cm, and the stance angle on the surface is 0 degrees. When the results obtained are taken into consideration, it has been observed that the measurement is made with an accuracy of 99.3% in long edge detection, 97.8% in short edge detection, 96.15% in height detection and 100% in angle detection. Figure 9, Figure 10, Figure 11, Figure 12, Figure 13, Figure 14 of the samples whose dimensions are given in Table 2 are shown. These pictures represent the objects in which size and angle measurements are made using the depth camera and the developed method.

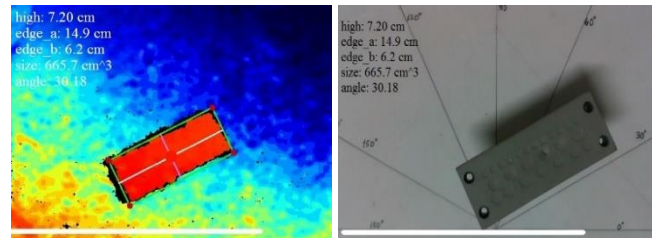


Figure 10. Sample-2 dimension and angle calculation

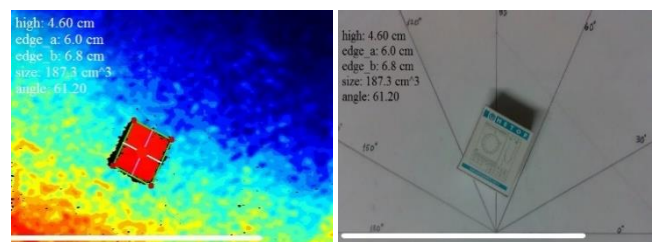


Figure 11. Sample-3 dimension and angle calculation

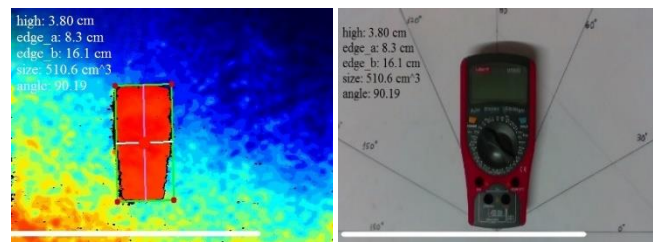


Figure 12. Sample-4 dimension and angle calculation

Table 2. Distance-dependent edge-to-pixel ratio of object

Sample Dimensions and Angle Measurements					
	Edge_a (cm)	Edge_b (cm)	Height (cm)	Angle (cm)	Size (cm <sup>3</sup> )
1	14.3	9.1	5.2	0	676.676
2	14.6	5.9	7.2	30	599.184
3	5.9	6.7	4.6	60	181.838
4	8.2	16.7	3.7	90	506.678
5	7.5	10.1	4.8	120	363.6
6	11.1	9.2	7	150	714.84

Results of The Measurement with Proposed Method					
	Edge_a (cm)	Edge_b (cm)	Height (cm)	Angle (cm)	Size (cm <sup>3</sup> )
1	14.4	8.9	5.4	0	690.7
2	14.9	6.2	7.2	30.18	665.7
3	6	6.8	4.6	61.2	187.3
4	8.3	16.1	3.8	90	510.6
5	7.5	10.2	4.9	120.66	372.4
6	11.4	9.3	7.2	150.95	758.5

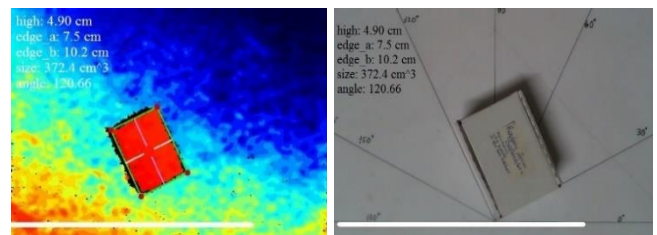


Figure 13. Sample-5 dimension and angle calculation

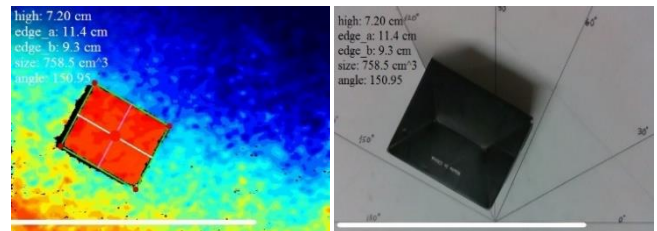


Figure 14. Sample-6 dimension and angle calculation

### 4. CONCLUSION

Two methods are generally used to calculate the size of objects. In the first method, a reference object of known dimensions is placed next to the object to be measured. The

lengths of the edges are determined by proportioning the object to be measured and the reference object. However, since the number of pixels increases with the approach of objects at different heights to the camera, the proportional study with the reference object begins to not give accurate results. In a second method, two depth cameras are pointed at the object at different angles. The edges of the object can be measured from the intersection areas. However, the large number of cameras affects the cost. With the method we developed, size and angle calculations of objects of different sizes were made without the need for a reference object and additional cameras. In this way, a system that is low cost and flexible in terms of object dimensions and does not require color separation has been developed. This developed system has also been applied to lines industrially and is currently in use. In this way, both academic and industrial gains were achieved with the study.

**Author contributions:** Concept – İ.P, F.Ç, B.G, R.G; Data Collection &/or Processing – R.G, S.E, F.G; Literature Search – M.Y, B.G, F.G, S.E; Writing – F.Ç, M.Y, F.G, B.G; Software and Hardware Development – R.G, S.E, F.G, M.Y.  
**Conflict of Interest:** This study was obtained from TUBITAK-2244 project named "Design, Development and Realization of Autonomous Storage and Logistics Management System" numbered "118C142".

**Financial Disclosure:** The products used in this study and other expenses were funded by OPTİMAK STU.


## REFERENCES

- [1] Ohio State University, "How the brain sees the world in 3-D: Scientists record visual cortex combining 2-D and depth info," *ScienceDaily*, 2017. %3Cwww.sciencedaily.com/releases/2017/03/170321110312.htm%3E
- [2] M. S. Ahn, H. Chae, D. Noh, H. Nam, and D. Hong, "Analysis and Noise Modeling of the Intel RealSense D435 for Mobile Robots," 2019. doi: 10.1109/URAI.2019.8768489.
- [3] S. Lee, "Depth camera image processing and applications," in 2012 19th IEEE International Conference on Image Processing, 2012, pp. 545–548.
- [4] J.-H. Cho, I.-Y. Chang, S. Kim, and K. H. Lee, "Depth image processing technique for representing human actors in 3DTV using single depth camera," in 2007 3DTV Conference, 2007, pp. 1–4.
- [5] J.-S. Jeong, K.-C. Kwon, M.-U. Erdenebat, Y. Piao, N. Kim, and K.-H. Yoo, "Development of a real-time integral imaging display system based on graphics processing unit parallel processing using a depth camera," *Opt. Eng.*, vol. 53, no. 1, p. 15103, 2014.
- [6] K. Adi and C. E. Widodo, "Distance Measurement With a Stereo Camera," *Int. J. Innov. Res. Adv. Eng.*, 2017.
- [7] J. B. Kim, "Efficient vehicle detection and distance estimation based on aggregated channel features and inverse perspective mapping from a single camera," *Symmetry (Basel)*, 2019, doi: 10.3390/sym11101205.
- [8] G. Lin, Y. Tang, X. Zou, J. Xiong, and J. Li, "Guava detection and pose estimation using a low-cost RGB-D sensor in the field," *Sensors (Switzerland)*, 2019, doi: 10.3390/s19020428.
- [9] B. Parr, M. Legg, and F. Alam, "Analysis of Depth Cameras for Proximal Sensing of Grapes," *Sensors*, vol. 22, no. 11, 2022, doi: 10.3390/s22114179.
- [10] P. Kurtser, O. Ringdahl, N. Rotstein, R. Berenstein, and Y. Edan, "In-field grape cluster size assessment for vine yield estimation using a mobile robot and a consumer level RGB-D Camera," *IEEE Robot. Autom. Lett.*, 2020, doi: 10.1109/LRA.2020.2970654.
- [11] Z. Wang, K. B. Walsh, and B. Verma, "On-tree mango fruit size estimation using RGB-D images," *Sensors (Switzerland)*, 2017, doi: 10.3390/s17122738.
- [12] N. Maeda, H. Suzuki, T. Kitajima, A. Kuwahara, and T. Yasuno, "Measurement of Tomato Leaf Area Using Depth Camera," *J. Signal Process.*, vol. 26, no. 4, pp. 123–126, 2022.
- [13] B. Zheng, G. Sun, Z. Meng, and R. Nan, "Vegetable Size Measurement Based on Stereo Camera and Keypoints Detection," *Sensors*, vol. 22, no. 4, 2022, doi: 10.3390/s22041617.
- [14] C. Vo-Le, P. Van Muoi, N. H. Son, N. Van San, V. K. Duong, and N. T. Huyen, "Automatic Method for Measuring Object Size Using 3D Camera," *ICCE 2020 - 2020 IEEE 8th Int. Conf. Commun. Electron.*, pp. 365–369, 2021, doi: 10.1109/ICCE48956.2021.9352115.
- [15] H. Xu, J. Xu, and W. Xu, "Survey of 3D modeling using depth cameras," *Virtual Reality and Intelligent Hardware*. 2019. doi: 10.1016/j.vrih.2019.09.003.
- [16] L. Wu, Y. Long, H. Sun, N. Liu, W. Wang, and Q. Dong, "Length Measurement of Potato Leaf using Depth Camera," 2018. doi: 10.1016/j.ifacol.2018.08.197.
- [17] A. Ruchay, V. Kober, K. Dorofeev, V. Kolpakov, and S. Miroshnikov, "Accurate body measurement of live cattle using three depth cameras and non-rigid 3-D shape recovery," *Comput. Electron. Agric.*, 2020, doi: 10.1016/j.compag.2020.105821.
- [18] B. A. Griffin and J. J. Corso, "Depth from Camera Motion and Object Detection," *Proc. IEEE Comput. Soc. Conf. Comput. Vis. Pattern Recognit.*, pp. 1397–1406, 2021, doi: 10.1109/CVPR46437.2021.00145.
- [19] L. Keselman et al., "Intel RealSense Stereoscopic Depth Cameras," *Comput. Vis. Pattern Recognit.*, 2017.



# Improving the Prediction Accuracy in Deep Learning-based Cryptocurrency Price Prediction

\*<sup>1</sup>Furkan BALCI

<sup>1</sup>Department of Electrical and Electronics Engineering, Faculty of Technology, Gazi University, Ankara, Türkiye, [furkanbalci@gazi.edu.tr](mailto:furkanbalci@gazi.edu.tr) 

## Abstract

Cryptocurrencies are popular today even though they do not have a physical form with their high-profit rates and increasing daily usage. However, the volatility of cryptocurrencies is higher than physical currencies. Furthermore, these volatilities change with the effect of social media rather than changes in exchange rates of physical currencies. For this reason, in this study, using Twitter data, one of the most widely used social media tools, real-time analysis of the values of four cryptocurrencies with the highest market value and the change in the estimated success compared to classical approaches were examined. This study's basic steps are obtaining Twitter data and financial data, performing sentiment analysis using Twitter data, and making predictions on MM-LSTM architecture. The approach is aimed to be a predictive method open to online learning. Furthermore, various filter steps were applied to remove the effect of bot users on Twitter that could prevent the prediction performance on the created data set, and the impact of the method on accuracy rate was tried to be reduced by eliminating the activity of bot accounts.

**Keywords:** Forecasting; Twitter Sentiment Score; MM-LSTM; Cryptocurrency; Deep Learning

## 1. INTRODUCTION

Cryptocurrencies have become a popular topic nowadays. Cryptocurrencies, which have varieties such as Bitcoin and Ethereum, do not have any physical form. After Bitcoin, Satoshi Nakamoto created in 2009, different cryptocurrencies were developed [1]. Cryptocurrencies other than Bitcoin are called altcoins. According to CoinMarketCap data, there are over 5500 cryptocurrencies today. The use of cryptocurrencies as a medium of exchange in various sectors, such as automotive and food, especially physical money, has made it widespread. As of October 2021, the total market capitalization of cryptocurrencies has exceeded \$2 trillion. The market value of Bitcoin, the first cryptocurrency, is at the level of \$1 trillion. The top 5 cryptocurrencies by market cap are Bitcoin (BTC), Ethereum (ETH), Cardano (ADA), XRP (XRP) and Solana (SOL).

The value of Bitcoin, which was at the level of 800 dollars at the beginning of 2017, increased to 18000 dollars at the end of the same year. This significant change has been heard worldwide thanks to social media and has aroused everyone's curiosity about cryptocurrencies. Regulations by states for the cryptocurrency market are pretty limited. Although there is no institution or state behind it, it is frequently used as an investment tool today, with the growth of the crypto money market and the high profits of many people. Although it allows investors to earn high profits in

some periods, cryptocurrencies' values are uncertain today. It is complicated to know the main factor causing this uncertainty. However, today, where interactions on social media affect daily life, the values of cryptocurrencies are also affected by these interactions. Twitter is the platform where text-based interaction is most common in social media. With the results of the studies, it has been revealed that social media has a guiding effect even in presidential elections [2]. Apart from the agendas created by many people, the tweets of some critical people play an essential role in the changes in the values of cryptocurrencies [3]. Television channels about the exchange rates of physical currencies broadcast 24 hours a day, 7 days a week. However, no publications can inform the public about the changes and developments in the cryptocurrency market. That's why people tweet about their feelings and thoughts about cryptocurrencies using social media platforms like Twitter. In behavioral economics, it has been proven that different people's emotions impact the individual's decision-making mechanism. For this reason, it is argued that tweets shared on Twitter create an agenda and affect people's interest in cryptocurrencies [4, 5]. The values of physical currencies are generally constant over time. These currencies are produced by states and protected by the same condition by various laws. Cryptocurrencies lack these safeguards [6]. As a result of the research on Binance, half of the Bitcoin (on average 6 million) held by users is used for short-term (< 1 year), and the remaining half is used for long-term (>1 year)

investment purposes. Most users do not use cryptocurrencies as a medium of exchange. The U.S. Securities and Exchange Commission has classified cryptocurrencies as commodities, not securities [5]. Speculation-free currencies are always more robust and more stable. There are studies on how cryptocurrencies are affected by speculation [7]. However, in some studies, it is revealed with GARCH models that cryptocurrencies have similar characteristics with gold and USD [8]. While investigating the effects of manipulations, an abnormal finding was encountered. Between 2010 and 2013, Bitcoin increased from 150 dollars to 1000 dollars with the purchase and sale of one person. Users who own the

majority of cryptocurrencies are called whales. These users are open to manipulation as a large amount of buying and selling transactions are not controlled by specific rules. It has been determined that the increase in cryptocurrencies between 2017 and 2018 occurred due to extensive manipulation [9]. There are various studies to make the crypto money exchange a regular use tool. The most critical work among financial institutions is establishing the Exchange-Traded Fund (ETF). With this money exchange method, more profit can be made by taking advantage of the differences between different prices in the stock markets [10].

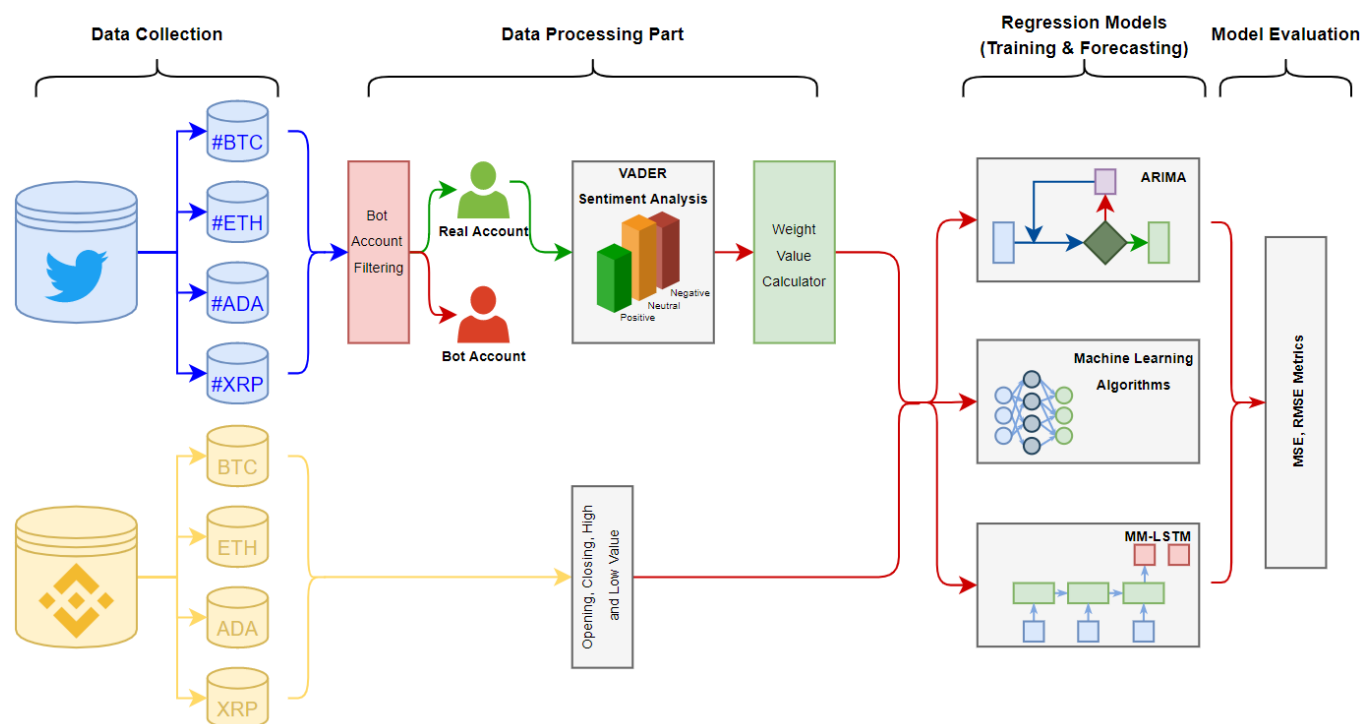


**Figure 1.** A general overview of the proposed methodology

It is complicated to predict the values of cryptocurrencies. For this reason, artificial intelligence techniques have been used frequently in addition to some classical methods in the financial field. These applications have had sufficient success in the short-term and low-volatility timeframes. Studies in the literature can be divided into three main categories: analysis with classical finance methods [7-10, 23], artificial intelligence-based forecasting, and artificial intelligence studies using different data (social media data, forum site data) in addition to financial data [16, 22, 26-28]. Applications that can interact with people over the internet, such as Twitter, allow the transfer of information and thoughts between people. Tweets can be shared about daily topics, politics, the economy and many similar topics. While sharing about issues, hashtags containing that topic are generally used. Various studies have been done on the push factors of the crypto money market [11-14]. Multiple factors were considered in these studies. Some of these factors are gold prices, the USD/EUR exchange rate, and the S&P 500. Twitter may also be among these factors. In the studies in the literature, it has been determined that investors are affected by the news and apply their investments in this direction [4]. The cryptocurrency market is instantly affected. Therefore, data consisting of various surveys and news in which

investors' tendencies are analyzed is somewhat cumbersome in the analysis of instantaneous changes. Thus, tweets shared on Twitter allow investors to access their ideas instantly. Since each tweet is 280 characters long, there are limits to conveying emotions.

Nevertheless, Twitter data contains a rich source of information about the changes in instant market values. Extensive studies use Twitter data to forecast financial markets [4-15]. High accuracy rates were achieved in these studies. These obtained accuracy rates have high accuracy for predictions 1 - 2 days later [16]. While most of these studies in the literature test the usability of Twitter data to increase prediction accuracy, various regression models and causality tests are applied. Long-term (30 - 90 days) and short-term (1 - 7 days) data are used to forecast financial data. Prediction studies using artificial intelligence techniques reach high accuracy. Methods such as Support Vector Machine (SVM) and Vector Autoregressive (VAR) are examples of these artificial intelligence techniques. However, when the studies in the literature are examined, some limitations are encountered. There are not enough estimation studies about altcoins in the literature [29, 31-37, 41-43, 45]. Generally, there are prediction studies about the

Bitcoin market. Although the findings obtained in the studies are valid during the research, the hypotheses produced due to the sudden changes in the crypto money market lose their validity. Another limitation is that there are limits on the data obtained through the Twitter API. There is a monthly limit of 5 million tweets for academic studies. Therefore, the sentiment analysis accuracy in the tweets obtained significantly affects the studies.

In this study, cryptocurrencies, including altcoins, are estimated by producing various solutions to the deficiencies of the studies in the literature. There are many suggested approaches with data from social networks such as Twitter. However, the most important of the shortcomings in these approaches is not paying attention to the fact that the effect of every tweet or every shared post is not the same. Unlike the studies in the literature, only tweets shared at the same minute were not taken as supporting data. Instead, a scoring approach was developed to reveal the effect of each tweet and its predictive performance was tested. Classical economics approaches such as ARIMA and regression algorithms such as Decision Tree, Random Forest, Linear Regression, and Logistic Regression were used for comparison. Against these algorithms, the prediction success of the MM-LSTM architecture fed by the Twitter score obtained by the weight value from Eq.1. In summary, forecast accuracy has been increased with a VADER sentiment score-based weight value equation developed for the problem of low forecast accuracy due to the extreme volatility of cryptocurrencies. To test the effectiveness of this developed sentiment analysis approach, both classical methods, machine learning methods and deep learning methods were used. The method with the lowest error rate among the methods used is MM-LSTM.

The remainder of this paper is structured as follows: Section 2 will explain the related works. Section 3 will explain the methodology. In Section 4, the experimental results of the proposed method and the outputs of the analyses. The results obtained will be discussed in Section 5. Finally, the findings of this study are summarized in Section 6.

## 2. RELATED WORKS

Studies in the literature follow two different methods: classification and regression. It provides information for future investments in the outputs of algorithms in studies that make the classification. In these studies, he usually makes predictions about whether the value of the cryptocurrency will increase or decrease for certain intervals such as 1 minute, 1 day, 15 minutes. Studies that predict the next 1 minute are very few due to the running times of the algorithms, and generally, simple machine learning methods are used in these studies.

The first studies on cryptocurrencies are about whether these assets are usable [17-20]. Wen et al. predicted that there would be some problems with cryptocurrencies in the coming years [21]. The biggest of these problems is that Chinese companies invest enough to determine the cryptocurrency market.

In the following years, with the increase in the value of cryptocurrencies, research topics began to be about predicting future values. Therefore, correlation studies have started between different data and the values of cryptocurrencies. The relationship of cryptocurrencies between Google Trends and Wikipedia search numbers was examined. A high correlation was found in this relationship [22]. In different studies, relations with varying assets with a market have been discussed. It does not correlate with assets such as Financial Stress Index and gold price [23]. The most comprehensive study analyzes 21 different parameters and shows that Google Trends searches have the highest correlation [24]. The relationship with the prices of assets such as stocks, oil barrel prices, and exchange rates is relatively low both in the expected period and when cryptocurrencies change abruptly [25]. The general result obtained in these studies is as follows, a high correlation is seen in data such as social media shares, Google search trends, and opinions on forum sites [7]. Studies about cryptocurrencies with high social media shares have been concentrated in the literature. Some studies forecast daily bitcoin, ripple and Ethereum prices with data from forum sites [26]. Different estimation methods, such as the Markov model, were also used in these studies [27]. It has been determined that the Coronavirus epidemic, which is one of the current issues, affects prices and expands transaction volumes [28].

Recent studies have revealed approaches based on predicting the prices of cryptocurrencies. In Table 1, studies in the literature are listed chronologically. The studies are divided into two subclasses, classification or regression, if the table is examined in detail. It contains brief information about the methods used. In each study, methods that will increase the predictive power, in general, are revealed. Different machine learning and deep learning methods are used in the literature. But there is no consensus on which way gives the highest accuracy. It is understood that only classical methods (such as ARIMA) have lower performance than machine learning and deep learning methods. Most studies only research on Bitcoin. Studies similar to the one performed in this article were performed in [29] and [30]. In these studies, different machine learning methods were used in the study.

Our main difference from the studies in the literature is not only on Bitcoin but also on Ethereum, XRP and Cardano with the Twitter sentiment. In addition, unlike the literature, estimates are not made for time intervals such as 15 minutes, 1 hour, and 1 day, but operations are carried out 1 minute later. Due to the extreme volatility of cryptocurrencies, classical economic forecasting methods (AR, MA, ARIMA, etc.) predict cryptocurrencies with high errors. In general, since artificial intelligence-based studies have a higher ability to learn the volatility of cryptocurrencies, there are often artificial intelligence-based studies in the literature.

## 3. MATERIALS AND METHODS

In this study, the usability of public Tweets shared on Twitter as a feature to increase the prediction of cryptocurrencies was investigated using deep learning architecture. The proposed method of the study is shown in Figure 1.

**Table 1.** Literature review

#	Cryptocurrency	Prediction	Data Length	Type	Method
[29]	Bitcoin	Daily	2011-2018	Regression Classification	It shows that the Long Short-Term Memory (LSTM) algorithm for regression gives better results than the Deep Neural Network (DNN) algorithm for classification.
[31]	Bitcoin	10 minutes	Since the discovery of Bitcoin	Classification	It uses Bitcoin closing price and 16 different features of Bitcoin as data. Both 10-minute and 10-second data were used as an additional amount of data. Classification results with 10-second data are higher. Random Forest and Binomial Logistic Regression (BLR) algorithms were used.
[26]	Bitcoin, Ethereum, Ripple	Daily	2013-2016	Classification	The classification was made with various commercial data and comments collected from online forums. Data collected from forum sites provided satisfactory improvement.
[32]	Bitcoin	15 minutes	1 month	Classification	Ten different technical analysis indicators about Bitcoin are used as features. In addition, a study on the average return was carried out with the algorithm developed based on Volume Weighted-SVM.
[33]	12 Cryptocurrencies	30 minutes	2015-2016	Regression	A regression-based on Convolutional Neural Networks (CNN) was made. In addition, forecasts of 12 different cryptocurrencies were carried out.
[34]	Bitcoin	Daily	2011-2017	Regression	Regression was performed using Bayesian neural networks (BNN), linear regression and SVM. In the study, it is argued that the BNN architecture is the best predictive method.
[35]	Bitcoin	Daily	2013-2016	Classification Regression	Regression was performed using Bayes repetitive nerve (RNN) and LSTM algorithms. It has been determined that the most suitable data amount for the LSTM algorithm is 100-120 days, and the most appropriate for the RNN algorithm is 15-20 days.
[36]	Bitcoin	15 minutes	2016-2018	Classification	The classification was made using artificial neural networks (ANN). 4 different technical analysis indicators were used.
[37]	Bitcoin	1 minute	2012-2017	Classification	The classification was made using Random Forest (RF). He used five different technical analysis indicators. He argues that 15-minute forecasts are more accurate.
[38]	1681 Cryptocurrencies	Daily	2015-2018	Regression	A collection of regression trees created by XGboost and the long-term memory network is used. As a result, a profitable forecasting system has been developed against up to 0.2% transaction fees.
[39]	Bitcoin, Ethereum, Litecoin, Ripple	Daily	2011-2017	Classification Regression	A hybrid neuro-fuzzy model (PATSOs) has been developed, and higher results have been obtained than classical machine learning methods.
[40]	Bitcoin, Ethereum, Litecoin, Ripple	Daily	2015-2017	Regression	Linear univariate and multivariate regression models and their selections and combinations were tested individually. It was observed that the results of combinations of univariate models were lower.
[41]	Bitcoin	Daily	2013-2018	Regression	SVM and ANN algorithms are used. It has been observed that the SVM method makes more protective decisions.
[42]	Bitcoin	Daily	2011-2018	Classification Regression	DNN, LSTM, CNN, Deep Residual Network (ResNet), CNNs and RNNs (CRNN) and their combinations were used. LSTM for regression achieved higher accuracy than DNN for classification.
[30]	Bitcoin, Ripple	Daily	2011-2018	Regression	A comparison was made between LSTM and Generalized Regression Neural Networks (GRNN). The prediction accuracy of LSTM is higher than GRNN.
[43]	Bitcoin	Daily	2011-2017	Classification Regression	Artificial neural networks (ANN) and SVM are used. It is argued that SVM is the best regression model. OHLC prices and various external financial variables are used as data.
[44]	100 Cryptocurrencies	1 minute	Until 2018	Classification	Logistic regression (LR), RF, SVM and Gradient Tree Boosting algorithms were used.
[45]	Bitcoin	5 minutes Daily	2017-2018	Classification	LR, Linear Discriminant Analysis (LDA), RF, XGBoost (XGB), SVM and LSTM algorithms are used. The LSTM achieved the highest accuracy in the 5-minute data.
[31]	42 Cryptocurrencies	Daily	6 months	Classification	LightGBM, SVM and RF methods were used for 2-week forecasts. The LightGBM method achieved the best results.

### 3.1. Financial Data

This study focuses on the improvement that can be made to the forecast of the four largest cryptocurrencies by market capitalization. Particularly focused on cryptocurrencies with high interaction. These cryptocurrencies are Bitcoin (BTC), Ethereum (ETH), Cardano (ADA), XRP (XRP) and Solana (SOL). Binance was used to collect financial data. Financial data were collected between September 6, 2021, and October 3, 2021. This period is a period of 4 weeks. Hourly and minute data was received from Binance. In order to express the value of cryptocurrencies, the physical currency USD, which has general usage in the world, was used. The labels of the financial data used as time series are used with the date and time of the relevant day.

### 3.2. Twitter Data

In order for the interaction with financial data to be examined, the time interval of the Twitter data and the time interval of the financial data must be the same. A data set was created by collecting tweets separately for each cryptocurrency. Twitter API developed by Twitter for researchers was used to collect Twitter data. Tweets shared publicly on Twitter can be accessed using the Twitter API. On Twitter, users use the hashtag (#) prefix before some keywords related to the topics they are talking about. Thanks to this use, both the agenda is created, and the Tweets shared about that subject can be easily accessed. The dataset was created using hashtags for each cryptocurrency. The prefix before some keywords are related to the topics they are talking about. The dataset was created using hashtags for each cryptocurrency. However, today, artificial agenda creation studies are also carried out for the crypto money market with the use of bot accounts. For this reason, it is necessary to clean the shares made by bot accounts before using the dataset. Bot accounts were identified and filtered by analyzing Tweets and the number of people who shared these Tweets, and the number of people following these users. There are many studies on the detection of bot accounts. In the detection of bot accounts, first of all, it should be understood how the sharing movements of bot accounts are. In this regard, some basic generalizations have been considered. These generalizations are: Tweets with content about free cryptocurrency giveaways, bot account link sharing, almost zero follower/follower ratio. By using these generalizations, the dataset is free of bots. Today, the intense use of social media has made it easier for these environments to be neglected by malicious people. Bot accounts can spread fake news using Twitter. Known for its corporate identity, Twitter social media application is used by every segment of society. The data shared by Twitter has more than 400 million users. According to Alexa, developed by Google, although Twitter ranks 13th among the most visited sites in the world, abuses on this social platform have also increased. The use of Twitter as a usable identity at the entrance of some applications makes it possible to access the Twitter application from different platforms easily. This situation attracts malicious users more. Generally, negative Twitter accounts have goals such as gaining more followers, influencing a specific community to make people join their organization, manipulating people for the stock market, spreading fake news, and blackmailing people using private

information. Bots in social networks are computer software that shows automatic reactions that mimic human behavior [48]. Today, it is thought that 15% of active Twitter users are bots [49]. Zi et al. used an entropy-based layered architecture to detect Twitter bot-human-Cyborg [50]. Software frameworks that account for Twitter bots' characteristics and detect accounts by automatic feature extraction have also been developed [49]. In the dataset used in another study, Twitter profiles were discussed according to the number of different followers [51]. The study used all samples in the data set for training and testing, thanks to the cross-validation method. In addition, the diversity of features in the dataset was also crucial in bot detection. The most comprehensive competition for detecting Twitter bots is "The DARPA Twitter Bot Challenge", held during the 2016 American Presidential Elections. The six teams participating in the competition worked on 7,038 accounts and approximately 4 million tweets [52]. Bot accounts on Twitter were detected with the "warped correlation" technique developed in another study. With this method, 544,868 bot accounts were detected annually, and the success rate was 94% [53]. In the Twitter environment, bot detection is essential for the security of society. Recently, new deep-learning networks have started to be used in Twitter bot detection [54]. Both machine learning and deep learning methods use metrics such as accuracy, precision and F-score in detecting bot accounts. Fred et al. contributed from a different point of view in evaluating these metrics [55]. In some approaches in the literature, many parameters are used to determine bot accounts. Some of these parameters are:

- Age of the account: The age of the account in days is higher for real users.
- The ratio of followers to friends: It is observed that the ratio of real users is close to 1.
- User favorites: The number of favorite tagging tweets by users is higher in real users.
- The number of retweets per tweet: Real users get more retweets due to original content and variety.
- Number of URLs: Real users share fewer URLs.
- Frequency of tweeting: Bot users share more tweets during the day.

To be able to do sentiment analysis later, the text content must be made available for Sentiment analysis. Some steps must be followed for this process. These steps are shown in Table 3. on a sample tweet, respectively. These steps were applied to all tweets, and as a result of these pre-processes, the dataset was ready for sentiment analysis. Statistical data and general information about the data obtained with the access permission obtained from Twitter are shown in Table 1. Some of the statistical information is important for artificial intelligence techniques. Especially the number of data is essential for training and testing. Therefore, the number of Tweets is shared in the table. Twitter can reshare another person's tweet. Therefore, information about unique shared tweets is also provided. There is standard deviation (STD) information about the daily data, which includes the average number of tweets and the difference from the average daily tweets. The average number of tweets and standard deviation information provide us with information about how volatile the agenda is. If the table is examined in

detail, Bitcoin is the most talked about cryptocurrency because it is both popular and dominates more than half of the market. There is not enough sharing to create an agenda on Twitter about other sub-cryptocurrencies. That's why only these four cryptocurrencies have been selected.

**Table 2.** Statistics of the filtered Twitter datasets

	Number of Tweets	Number of Unique Tweets	Mean Daily Tweets	STD of Daily Tweets
BTC	3.101.251	1.352.077	110.759	33.985
ETH	738.192	379.124	26.364	3.846
ADA	486.224	203.218	17.365	5.199
XRP	375.117	79.826	13.397	2.491

Not every Tweet has the same effect. Some people can affect the agenda more due to the high number of followers. This effect needs to be measurable. Using a scoring system to understand the impact of users' Tweets makes Twitter's impact more meaningful. There are various scoring systems in the literature. VADER (Valence Aware Dictionary and Sentiment Reasoner) approach will be used in this study to measure the effect of Tweets shared by users publicly. In the VADER method, Tweets shared by users are analyzed and classified according to their emotions. The words in the dictionary within the VADER structure play an essential role

in this scoring process. The compound score is calculated with this dictionary. The punctuation marks used are necessary for the compound score. The Tweet's language was translated into English using the Python module developed by Google on Tweets shared in different languages. The compound score takes a normalized value between -1 and +1. A value of -1 means the most extreme negative, and a value of +1 means the most positive. Positive sentiment analysis means buying, neutral sentiment analysis means waiting, and positive sentiment analysis means selling cryptocurrencies. In this scoring system, an equation developed outside of the VADER structure will be used to turn the effect of the Tweet shared by the user into usable numerical data in the deep learning structure. In Eq. (1), the compound score (CS), the number of followers (FC), the number of likes (TL) and the number of retweets of the shared Tweet (RT) are used as a multiplier. This designed score number is updated instantly and creates a supporting feature for the cryptocurrency closing data, which is planned to be predicted for the next minute. To investigate the contribution of this data, prediction performances on different algorithms will be compared. A comparison of supported and unsupported algorithms will also be made with this data.

$$WeightValue = CS * FC * (TL + 1) * (RT + 1) \quad (1)$$

**Table 3.** Example of pre-processing steps to be applied to tweet for Twitter score

Process Number	Process Definition	Example
0	Initial Tweet	RT @ethereum https://t.co/FT/status/98342573428 Bitcoin will make us richeeeerr than yesterday!!! Go and buy lol, end of the year it will be \$100000 #BUY #ETHEREUM \$BTC \$ETC
1	Removing "RT" text	@ethereum https://t.co/FT/status/98342573428 Bitcoin will make us richeeeerr than yesterday!!! Go and buy lol, end of the year it will be \$100000 #BUY #ETHEREUM \$BTC \$ETC
2	Removing links	Bitcoin will make us richeeeerr than yesterday!!! Go and buy lol, end of the year it will be \$100000 #BUY #ETHEREUM \$BTC \$ETC
3	Reducing repeated characters	Bitcoin will make us richeerr than yesterday!!! Go and buy lol, end of the year it will be \$100000 #BUY #ETHEREUM \$BTC \$ETC
4	Uppercase character conversion	bitcoin will make us richeerr than yesterday!!! go and buy lol, end of the year it will be \$100000 #buy #ethereum \$btc \$etc
5	Removing hashtags	bitcoin will make us richeerr than yesterday!!! go and buy lol, end of the year it will be \$100000 \$btc \$etc
6	Expansion of abbreviations	bitcoin will make us richeerr than yesterday!!! go and buy laughing out loud, end of the year it will be \$100000 \$btc \$etc
7	Removing punctuation	bitcoin will make us richeerr than yesterday go and buy laughing out loud, end of the year it will be 100000 btc etc
8	Removing numeric expressions	bitcoin will make us richeerr than yesterday go and buy laughing out loud, end of the year it will be btc etc

### 3.3. Statistical Analysis

The value of cryptocurrencies and the number of tweets shared are time-dependent data. These data types are called time series. The stationarity of the time series is one of the most important criteria. Stationarity is when the mean and variance of the time series are not dependent on time. The covariance value depends on the mean and variance values.

Various statistical models should be used first to see that the approach can benefit the deep learning model in examining the relationship between the cryptocurrency values data used in this study and the number of tweets shared in the relevant period. Correlation analysis gives us information about the relationship between two data and the direction of this relationship. Simple correlation analyzes may be insufficient because there will be a time difference between the two data.

If the values in two different time series have a relationship over time concerning a particular lag time, and it is desired to determine the direction of this relationship, one of the tests that can be used is the Granger causality test. The Granger causality test can be defined as follows: If an X variable causes a change in a Y variable, changes in X will lead to changes that will occur in Y after a while. That is, if the estimation is significantly improved when variable X or the delayed values of variable X are added to the regression of variable Y with other variables, then variable X is the Granger cause of variable Y [46].

Although there are many views on the definition of causality, there is a common view on establishing a cause-effect relationship between the variables. The existence of a strong relationship or correlation between the variables does not necessitate the existence of causality. For example, regression analysis establishes a statistical relationship between variables and does not deal with cause-effect relationships.

In this context, Granger developed a relatively simple test in 1969 to reveal the cause-effect relationship between the variables. According to Granger, if the success of the estimation increases with the inclusion of the past values of the X independent variable in the estimation of any Y variable, the X variable is a cause of the Y variable. The Granger causality test is expressed in the context of linear regression models. For example, it is described as a linear autoregressive model with two variables such as  $X_1$  and  $X_2$ . It is expressed mathematically as follows [46]:

$$x_1(t) = \sum_{j=1}^p A_{11}X_1(t-j) + \sum_{j=1}^p A_{12}X_2(t-j) + E_1(t) \quad (2)$$

$$x_2(t) = \sum_{j=1}^p A_{21}X_1(t-j) + \sum_{j=1}^p A_{22}X_2(t-j) + E_2(t) \quad (3)$$

In the equation above, p represents the maximum number of delayed observations included in the model. If the variance of  $E_1$  decreases when the term  $X_2$  is included in the equation above, it is understood that  $X_1$  is the Granger cause of  $X_2$ . Likewise, if the variance of  $E_2$  decreases when the term  $X_1$  is included in the equation above, it is understood that  $X_2$  is the Granger cause of  $X_1$ . In other words,  $X_2$  becomes the Granger cause of  $X_1$  if the coefficients in  $A_{12}$  together are unique in relation to zero. This situation can be understood by performing the F-test of the  $H_0$  hypothesis with when  $A_{12}$  is 0, when the assumption of covariance stationarity for  $X_1$  and  $X_2$  is accepted. The magnitude of a Granger causality relationship is measured by taking the logarithm of the corresponding F-statistic. Choice of criteria methods like Hannan-Quinn Information Criteria (HQ), Schwartz Information Criteria (SIC) or Akaike Information Criteria (AIC) can be utilized to decide the fitting number of delays.

### 3.4. Multi-step Multivariate Long Short-Term Memory

This paper created a deep learning structure to predict the value of cryptocurrencies. This deep learning structure is based on the Recurrent Neural Network (RNN) structure. The value to be estimated in RNN structures does not only analyze based on the current value but also based on historical data. Therefore, RNN structures are frequently used in time series data [47, 56]. RNN structures do not

delete old data, such as the work of the human brain. Classical neural network structures delete after using old data in the weighting setting [56]. RNN structures have been developed to cover this gap. The data used in RNN-based structures are stored in memory units until the cycle is completed. RNN structure is basically the same as classical neural networks [57]. This structure is formed by listing the same networks. The input of each network depends on the output of the previous network. There are varieties of RNN structures. Long Short-Term Memory (LSTM) structure is used in this paper. LSTM structure has begun to be used widely in estimation processes based on historical data. RNN structure has a single-layer network structure.

The LSTM structure has a four-layer network structure. There are structures called gates in the LSTM structure. These gate structures perform tasks such as adding and removing information to the neural cell. The sigmoid function used in the neural network layer gives values between 0 and 1. The sigmoid function determines how much of the signal is allowed to pass. This value varying between 0 and 1 is used as a ratio. The first of these gates is called the forget gate. This gate investigates the prior output and the current input and produces a value between 0 and 1. On the off chance that the produced value is 0, it signifies "forget this state"; assuming the produced value is 1, it represents "keep this state" [47]. The forget gate is indicated by  $f_t$ . Eq. (4) shows the equation of the forget gate result.

$$f_t = \text{sigmoid}(W_f[h_{t-1}, x_t] + b_f) \quad (4)$$

Another gate layer is the input gate. This gate structure decides which new values to keep. In this step, both sigmoid and tanh functions are used. The sigmoid structure produces the value to be updated, and the tanh structure produces the intermediate value  $C_{tx}$ . Eq. (5) shows the equation of the sigmoid function. Eq. (6) shows the equation of the tanh function. Then these values are combined.

$$i_t = \text{sigmoid}(W_i[h_{t-1}, x_t] + b_i) \quad (5)$$

$$C_{tx} = \text{tanh}(W_c[h_{t-1}, x_t] + b_c) \quad (6)$$

Using it and  $C_{tx}$  values,  $C_t$  is generated, allowing the old data to be transferred to the next cell. For example, Eq. (7) shows the current data equation  $C_t$  obtained with old data and new entries.

$$C_t = f_i * C_{t-1} + i_t * C_{tx} \quad (7)$$

In the next step, the output of that cell must be calculated. This calculated output is branched to be used in the next cell. Finally, deciding which data will be used as output from the cell is necessary. The sigmoid function is used to make this decision. Eq. (8) shows the equation of the sigmoid function. The tanh function converts the sigmoid function's result to -1 and 1. The final cell output is obtained after this transformation. Eq. (9) shows the equation of the last cell output.

$$o_t = \text{sigmoid}(W_o[h_{t-1}, x_t] + b_o) \quad (8)$$

$$h_t = o_t * \tanh(C_t) \quad (9)$$

**Table 4.** Pseudocode of the proposed MM-LSTM architecture**Algorithm 1.** MM-LSTM Architecture**Input:** Multivariate Cryptocurrency Data, Learning Rate( $\lambda$ ), Twitter Score**Output:** Predicted Value ( $x_{N+1}^{(1)}$ ), Test MSE, Test RMSE

Initialize the parameters of MM-LSTM

 $test\ size \leftarrow length(data) \times (100 - \lambda)$ **for**  $i \in (1, \dots, epoch)$  **do** $\hat{x}_t^{(1)} \leftarrow LSTM(x_t, \dots, x_{t-slidingwindowsize+1})$ Loss  $\leftarrow \|\hat{x}_t^{(1)} - x_t^{(1)}\|$ 

Optimize the parameters based on Loss

Back propagation method with  $\lambda$ **end for**Predicted Value List  $\leftarrow x_{N+1}^{(1)}$ Test RMSE  $\leftarrow \sqrt{\frac{\sum_{i=1}^{testsize} (x_{N+1}^{(1)} - x_{N+1})^2}{testsize}}$ **return** Predicted Value List, Test RMSE

The Multivariate Multi-step LSTM structure used in this study is similar to the classical LSTM structure described above. However, it has 2 differences from the classical LSTM structure. These differences:

- The dependent variable estimation result is estimated with more than one independent variable.
- The estimated value includes more steps than a single step.

LSTM architecture is used in the study carried out in various academic fields, such as biomedical data in time series, economic data, and time series data related to the process [58 – 61].

#### 4. RESULTS AND ANALYZES

Two separate data sets are needed to carry out this study. First of all, the dataset that needs to be pre-processed and analyzed is the Twitter dataset. Table 2 contains statistical data on Twitter data. In light of these data, it has been determined that the tweets of bot users at various rates (1% - 17%) set the agenda. These accounts, created to share false information and manipulate, need to be filtered out. The posts of bot accounts are mostly about low-value cryptocurrencies. If Table 2 is examined, the effect of bot accounts on each cryptocurrency is also shown as a percentage distribution. Some essential criteria detect these bot accounts. It can be said that there may be some bot accounts that exceed these criteria. During the detection of bot accounts, attention was paid to the fact that the follower/following ratio was almost zero and that the tweet content included giving away crypto money. This study's sentiment analysis on publicly shared Tweets investigates the predictability of cryptocurrencies' values. The analysis method used to examine this relationship is Granger causality analysis. To search for causality between series, stationarity information is needed. If the series are stationary

of the same order, a cointegration relationship can be sought between them. If a cointegration relationship is not observed, causality can be investigated in the order that the series are stationary. Thanks to the Granger causality test, it is revealed whether tweets shared by users cause a change in the value of cryptocurrencies. It plays a vital role in seeing the relationship between the scoring process using the compound score calculated with the VADER method and the value of the relevant cryptocurrency at that moment. With these scores, the Granger causality test was applied. Here, the Granger causality test was applied for both cases to understand whether Twitter data contains causality on cryptocurrencies or on Twitter data. The Granger causality test results, the maximum order of integration and p values for each cryptocurrency are shown in Tables 5 to 8. The section shown in red shows the Twitter score calculated per minute, obtained within the framework of our approach. The part shown in blue is the closing data of the cryptocurrency received on Binance at that minute. It is important here that there are statistically significant relationships ( $p < 0.05$ ). Cryptocurrencies with lower market caps are more susceptible to manipulation. For this reason, if we look at the results of the Granger analysis, the causality relationship is higher for cryptocurrencies with lower market capitalization.

Eight different methods were used to analyze the performance of the proposed method. First, ARIMA, LTSM, Support Vector Regressor, Decision Tree Regressor, Random Forest Regressor, Linear Regressor, Logistic Regressor, Gaussian Process Regressor and MM-LSTM architectures were tested only with cryptocurrency closing data. Then these architectures were tested with Twitter sentiment analysis score and cryptocurrencies' opening, closing, high and low data. Next, the Root Mean Square Error (RMSE) calculation was calculated separately for all methods to make the performances comparable. RMSE is a metric used to create a comparison of predicted values. It explains how far each predicted value deviates from the correct value. The RMSE result can start from 0 and take forever. Eq. (10) shows the equation for calculating the RMSE value. Each RMSE result is given in Tables 9 and 10.

$$RMSE = \sqrt{\frac{\sum_{i=1}^N (Predicted_i - Actual_i)^2}{N}} \quad (10)$$

Since different types of data (Cryptocurrency value, Twitter score) are used in the MM-LSTM structure, the data were normalized before using the deep learning model for training and testing. The Min-Max Scaling method was used, one of the various normalization methods in the literature. Due to the use of the minute dataset, there are 40200 samples in each feature for all three methods between the relevant dates. Finally, the closing data of each cryptocurrency is used to make predictions with eight regression algorithms.

ARIMA models are applied to non-stationary series but converted to stationary by differencing. Models used to non-stationary series but converted to stationary by difference-taking are called non-stationary linear stochastic models. These models are AR, applied to series with a d-degree difference, in which the value of the variable in the t-period is expressed as a linear function of a certain number of back-period values and the error term in the same period. The



variable's value in the t-period is a linear function of the error term in the same period and a certain number of back-period error terms. They are a mix of MA models expressed as the general representation of the models is ARIMA (p, d, q). Here, p and q are the levels of the autoregressive model (AR) and the moving average model (MA) separately, and d is the level of difference. The general ARIMA (p, d, q) model is formulated as Eq. (11).

$$Z_t = \Phi_1 Z_{t-1} + \Phi_2 Z_{t-2} + \dots + \Phi_p Z_{t-p} + \delta \alpha_t - \Theta_1 \alpha_{t-1} - \Theta_2 \alpha_{t-2} - \dots - \Theta_q \alpha_{t-q} \quad (11)$$

In Eq. (11);  $Z_t, Z_{t-1}, \dots$  d-degree observation values,  $\Phi_1, \Phi_2, \dots$  coefficients for d-degree differentiated observation values,  $\delta$  constant value,  $\alpha_t, \alpha_{t-1}, \dots$  error terms and  $\Theta_1, \Theta_2, \dots$  error show the coefficients related to the terms.

**Table 5.** Bitcoin Granger causality test results

BTC Number of Lags: 1 (dfdenom=40196)				BTC Number of Lags: 2 (dfdenom=40193)			
F test on SSR	23.166	p=0.0000	num=1	F test on SSR	8.259	p=0.0003	num=2
chi2 test on SSR	23.168	p=0.0000	df=1	chi2 test on SSR	16.521	p=0.0003	df=2
Likelihood ratio test	23.161	p=0.0000	df=1	Likelihood ratio test	16.518	p=0.0003	df=2
F test parameter	23.166	p=0.0000	num=1	F test parameter	8.259	p=0.0003	num=2
BTC Number of Lags: 3 (dfdenom=40190)				BTC Number of Lags: 4 (dfdenom=40187)			
F test on SSR	3.347	p=0.0182	num=3	F test on SSR	1.517	p=0.1942	num=4
chi2 test on SSR	10.042	p=0.0182	df=3	chi2 test on SSR	6.069	p=0.1940	df=4
Likelihood ratio test	10.040	p=0.0182	df=3	Likelihood ratio test	6.069	p=0.1941	df=4
F test parameter	3.347	p=0.0182	num=3	F test parameter	1.517	p=0.1942	num=4

**Table 6.** Ethereum Granger causality test results

ETH Number of Lags: 1 (dfdenom=40196)				ETH Number of Lags: 2 (dfdenom=40193)			
F test on SSR	103.098	p=0.0000	num=1	F test on SSR	28.923	p=0.0000	num=2
chi2 test on SSR	103.105	p=0.0000	df=1	chi2 test on SSR	57.852	p=0.0000	df=2
Likelihood ratio test	102.973	p=0.0000	df=1	Likelihood ratio test	57.811	p=0.0000	df=2
F test parameter	103.098	p=0.0000	num=1	F test parameter	28.923	p=0.0000	num=2
ETH Number of Lags: 3 (dfdenom=40190)				ETH Number of Lags: 4 (dfdenom=40187)			
F test on SSR	7.588	p=0.0000	num=3	F test on SSR	2.434	p=0.0451	num=4
chi2 test on SSR	22.767	p=0.0000	df=3	chi2 test on SSR	9.738	p=0.0451	df=4
Likelihood ratio test	22.760	p=0.0000	df=3	Likelihood ratio test	9.737	p=0.0451	df=4
F test parameter	7.588	p=0.0000	num=3	F test parameter	2.434	p=0.0451	num=4

**Table 7.** Cardano Granger causality test results

ADA Number of Lags: 1 (dfdenom=40196)				ADA Number of Lags: 2 (dfdenom=40193)			
F test on SSR	24.711	p=0.0000	num=1	F test on SSR	8.605	p=0.0002	num=2
chi2 test on SSR	24.713	p=0.0000	df=1	chi2 test on SSR	17.213	p=0.0002	df=2
Likelihood ratio test	24.706	p=0.0000	df=1	Likelihood ratio test	17.209	p=0.0002	df=2
F test parameter	24.711	p=0.0000	num=1	F test parameter	8.605	p=0.0002	num=2
ADA Number of Lags: 3 (dfdenom=40190)				ADA Number of Lags: 4 (dfdenom=40187)			
F test on SSR	4.417	p=0.0041	num=3	F test on SSR	2.505	p=0.0401	num=4
chi2 test on SSR	13.254	p=0.0041	df=3	chi2 test on SSR	10.022	p=0.0401	df=4
Likelihood ratio test	13.252	p=0.0041	df=3	Likelihood ratio test	10.021	p=0.0401	df=4
F test parameter	4.417	p=0.0041	num=3	F test parameter	2.505	p=0.0401	num=4

**Table 8.** XRP Granger causality test results

XRP Number of Lags: 1 (dfdenom=40196)				XRP Number of Lags: 2 (dfdenom=40193)			
F test on SSR	91.789	p=0.0000	num=1	F test on SSR	48.881	p=0.0002	num=2
chi2 test on SSR	91.796	p=0.0000	df=1	chi2 test on SSR	97.775	p=0.0002	df=2
Likelihood ratio test	97.657	p=0.0000	df=1	Likelihood ratio test	97.657	p=0.0002	df=2
F test parameter	91.789	p=0.0000	num=1	F test parameter	48.881	p=0.0002	num=2
XRP Number of Lags: 3 (dfdenom=40190)				XRP Number of Lags: 4 (dfdenom=40187)			
F test on SSR	20.967	p=0.0041	num=3	F test on SSR	9.847	p=0.0401	num=4
chi2 test on SSR	62.913	p=0.0041	df=3	chi2 test on SSR	39.398	p=0.0401	df=4
Likelihood ratio test	62.863	p=0.0041	df=3	Likelihood ratio test	39.379	p=0.0401	df=4
F test parameter	20.967	p=0.0041	num=3	F test parameter	9.847	p=0.0401	num=4

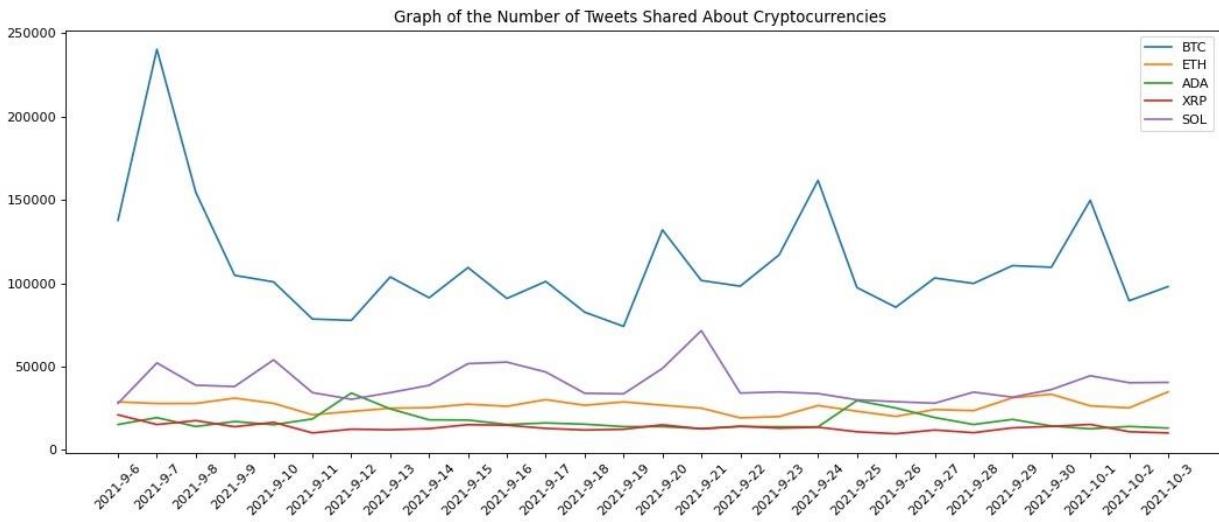


**Figure 2.** Daily tweet volumes of four cryptocurrencies between September 6 and October 3, 2021

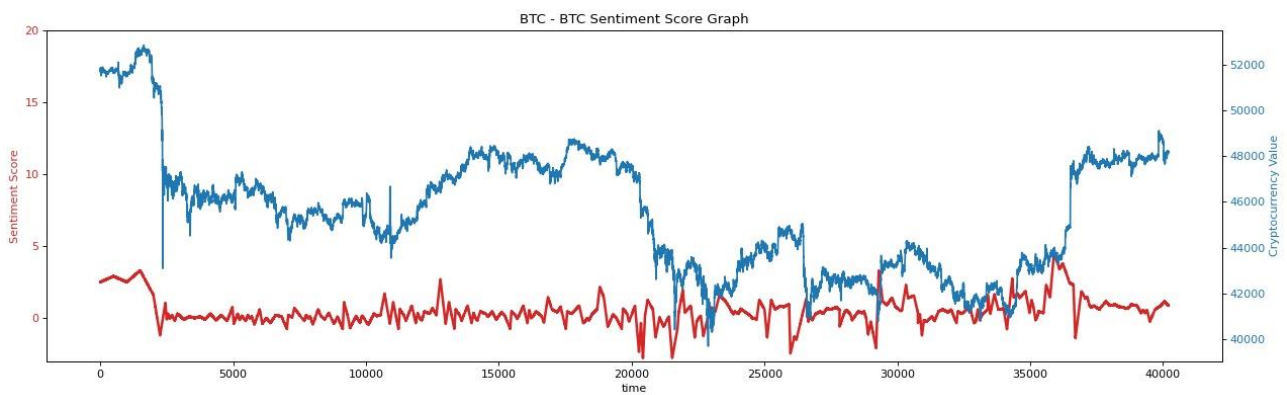


**Figure 3.** Twitter sentiment analysis score chart with Bitcoin closing data

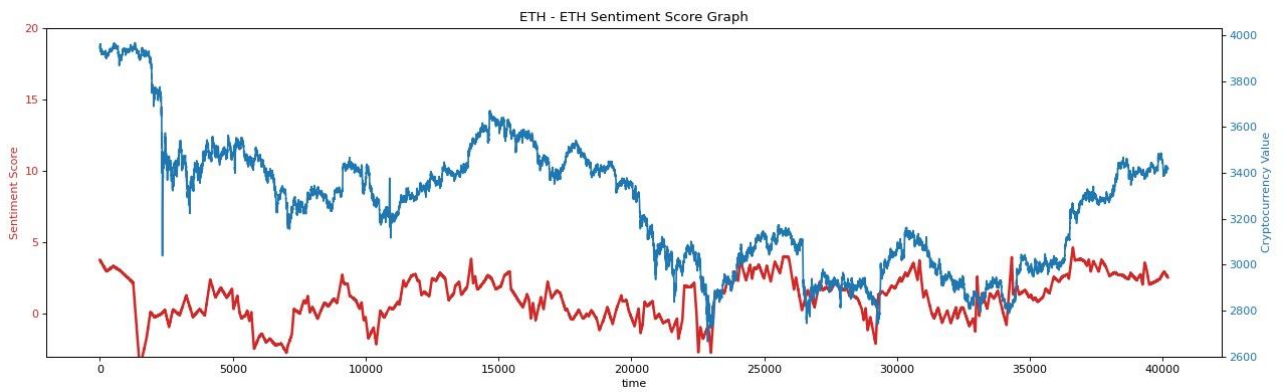


**Figure 4.** Twitter sentiment analysis score chart with Ethereum closing data

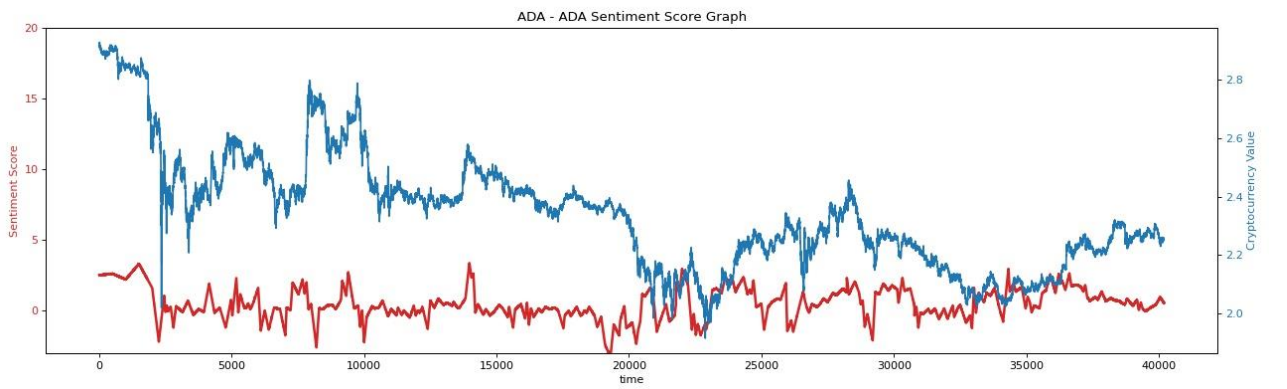


**Figure 5.** Twitter sentiment analysis score chart with Cardano closing data

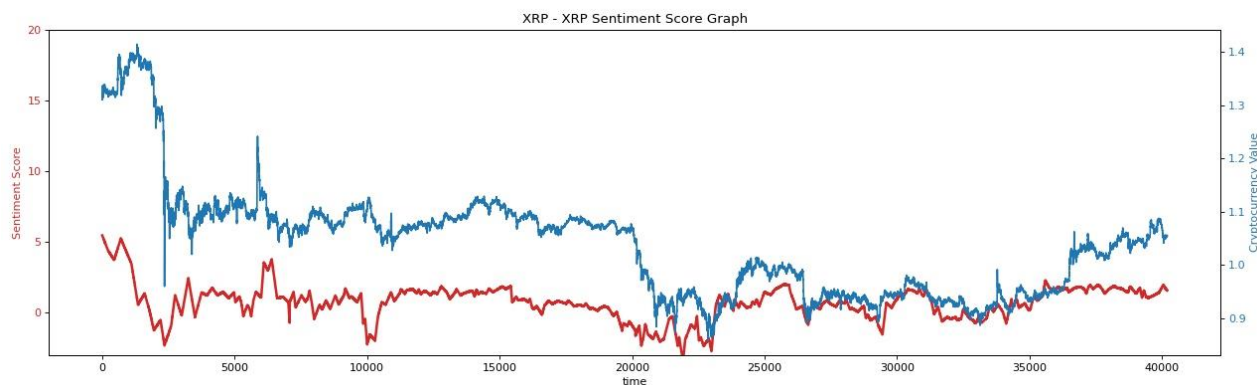


**Figure 6.** Twitter sentiment analysis score chart with XRP closing data

The total length of the data collected in 4 weeks (28 days x 24 hours x 60 minutes) is 40200. 65% of the whole data set was used as training data, and the remaining 35% as test data. According to these ratios, three different methods were trained and tested. Table 10 shows that the ARIMA method has a higher MSE & RMSE value for each cryptocurrency. Although the ARIMA method is a widely used method for estimating time series, the main reason for having high RMSE values is the volatility of cryptocurrencies. As it is known, the values of cryptocurrencies are not stationary time series. While creating the ARIMA model,  $p$ ,  $d$ , and  $q$  parameters were selected as 0, 1 and 0, respectively, from the values showing the highest performance by trial. Examining the prediction performance using the ARIMA method, the primary purpose is to compare LSTM based on deep learning and MM-LSTM, another improved version of LSTM. Parameters of LSTM structures: number of layers is 2, and the number of hidden units is 7. The performances of the algorithms that are frequently used in regression problems (Decision Tree Regressor, Random Forest Regressor, Linear Regressor, Logistic Regressor, and Gaussian Process Regressor) are shown in Table 10. The analysis of the comparative performance of the algorithms is demonstrated with the MSE and RMSE results. According to these results, it is seen that the Twitter score (TS) approach created in equation 1 has an improving effect on the accuracy rate for each algorithm. In addition, the data were divided into 1-7-14 and 28-day parts, and the impact of the amount of data was wanted to be observed. The amount of data used in forecasts, such as cryptocurrency or dollar rate in the literature, is 4 weeks (28 days). Many of the results we obtained were higher in 4-week data.

In order to compare the method applied in this article with similar studies in the literature, a brief summary of the studies in the literature is given in Table 10. At the point when this table is analyzed, it is seen that the applied MM-LSTM structure has achieved results that can rival the LSTM-based approaches.

## 5. DISCUSSION

Various problems were encountered in the study of this article. First of all, the Twitter API used to collect Twitter data, which forms the main frame of the article, has a data limitation. Due to these limitations, various problems were encountered in accessing historical Twitter data. Despite these limitations, approximately 5 million tweets were

analyzed. Another problem is the filtering of tweets shared by bot users. The tweets shared by bot users, which are used to be among the prominent hashtags on Twitter, are effective. Although Twitter is seen as a knowledge bank, it can also turn into a social media network that can cause manipulation with the shares of these bot accounts. Although various approaches are used to detect bot user accounts in this study, some bot accounts got rid of these filters, and some real users were stuck with these filters. For example, the most important of these filters is that the ratio of the number of followers to the number of people followed is close to zero. Since some bot accounts have been active for a long time, this rate has moved away from zero. Apart from this, since some real users share without caring about the number of followers, the ratio of the number of followers to the number of people followed is close to zero.

There are some problems with the filter for accounts in these two groups. Apart from these problems, users sometimes use more than one hashtag while sharing a tweet. Therefore, there are some overlapping tweets in the obtained dataset. The most important of the deficiencies in the studies in the literature is a weighting according to the effect of tweets. Not all tweets shared by users have the same effect. Factors such as the number of people following the user, the number of likes, and the number of retweets determine the interaction. Using these factors, a score was generated for each tweet. One-word tweets shared by users with high followers can be scored with this method. However, even if these tweets have a very high impact factor, they do not have enough words for sentiment analysis. In addition, it will not be possible to conduct sentiment analysis and use the weight value in Eq.1 from tweets (only links, hashtags, etc.) consisting of the parts cleaned in the pre-processing steps in Table 3.

**Table 9.** Performance Metrics Results of MM-LSTM with Twitter Score Data (RMSE Results)

Data	1 Day Data	3 Days Data	7 Days Data	14 Days Data	28 Days Data
BTC	7.253	21.803	18.625	9.322	<b>3.401</b>
ETH	6.406	18.211	12.376	6.601	<b>2.729</b>
ADA	3.782	12.384	9.107	4.598	<b>1.902</b>
XRP	2.625	10.206	6.294	2.713	<b>1.726</b>

**Table 10.** Performance metrics results of Twitter score data (RMSE results)

Data	ARIMA	Support Vector Regressor	Decision Tree Regressor	Random Forest Regressor	Linear Regressor	Logistic Regressor	Gaussian Process Regressor	Proposed Method MM-LSTM
28-Days Data - Prediction Results Without Using Twitter Score Data								
BTC	117.529	19.305	16.263	16.329	27.264	21.407	22.345	13.352
ETH	88.762	16.347	13.229	13.283	14.645	15.346	15.963	12.412
ADA	62.904	10.029	8.156	8.297	9.803	8.206	9.056	5.456
XRP	24.203	4.971	4.294	4.362	4.614	3.742	4.391	4.634
28-Days Data - Prediction Results With Using Twitter Score Data								
BTC	43.646	13.275	10.857	11.016	18.291	15.386	14.051	<b>3.401</b>
ETH	24.016	8.701	7.216	7.615	15.204	10.056	9.108	<b>2.729</b>
ADA	12.052	5.104	3.729	4.026	9.381	6.319	5.827	<b>1.902</b>
XRP	7.102	1.916	1.895	2.004	3.519	2.542	2.168	<b>1.726</b>

**Table 11.** Relative comparison for cryptocurrency value prediction

Objective	Methodology	Forecast Duration	Results
A study has been made on selecting the inputs in the LSTM structure. [62]	LSTM & AR	71 Days	RMSE: 247.33
A study has been made about the effect of the parameters used in estimating the Bitcoin value in deep learning methods. [63]	CNN, LSTM, GRU	1&3 Months	Gold Price: CNN RMSE: 201.34 LSTM RMSE: 151.67 GRU RMSE: 32.98 Twitter: LSTM RMSE: 32.98
ANN and LSTM method were used to find out how the price dynamics of cryptocurrencies changed in various time intervals. [64]	ANN, LSTM	1, 3, 5, 7, 14 Days	Min-MSE: ~2 Max-MSE: ~66
The performances of ARIMA, LSTM and GRU methods in time series forecasting are compared using only the opening values of cryptocurrencies. [65]	ARIMA, LSTM, GRU	492 Days	ARIMA RMSE: 302.53 LSTM RMSE: 603.68 GRU RMSE: 381.34
The performances of forecasting the price of different cryptocurrencies with the LSTM method were compared. [66]	LSTM	1, 10, 20, 30 Days	1 Day RMSE: 53.30 10 Days RMSE: 67.99 20 Days RMSE: 91.41 30 Days RMSE: 45.71
Proposed Method	ARIMA, LSTM, MM-LSTM	28 Days (4 Weeks)	Twitter Score and MM-LSTM: BTC RMSE: <b>3.401</b> ETH RMSE: <b>2.729</b> ADA RMSE: <b>1.902</b> XRP RMSE: <b>1.726</b>

Different amounts of data are used in the literature. Therefore, in this study, first of all, the methods used in the literature were used and it was determined that the most suitable model was MM-LSTM. Table 10 shows the results of different methods. Since these methods are not supported by Twitter data, they estimate with rather high errors. It has been determined that the best model is LSTM. The high volatility of cryptocurrencies negatively affects the success of machine learning methods and methods such as ARIMA. In the literature, it was seen that higher results were obtained in the estimations made using 4-week data. In order to test the accuracy of this, the performance of the MM-LSTM algorithm supported by the Twitter score was tested with 1-3-7-14 and 28-day data. The highest performances obtained are shown in Table 9. Data diversity can be increased by

expanding the data collected in four weeks. But here, Twitter's service policy comes into play as a limiting effect. Twitter allows the analysis of 500,000 tweets for hobbyists, and 5 million tweets for academic research users, provided that they prove they are academic staff. In addition, there are not enough tweets about altcoins other than Ethereum, XRP and Cardano. Therefore, no agenda can affect people. Thus, the proposed approach may not be appropriate for cryptocurrencies other than these altcoins. The number of data for 4 weeks (28 days) is approaching 5 million. Therefore, the number of days is limited to 4 weeks. According to these results, the highest performance was obtained using 28 days (4 weeks) of data. Forecast using 1-day data has the second-best accuracy. Since there is less speculation about XRP, the prediction accuracy seems to be

relatively high. These results show us that social media data such as Twitter can cause speculation. However, the estimation performance has been considerably improved thanks to the data created with the scoring system developed in this study.

While performing the sentiment analysis, the words are examined one by one. For this reason, typos or unique jargons in tweets affect the scoring. In addition, the model's input is increased by using the MM-LSTM structure instead of the classical LSTM structure. In this way, Twitter scores of cryptocurrencies, opening, closing, highest and lowest values in that minute can be used as the input of the proposed method. The study's primary purpose is to observe the effect of the calculated weight value for each tweet shown in Eq.1 on the RMSE results. Therefore, in the study, it is checked whether the prediction accuracy increases rather than the selection of the regression algorithm. It is observed that our VADER architecture-based weight value generation approach makes improvements in each algorithm. Therefore, future studies can focus on algorithm selection. When the results in Table 10 are examined, it is seen that the ARIMA model, which economists generally use, is unsuitable for cryptocurrency prediction. In addition, the LSTM architecture is a deep learning architecture developed for predicting and classifying time series. The MM-LSTM architecture developed based on LSTM has a lower RMSE value than the machine learning algorithms frequently used in regression studies in Table 11. This is important for the hybrid model development part, which can be applied to us in future studies. In particular, it gives us a clue that the basic algorithm that should be used should be a deep learning algorithm. However, Gaussian Process Regressor and Logistic Regressor methods, which are machine learning methods, have very successful results.

## 6. CONCLUSION

In this article, the scoring of Twitter sentiment analysis is used as another additional data that increases the performance of methods performed on predicting cryptocurrencies. When the studies in the literature were checked, it was seen that the tweets shared on Twitter had the power to affect other users. With these shared tweets, successful results have been obtained for predicting stock prices, elections and cryptocurrencies. With the Granger causality analysis, it is seen that one of the reasons for the fluctuations in the cryptocurrency market is the effect of tweets shared on Twitter. This article argues that the amount of influence of shared tweets is also a quality. Since it has a data line that can access historical data, the LSTM structure has a high predictive ability in time series data. This forecasting performance can be enhanced with supporting input data. Tweets shared on Twitter were used as supporting data. However, there are tweets (1% - 17%) shared by bot accounts. This article successfully reduced the RMSE value, one of the performance measures frequently used in time series forecasting studies, with the analyzed Twitter score data. This improvement rate is different for each cryptocurrency. Estimation was also made with the ARIMA method, the most widely used method of classical economics. The RMSE performances of these three different methods were compared.

The method applied in this article is open to improvement. For example, improvements can be made to make predictions in real-time in future studies. Furthermore, Twitter is not the only social media network that people interact with. For this reason, the scoring system used in this article can be developed by using data from different social media networks.

**Conflict of Interest:** No conflict of interest was declared by the authors.

**Financial Disclosure:** The authors declared that this study has received no financial support.

## REFERENCES


- [1] S. Nakamoto, Bitcoin: A peer-to-peer electronic cash system, *Decentralized Business Review*, 2008.
- [2] H. Wang, D. Can, A. Kazemzadeh, F. Bar and S. Narayanan, A System for Real-time Twitter Sentiment Analysis of 2012 U.S. Presidential Election Cycle, *Proceedings of the ACL 2012 System Demonstrations*, pp. 115-120, 2012.
- [3] D. R. Pant, P. Neupane, A. Poudel, A. K. Pokhrel and B. K. Lama, Recurrent neural network-based bitcoin price prediction by twitter sentiment analysis, 2018 IEEE 3<sup>rd</sup> International Conference on Computing, Communication and Security, Kathmandu, Nepal, (2018) 128-132.
- [4] J. Bollen, H. Mao and X. Zeng, Twitter mood predicts the stock market, *Journal of computational science*, (2011) 2.1: 1-8.
- [5] X. Li and C. A. Wang, The technology and economic determinants of cryptocurrency exchange rates: The case of Bitcoin, *Decision support systems*, (2017) 95: 49-60.
- [6] P. Ciaian, M. Rajcaniova and D. Kancs, The economics of Bitcoin price formation, *Applied Economics*, (2016) 48.19: 1799-1815.
- [7] D. G. Baur, K. Hong and A. D. Lee, Bitcoin: Medium of Exchange or Speculative Assets?, *Journal of International Financial Markets, Institutions and Money*, (2018) 54: 177-189.
- [8] A. H. Dyhrberg, Bitcoin, gold and the dollar—A GARCH volatility analysis, *Finance Research Letters*, (2016) 16: 85-92.
- [9] N. Gandal, Price manipulation in the Bitcoin ecosystem, *Journal of Monetary Economics*, (2018) 95: 86-96.
- [10] M. Baker and J. Wurgler, Investor sentiment and the cross-section of stock returns, *The journal of Finance*, (2006) 61.4: 1645-1680.
- [11] Y. Sovbetov, Factors influencing cryptocurrency prices: Evidence from bitcoin, Ethereum, dash, bitcoin, and monero, *Journal of Economics and Financial Analysis*, (2018) 2.2: 1-27.


- [12] O. Poyser, Exploring the dynamics of Bitcoin's price: a Bayesian structural time series approach, *Eurasian Economic Review*, (2019) 9.1: 29-60.
- [13] Z. H. Munim, M. H. Shakil and I. Alon, Next-day bitcoin price forecast, *Journal of Risk and Financial Management*, (2019) 12.2: 103.
- [14] M. Polasik, A. I. Piotrowska, T. P. Wisniewski, R. Kotkowski and G. Lightfoot, Price fluctuations and the use of bitcoin: An empirical inquiry, *International Journal of Electronic Commerce*, (2015) 20.1: 9-49.
- [15] T. Rao and S. Srivastava, Modeling movements in oil, gold, forex and market indices using search volume index and twitter sentiments, *Proceedings of the 5th annual ACM Web science conference, Paris, France*, (2013) 336-345.
- [16] V. Karalevicius, N. Degrande and J. De Weerd, Using sentiment analysis to predict interday Bitcoin price movements, *The Journal of Risk Finance*, (2018) 19.1: 56-75.
- [17] D. Yermack, Is bitcoin a real currency? An economic appraisal, In: *Handbook of digital currency*. Academic Press, London, (2015) 31-43.
- [18] G. P. Dwyer, The economics of Bitcoin and similar private digital currencies, *J Financ Stab*, (2015) 17:81-91.
- [19] A. Cheung, E. Roca, J. J. Su, (2015) Crypto-currency bubbles: an application of the Phillips-Shi-Yu (2013) methodology on Mt.Gox Bitcoin prices. *Appl Econ* 47(23):2348-2358
- [20] E. T. Cheah and J. Fry, Speculative bubbles in Bitcoin markets? An empirical investigation into the fundamental value of Bitcoin, *Econ Lett*, (2015) 130:32-36.
- [21] F. Wen, L. Xu, G. Ouyang and G. Kou, Retail investor attention and stock price crash risk: Evidence from China, *Int Rev Financ Anal*, (2019) 65:101376.
- [22] L. Kristoufek, BitCoin meets Google trends and wikipedia: quantifying the relationship between phenomena of the Internet era, *Sci Rep*, (2013) <https://doi.org/10.1038/srep03415>
- [23] L. Kristoufek, What are the main drivers of the bitcoin price? Evidence from wavelet coherence analysis, *PLoS ONE*, (2015) 10(4):e0123923.
- [24] T. Panagiotidis, T. Stengos and O. Vravosinos, On the determinants of bitcoin returns: a LASSO approach. *Finance Res Lett*, (2018) 27:235-240.
- [25] E. Bouri, P. Molnár, G. Azzi, D. Roubaud and L. I. Hagfors, On the hedge and safe haven properties of Bitcoin: Is it really more than a diversifier?, *Finance Res Lett*, (2017) 20:192-198.
- [26] Y. B. Kim, J. G. Kim, W. Kim, J. H. Im, T. H. Kim, S. J. Kang and C. H. Kim, Predicting fluctuations in cryptocurrency transactions based on user comments and replies, *PLoS ONE*, (2016) 11(8):e0161197.
- [27] R. C. Phillips and D. Gorse, Predicting cryptocurrency price bubbles using social media data and epidemic modelling, In: *2017 IEEE symposium series on computational intelligence (SSCI)*, (2017) <https://doi.org/10.1109/SSCI.2017.8280809>
- [28] C. Chen, L. Liu and N. Zhao, Fear sentiment, uncertainty, and bitcoin price dynamics: the case of COVID-19, *Emerg Mark Finance Trade*, (2020) 56(10):2298-2309.
- [29] S. Ji, J. Kim and H. Im, A comparative study of bitcoin price prediction using deep learning, *Mathematics*, (2019) 7(10):898.
- [30] T. A. Borges and R. F. Neves, Ensemble of machine learning algorithms for cryptocurrency investment with different data resampling methods, *Appl Soft Comput*, (2020) 90:106187.
- [31] I. Madan, S. Saluja and A. Zhao, Automated bitcoin trading via machine learning algorithms, (2015) <http://cs229.stanford.edu/proj2014/Isaac%20Madan,20>
- [32] K. Żbikowski, Application of machine learning algorithms for bitcoin automated trading, In: *Machine intelligence and big data in industry*. Springer, Cham, (2016) 161-168.
- [33] Z. Jiang and J. Liang, Cryptocurrency portfolio management with deep reinforcement learning, In: *2017 intelligent systems conference (intelliSys)*. IEEE, New York, (2017) 905-913.
- [34] H. Jang and J. Lee, An empirical study on modeling and prediction of Bitcoin prices with Bayesian neural networks based on blockchain information, *IEEE Access*, (2018) 6:5427-5437.
- [35] S. McNally, J. Roche and S. Caton, Predicting the price of Bitcoin using machine learning, In: *2018 26th Euromicro international conference on parallel, distributed and network-based processing (PDP)*, IEEE, New York, (2018) 339-343.
- [36] M. Nakano, A. Takahashi and S. Takahashi, Bitcoin technical trading with artificial neural network, *Phys A*, (2018) 510:587-609.
- [37] A. Vo and C. Yost-Bremm, A high-frequency algorithmic trading strategy for cryptocurrency, *J Comput Inf Syst*, (2018) <https://doi.org/10.1080/08874417.2018.1552090>
- [38] L. Alessandretti, A. ElBahrawy, L. M. Aiello and A. Baronchelli, Anticipating cryptocurrency prices using machine learning, *Complexity*, (2019) 2018:8983590.
- [39] G. S. Atsalakis, I. G. Atsalaki, F. Pasiouras and C. Zopounidis, Bitcoin price forecasting with neuro-fuzzy techniques, *Eur J Oper Res*, (2019) 276(2):770-780.
- [40] L. Catania, S. Grassi and F. Ravazzolo, Forecasting cryptocurrencies under model and parameter instability, *Int J Forecast*, (2019) 35(2):485-501.

- [41] J. B. Han, S. H. Kim, M. H. Jang and K. S. Ri, Using genetic algorithm and NARX neural network to forecast daily bitcoin price, *Comput Econ*, (2019) <https://doi.org/10.1007/s10614-019-09928-5>
- [42] S. Lahmiri and S. Bekiros, Cryptocurrency forecasting with deep learning chaotic neural networks, *Chaos Solitons Fractals*, (2019) 118:35–40.
- [43] D. C. Mallqui and R. A. Fernandes, Predicting the direction, maximum, minimum and closing prices of daily Bitcoin exchange rate using machine learning techniques, *Appl Soft Comput*, (2019) 75:596–606.
- [44] Z. Chen, C. Li and W. Sun, Bitcoin price prediction using machine learning: an approach to sample dimension engineering, *J Comput Appl Math*, (2020) 365:112395.
- [45] X. Sun, M. Liu and Z. Sima, A novel cryptocurrency price trend forecasting model based on LightGBM, *Finance Res Lett*, (2020) 32:101084.
- [46] C. WJ. Granger, Investigating causal relations by econometric models and cross-spectral methods, *Econometrica: journal of the Econometric Society*, (1969) 424-438.
- [47] L. Deng and D. Yu, Deep learning: methods and applications, *Foundations and trends in signal processing*, (2014) 7.3–4: 197-387.
- [48] M. Shafahi, L. Kempers and H. Afsarmanesh, Phishing through social bots on Twitter, In 2016 IEEE international conference on big data, (2016) 3703-3712). IEEE.
- [49] O. Varol, E. Ferrara, C. Davis, F. Menczer and A. Flammini, Online human-bot interactions: Detection, estimation, and characterization, In Proceedings of the international AAAI conference on web and social media, (2017) 11(1):280-289.
- [50] Z. Chu, S. Gianvecchio, H. Wang and S. Jajodia, Detecting automation of twitter accounts: Are you a human, bot, or cyborg?, *IEEE Transactions on dependable and secure computing*, (2012) 9(6):811-824.
- [51] Z. Gilani, E. Kochmar and J. Crowcroft, Classification of twitter accounts into automated agents and human users, In Proceedings of the 2017 IEEE/ACM international conference on advances in social networks analysis and mining, (2017) 489-496.
- [52] V. S. Subrahmanian, A. Azaria, S. Durst, V. Kagan, A. Galstyan, K. Lerman and F. Menczer, The DARPA Twitter bot challenge, *Computer*, (2016) 49(6):38-46.
- [53] N. Chavoshi, H. Hamooni and A. Mueen, Debot: Twitter bot detection via warped correlation, In *Icdm*, (2016) 817-822.
- [54] C. Cai, L. Li and D. Zengi, Behavior enhanced deep bot detection in social media, In 2017 IEEE International Conference on Intelligence and Security Informatics (ISI), (2017) 128-130, IEEE.
- [55] F. Morstatter, L. Wu, T. H. Nazer, K. M. Carley and H. Liu, A new approach to bot detection: striking the balance between precision and recall, In 2016 IEEE/ACM International Conference on Advances in Social Networks Analysis and Mining (ASONAM), (2016) 533-540, IEEE.
- [56] D. Ciregan, U. Meier and J. Schmidhuber, Multi-column deep neural networks for image classification, 2012 IEEE conference on computer vision and pattern recognition, USA, (2012) 3642-3649.
- [57] K. Fukushima and S. Miyake, Neocognitron: A self-organizing neural network model for a mechanism of visual pattern recognition, *Competition and cooperation in neural nets*, (1982) 267-285.
- [58] F. Balcı, Z. Oralhan, LSTM ile EEG Tabanlı Kimliklendirme Sistemi Tasarımı, *Avrupa Bilim ve Teknoloji Dergisi*, (2020) 135-141.
- [59] M. F. Stollenga, B. Wonmin, M. Liwicki and J. Schmidhuber, Parallel multi-dimensional LSTM, with application to fast biomedical volumetric image segmentation, *Advances in neural information processing systems*, (2015) 28: 2998-3006.
- [60] S. Song, H. Huang and T. Ruan, Abstractive text summarization using LSTM-CNN based deep learning, *Multimedia Tools and Applications*, (2019) 78.1: 857-875.
- [61] Y. Yin, X. Zheng, B. Hu, Y. Zhang and X. Cui, EEG emotion recognition using fusion model of graph convolutional neural networks and LSTM, *Applied Soft Computing*, (2021) 100: 106954.
- [62] C. Wu, C. Lu, Y. Ma and R. Lu, A new forecasting framework for bitcoin price with LSTM, 2018 IEEE International Conference on Data Mining Workshops (ICDMW), Singapore, (2018) 168-175.
- [63] A. Aggarwal, I. Gupta, N. Garg and A. Goel, Deep learning approach to determine the impact of socio economic factors on bitcoin price prediction, 2019 Twelfth International Conference on Contemporary Computing (IC3), Noida, India, (2019) 1-5.
- [64] W. Yiyang and Z. Yeze, Cryptocurrency price analysis with artificial intelligence, 2019 5th International Conference on Information Management (ICIM), Cambridge, UK, (2019) 97-101.
- [65] P. Yamak, L. Yujian and P. K. Gadosey, A comparison between arima, lstm, and gru for time series forecasting, 2nd International Conference on Algorithms, Computing and Artificial Intelligence, Sanya, China, (2019) 49-55.
- [66] W. Zhengyang, L. Xingzhou, R. Jinjin and K. Jiaqing, Prediction of cryptocurrency price dynamics with multiple machine learning techniques, 4th International Conference on Machine Learning Technologies, Nanchang, China, (2019) 15-19.

# Estimation of the Daily Production Levels of a Run-of-River Hydropower Plant using the Artificial Neural Network

\*<sup>1</sup>Hüseyin ALTINKAYA, <sup>2</sup>Mustafa YILMAZ

<sup>1</sup>Department of Electrical and Electronics Engineering, Karabük University, Karabük, Türkiye, [haltinkaya@karabuk.edu.tr](mailto:haltinkaya@karabuk.edu.tr) 

<sup>1</sup>Department of Electrical Engineering, Faculty of Technology, Karabük University, Karabük, Türkiye, [mustafayilmaz@karabuk.edu.tr](mailto:mustafayilmaz@karabuk.edu.tr) 

## Abstract

Renewable energy sources, as well as the studies being conducted regarding these energy sources, are becoming increasingly important for our world. In this manuscript, the daily energy production level of a small (15 MW) run-of-river hydropower plant (RRHPP) was estimated using the artificial neural network (ANN) model. In this context, the model utilized both meteorological data and HPP-related data. The input parameters of the artificial neural network included the daily total precipitation, daily mean temperature, daily mean water vapour pressure, daily mean relative humidity, and the daily mean river water elevation at the hydropower plant, while the only output parameter consisted of the total daily energy production. For the ANN, data from the four years between 2017 and 2020 were used for training purposes, while data from the first eight months of 2021 were used for testing purposes. Ten different ANN networks were tested. A comparison of the ANN data with the real data indicated that the model provided satisfying results. The minimum error rate was 0.13%, the maximum error rate was 9.13%, and the mean error rate was 3.13%. Furthermore, six different algorithms were compared with each other. It was observed that the best results were obtained from the Levenberg-Marquardt algorithm. This study demonstrated that the ANN can estimate the daily energy production of a run-of-river HPP with high accuracy and that this model can potentially contribute to studies investigating the potential of renewable energies.

**Keywords:** Artificial Neural Network; Run-of-River Hydropower Plant; Renewable Energy

## 1. INTRODUCTION

In our ever-growing and developing world, the need for energy is constantly increasing. Nowadays, electricity inarguably represents the most commonly used and indispensable form of energy. Electric energy can be produced from fossil fuel sources such as coal, oil, and natural gas, and renewable energy sources such as water, wind, and solar energy. As fossil fuels are limited in supply (with most forms of fossil fuels expected to be depleted in less than 100 years) and contribute to environmental pollution, environment-friendly alternative energy sources are becoming increasingly important. In both Turkey and around the world, fossil fuels have a significant share in electricity production as compared to renewable energy sources. According to the report on the share of different energy sources in world electricity production in 2020, the share of hydroelectric power plants is 16% [1].

Renewable energy sources have a considerably smaller share in electricity production than fossil fuels. In Turkey, natural gas is the energy source with the largest share in electricity production, while hydropower-based sources rank second.

Turkey is a natural gas and oil importing country; this renders the effective use of hydro sources in Turkey even more important. Another noteworthy point is that as of the end of 2021, HPPs with dams have a 23.3% share in total installed power capacity. However, their share in total electricity production is only 12.3%. On the other hand, run-of-river HPPs have an 8.2% share in installed power capacity, and a 4.6% share in electricity production [2,3]. Based on these data, it is possible to see that most dam and run-of-river HPPs in Turkey are operating below capacity. The production capacity of HPPs is directly related to the quantity of water. Therefore, meteorological parameters, such as the amount of precipitation, needs to be taken into account. These parameters are even more important for run-of-river HPPs, which lack dams and use water directly.

An evaluation of the literature shows that studies regarding run-of-river HPPs and dam HPPs generally focus on topics such as production capacity of reservoir [4-6]; climate change potential effects on the run-of-river plant [7]; water flow management [8]; estimating the water collection capacity and the water elevation of dams [9,10]; determining the type of turbines most suitable for run-of-river plants



[11,12]; determining the optimal sizing of run-of-river plants; assessing the costs of small HPP projects [13-15]; management of the HPP [16-18]; and controlling HPPs with expert systems [19-22].

This study is genuine in terms of estimating the daily production amount of the RRHPP based on meteorological data. In the literature, we encountered a single study which modelled a dam HPP based on meteorological data [23]. However, no studies were encountered that estimated the production levels of run-of-river HPPs by using meteorological data.

In this respect, this manuscript intends to bring a new perspective to current studies conducted on run-of-river HPPs. The paper is organized as described below.

Chapter 1 provides an introduction to the research topic and the main objectives of the study. In chapter 2, the working principle of RRHPP is explained in detail. Section 3 presents technical data and information related exclusively to RRHPP. Chapter 4 offers a brief overview of artificial neural networks (ANN), which are used in the study to estimate the daily electricity generation level of RRHPP. In section 5, the methodology for using ANN to estimate daily electricity generation is explained in detail, and the results are presented and analyzed through tables and graphs. Finally, in chapter 6, the conclusion is presented along with suggestions for future studies.

## 2. WORKING PRINCIPLE OF THE RUN-OF-RIVER PLANTS

Both run-of-river and dam HPPs operate depending on some energy conversion stages. Firstly, the potential energy in water is converted into kinetic energy. Then, the obtained kinetic energy is converted into mechanical energy, and

eventually, the mechanical energy is converted into electrical energy.

The process of electrical energy production in most of the run-of-river plants is conducted as follows: firstly, water from the river is transferred to a waterway by the use of a weir or a regulator, and then, it is carried into the forebay through the waterway. Using the penstocks, stagnant water collected in the forebay is transferred to a turbine, thus, causing blades of the turbine to turn along with a generator rotor which is connected to the turbine with a shaft. Accordingly, the conversion of potential energy stored in the water into kinetic energy is carried out by the penstock; the conversion of kinetic energy into mechanical energy is carried out by the turbines; and the conversion of mechanical energy into electrical energy is carried out by the generator. After amplifying the electrical energy obtained by the generator using transformers, it is fed to power transmission lines. The working principle of run-of-river plants is illustrated in the diagram shown in Figure 1.

There are several equipment and intermediate stages used in the electricity production process in HPPs. Not going into details of electricity production process, we will be providing information about the alternators, turbines and power control systems considered to be one of the most important elements.

The kinetic energy of the water falling from a higher level to a lower level through the penstocks is captured by the turbines and their blades convert the obtained kinetic energy into mechanical energy. Based on flow rate as well as the pressure of the water which will rotate the turbine in a plant, the turbine type to be used is selected. The rotating part in all turbines is known to be rotor, whereas the non-moving part is known to be spiral casing. Currently, there are three turbine types being used: Kaplan, Francis, and Pelton turbines.

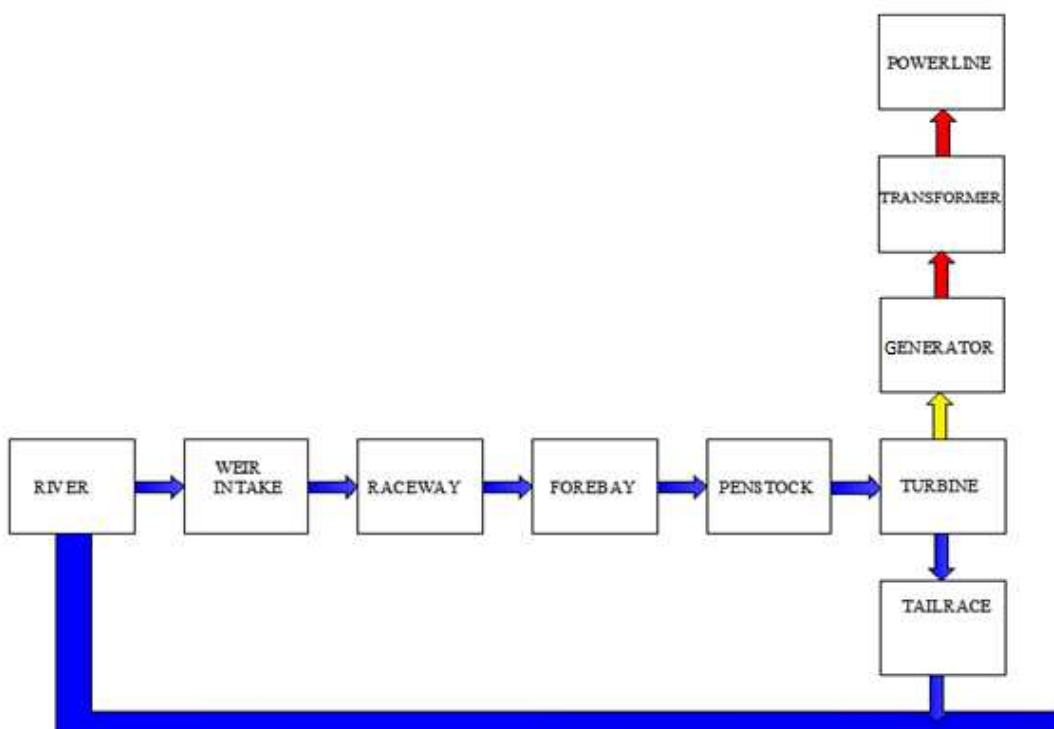


**Figure 1.** Energy production process in run-of-river plants.

According to the reference values, previously determined frequency and voltage values are continually adjusted and controlled. During the charging process of the generator, the turbine speed decreases. In order to bring the generator frequency and the turbine speed to the desired values, the water flow rate is increased by adjusting the valves and turbine wicket gates. Adjusting the valves and turbine wicket gates become necessary as the water flow rate is decreased in case of a decrease in generator charge. Nowadays, PID control systems are used to perform modern speed/rate controls. Such systems are being constantly monitored with the help of PLC-SCADA, and a database stores the relevant recorded data.

Depending on their power capacity, HPPs are classified as large capacity (> 50 MW), small capacity (10-50 MW), mini capacity (0.1-10 MW), and micro capacity (<0.1 MW) HPPs.

The formulae for potential energy and kinetic energy are given as follows:

$$E_p = m \cdot g \cdot h \quad (1)$$

$$E_k = \frac{1}{2} \cdot m \cdot v^2 \quad (2)$$

where  $E_p$  represents potential energy (J);  $m$  represents the object's mass (kg);  $g$  represents the gravitational acceleration ( $9.81 \text{ m/s}^2$ );  $h$  represents height (m);  $E_k$  represents kinetic energy (J); and  $v$  represents speed (m/s).

The electric power generated by HPPs is calculated using the formula below:

$$P = \rho \cdot g \cdot Q \cdot h \cdot \eta \quad (3)$$

where  $P$  represents electric power (W);  $\rho$  represents the specific density of water ( $1000 \text{ kg/m}^3$ );  $Q$  represents the flow rate of the water reaching the turbine ( $\text{m}^3/\text{s}$ );  $h$  represents the net falling height (elevation difference between the inlet and outlet, m); and  $\eta$  represents the system's efficiency (total efficiency comprising the

respective efficiencies of the penstock, turbine and generator, %). In case  $\rho$  is not used in the formula, the calculated power will be expressed in kW.

### 3. THE YALNIZCA RUN-OF-RIVER HYDROPOWER PLANT

Filyos Yalnızca Energy run-of-river HPP is situated in Karabük province located within Western Black Sea region of Turkey. The plant was inaugurated in September 2009 and has 15 MW installed power capacity consisting of three units with 5 MW power capacity each.

Yalnızca Hydropower Plant is situated on Filyos (Yenice) River and receives water from a 2 km waterway passing through a tunnel. The penstocks diameter of the plant is found to be 2.75 m, whereas the length is found to be 43 m. The water flow rate via the penstocks is observed to be  $25 \text{ m}^3$  per second. The water altitude of the forebay is 221.6 m, and the water altitude of tailwater channel is found to be 199.2 m. The falling height or the net head of the plant is observed to be 22 m, on average. The alternators or the generators have nominal power of 5100 kW. The voltage, nominal current, revolution speed and frequency are found to be 6.3 kV, 550 A, 333.3 rpm and 50 Hz, respectively. The afore-mentioned HPP uses Kaplan type horizontal-axis turbines. As seen in Figure 2, the fully automated plant is monitored and controlled with the SCADA system. Geographically, the HPP is located at 41.1633 parallel north and 32.5176 meridian east.

### 4. ARTIFICIAL NEURAL NETWORKS (ANN)

ANNs have been successfully used in learning, generalization, association, determining features classification and optimization. Using this technique, the information obtained from samples are recorded in the networks, and through the experiences, networks tend to give identical decisions in similar situations. Technically, the ANN, as its primary task, determines a set of outputs which meet input sets submitted to it [26].

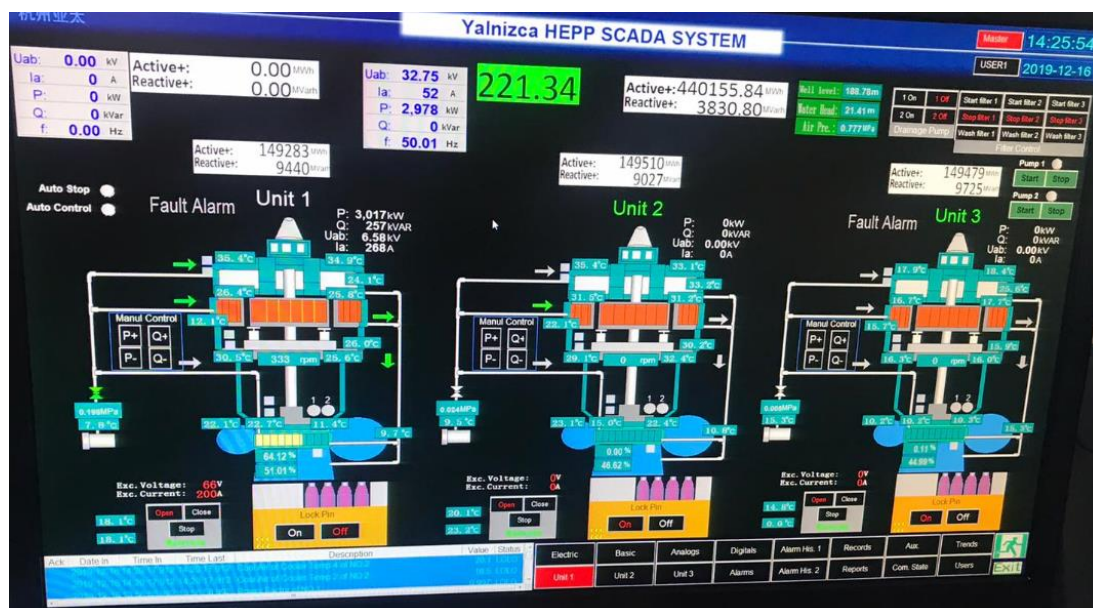
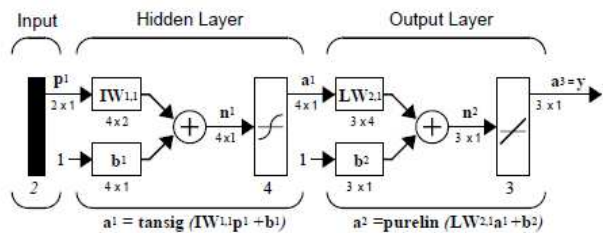


Figure 2. Yalnızca RRHPP SCADA main screen.

The ANN comprises artificial neural neurons. The neurons are assembled in three layers namely input, hidden and output layers as shown in Figure 3. Data obtained from the surrounding and fed into the input layer are transmitted to the hidden layer. Every process element in the layer consists of only one output, which is sent to each process elements present in the next layer. The information obtained from input layer is initially processed and then transferred to the next layer. In each layer, there might be more than one process and more than one hidden layer. The data received from hidden layers are processed in the output layer, and the generated outputs are sent to outside world by the network [24-26].



**Figure 3.** Architecture of feedforward network [27].

As our previous article [28] and the literature already provide a significant amount of information regarding the ANN, we will only provide the sigmoid function, RMSE,  $R^2$ , and MAPE equations in this context. Although there are several activation functions that can be considered, usually sigmoid function is used in the multilayer perceptron model. This function is expressed as follows [26].

$$f(x) = \frac{1}{1+e^{-x}} \quad (4)$$

The errors that occur during the training and test phases are referred to as root mean square errors (RMSE):

$$RMSE = \sqrt{\frac{\sum_{j=1}^n (t_j - o_j)^2}{n}} \quad (5)$$

Absolute fraction of variance ( $R^2$ ) and mean absolute percentage error (MAPE) are given as follows: [29-38]

$$R^2 = 1 - \left( \frac{\sum_{j=1}^n (t_j - o_j)^2}{\sum_{j=1}^n (t_j)^2} \right) \quad (6)$$

$$MAPE = \frac{1}{n} \sum_{j=1}^n \frac{|t_j - o_j|}{t_j} \times 100 \quad (7)$$

where,  $o$  is the output value,  $t$  is the target value and  $n$  is the pattern number.

The multilayer perceptron is part of the latent layered feed forward neural networks [39]. The performance of an ANN is significantly affected by the training algorithms, which optimize the biases and weights of the network based on the input-output pattern. Gradient methods and meta-heuristic methods are two commonly used types of training algorithms. Among the two, gradient methods are known to be effective, however, they have some drawbacks. One major disadvantage of gradient methods is that they can converge prematurely, and their performance depends

highly on the initial positions and parameters. Additionally, gradient methods can become trapped in local optima. Typically, gradient methods initiate the optimization process with a solution, thus guiding it to an optimum. Although the convergence is known to be fast, the solution's quality is greatly influenced by the initial solution. Mostly, the global optimum cannot be found using gradient method. Hence, meta-heuristic algorithms may be considered as alternative training algorithms. Different metaheuristic algorithms have been proposed by now. These algorithms can be listed as hybrid atom search optimization-simulated annealing (hASO-SA) [40], dragonfly [41], self-adaptive global best harmony search (SGHS) [42], cuckoo search algorithm [43], monarch butterfly optimization (IMBO) [44], particle swarm optimization and hybrid particle swarm optimization [45,46], grey wolf optimization [47, 48], dynamic group optimization [49], ant lion optimization [50], chimp optimization [51], grasshopper optimization [52], salp swarm [53], hybrid monarch butterfly and artificial bee colony optimization [54]. It is observed that the studies concentrate on the comparison of existing algorithms, improved algorithms or hybrid algorithms using various datasets.

## 5. ESTIMATION OF THE LEVEL OF ENERGY PRODUCTION WITH ANN

The Yalnızca run-of-river HPP is a plant located on the Yenice River, which is formed by the merging of the Araç and Soğanlı Streams. These two streams originate within the Kastamonu province, and then flow through the Karabük province. The Araç and Soğanlı Streams cover a distance of approximately 90 km before reaching the power plant. The watershed areas of the Araç and Soğanlı Streams are 2843 km<sup>2</sup> and 5102 km<sup>2</sup>, respectively. The amount of water reaching the plant is directly associated with the water flow of these two streams, which, in turn, are closely related to the meteorological parameters in the provinces of Karabük and Kastamonu.

For this reason, while developing the ANN architecture, the input parameters of the model included daily total precipitation, daily mean temperature, daily mean water vapour pressure and daily mean relative humidity for both provinces, as well as daily mean river water elevation at the hydropower plant. On the other hand, the only output parameter of the model consisted of the total daily energy production. Meteorological data were obtained from the Provincial Meteorology Directorates of Karabük and Kastamonu, which are branches of the General Directorate of Meteorology, while data regarding river water elevation and energy production levels of the power plant were obtained from the Yalnızca power plant. Water elevation data was transferred to the power plant by a GPRS system located 5 km upstream on the river. Data obtained during the period between 2017 and 2020 were used as training data for the ANN, while data from the first eight months of 2021 were used for testing purposes. Days during which technical issues at the power plant and/or meteorology centers caused data loss were not taken into consideration. Such days with data loss represented less than 3% of the total number of days.

The obtained data were normalized in such a way to have values ranging from 0.1 and 0.9. The formula used for normalization is given as follows:

$$V_N = 0.8 \times \left( \frac{V - V_{min}}{V_{max} - V_{min}} \right) + 0.1 \tag{8}$$

Where;  $V_N$  is the normalized value,  $V_{min}$  is the minimum value,  $V$  is the original value, and  $V_{max}$  is the maximum value. To determine the original value obtained from the normalized value, the formula used is given as follows:

$$V = \frac{V_N(V_{max} - V_{min}) - 0.1V_{max} + 0.9V_{min}}{0.8} \tag{9}$$

Tables 1 and 2 provide examples of non-normalized and normalized data sets.

**Table 1.** A sample of non-normalized dataset in Jan 2020.

Date	Krb DTP (mm)	Krb DMT (°C)	Krb DMWVP (hpa)	Krb DMRH (%)	Kst DTP (mm)	Kst DMT (°C)	Kst DMWVP (hpa)	Kst DMRH (%)	DMRWE (cm)	Prod (MWh)
1	0.2	4.2	7.5	92	0	3.4	7.4	97.6	57.46	33.25
2	0.8	2.6	6.3	88.6	0.4	1	5.7	88	64.29	25.53
3	0	1.2	5.6	86	0	0.3	5.5	89.5	65.46	36.50
4	0	1.3	5.8	89.3	0	0	5.7	93.6	67.71	41.58
5	1.4	2.3	6.5	93.9	0.3	2.1	5.8	85.9	64.5	38.17
6	0	0.8	6	96.5	0	-0.6	5.6	95.5	69.54	42.15
7	5.7	2.5	7	98.5	0.1	2.1	6.8	98.4	69.12	42.38
8	3.8	4.1	7.9	96.5	3.3	2.9	7.2	99	65.83	36.36
9	1.8	1.3	5.7	86.5	2	0.7	5.7	90	68.29	40.46
10	0	1.4	5.4	81.8	0	-1.1	5.1	90.5	69.12	41.14

**Table 2.** A sample of normalized dataset in May 2020

Date	Krb DTP (mm)	Krb DMT (°C)	Krb DMWVP (hpa)	Krb DMRH (%)	Kst DTP (mm)	Kst DMT (°C)	Kst DMWVP (hpa)	Kst DMRH (%)	DMRWE (cm)	Prod (MWh)
1	0.1049	0.1000	0.2810	0.1000	0.1196	0.1024	0.1147	0.1000	0.1073	0.1881
2	0.7232	0.6370	0.5994	0.6083	0.6370	0.6326	0.6238	0.6348	0.6083	0.6525
3	0.4629	0.6155	0.5041	0.4835	0.5536	0.5330	0.5206	0.5619	0.5948	0.5660
4	0.2695	0.5496	0.5735	0.4316	0.5283	0.5207	0.4805	0.5396	0.6388	0.4680
5	0.1000	0.3433	0.4023	0.1000	0.1737	0.1000	0.1479	0.1000	0.1000	0.1000
6	0.6811	0.6347	0.5800	0.6368	0.6305	0.6095	0.6179	0.6326	0.6474	0.6811
7	0.5889	0.7123	0.5444	0.5296	0.5938	0.5938	0.5790	0.5938	0.6037	0.6086
8	0.4938	0.7523	0.6538	0.5185	0.6169	0.6662	0.6169	0.6046	0.5677	0.5062
9	0.2059	0.2039	0.2137	0.2196	0.2118	0.2098	0.2176	0.2176	0.2216	0.2294
10	0.2466	0.2279	0.2567	0.2735	0.2546	0.2642	0.2651	0.2638	0.2725	0.2914

**Table 3.** The number of hidden layer(s) and neurons of the networks

Networks	Hidden Layer(s) Number	Neurons Number in the First Hidden Layer	Neurons Number in the Second Hidden Layer
Network 1	1	10	-
Network 2	1	15	-
Network 3	1	20	-
Network 4	1	25	-
Network 5	1	30	-
Network 6	2	13	5
Network 7	2	21	3
Network 8	2	15	4
Network 9	2	16	2
Network 10	2	30	3

In the study, the daily total precipitation was coded as DTP, the daily mean temperature as DMT, the daily mean water vapour pressure as DMWVP, the daily mean relative humidity as DMRH, and the daily mean river water elevation as DMRWE. Krb was used as the abbreviation for Karabük, and Kst was used as the abbreviation for Kastamonu.

The network type was chosen as feed-forward backpropagation. Among different algorithms as well as intermediate layers, the best results were observed to be obtained from the algorithm known as Levenberg-Marquardt (LM) having two hidden layers. The transfer functions selected were Tansig (Tan-sigmoid transfer function), Purelin (linear transfer function) and Logsig (Log-sigmoid transfer function), and using these three transfer functions, similar results were obtained. The ANN was trained using MATLAB software.

There is no agreed rule in literature for determining the hidden layer and neuron numbers in these layers. However, researchers have proposed some approaches regarding the determination of these afore-mentioned numbers of hidden layers and neurons [55-59].

The ten networks which have different hidden layers and/or neurons were tested. First network had one hidden layer with 10 neurons; the second had one hidden layer with 15 neurons; the third had one hidden layer with 20 neurons; the fourth had one hidden layer with 25 neurons; the fifth had one hidden layer with 30 neurons; the sixth network comprised two hidden layers having 13 neurons and 5 neurons in the first and in the second layer, respectively; the seventh network comprised two hidden layers having 21 neurons and 3 neurons in the first and in the second layer, respectively; the eighth network comprised two hidden layers having 15 neurons and 4 neurons in the first and in the second layer, respectively; the ninth network comprised two hidden layers having 16 neurons and 2 neurons in the first and in the second layer, respectively; the tenth network comprised two hidden layers having 30 neurons and 3 neurons in the first and in the second layer, respectively. The number of hidden layers and neurons of the networks are shown in Table 3.

Results obtained from the networks with one hidden layer were close to each other, while results from the networks with two hidden layers were quite different from each other. Statistical values of the ten networks are presented in Table 5.

Among the artificial neural networks trained using varying architectures, the ANN architectures which provided the best, the second-best and the worst results and consisted of two hidden layers having 16 and 2 neurons in the first and in the second layer (the ninth network), respectively; two hidden layers with 13 neurons in the first layer and 5 neurons in the second layer (the sixth network); two hidden layers with 30 neurons in the first layer and 3 neurons in the second layer (the tenth network) were used, respectively. Architecture of the second-best and the best networks are illustrated in Figures 4 and 5.

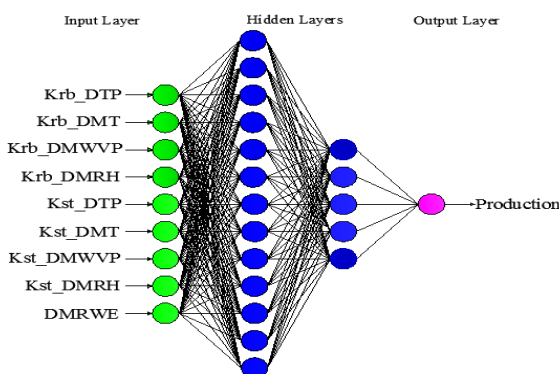


Figure 4. Architecture of the second-best ANN.

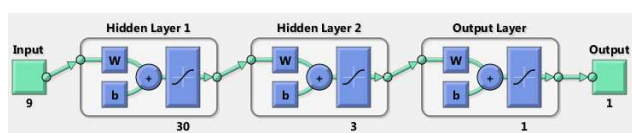


Figure 5. View of the best ANN in Matlab.

The common practice while training multi-layer networks using MATLAB environment is to initially split the data into three subsets as follows. The first subset used in order to compute the gradient as well as to update the network biases and weights, is the training set. The second subset is known to be the validation set. During the training process, the validation set error, which normally decreases in the initial phase of the training, is monitored. However, the validation set error starts increasing when the data are overfitted by the network. The network biases and weights are recorded at the minimum value of validation set error. While training the networks, test set error is not used. The test set error is used merely to compare different models [24]. Figure 6 shows the best (tenth) neural network regression results. These regression results represent the best results from 30 different trials using different random initial weights in each trial.

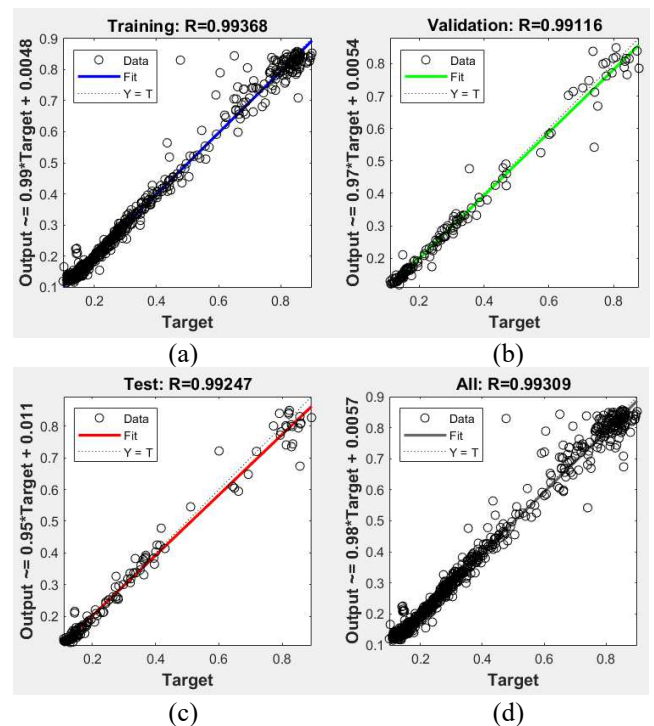


Figure 6. The tenth neural network regression results: (a) Training, (b) Validation, (c) Test, (d) All

For instance, Figures 7-9 are the graphical representations of the daily production levels in Jan, Apr and Aug 2021 respectively.

When actual values and ANN-derived values are compared, the min, max and mean error rates for daily production levels in January are found to be 0.41% (on Jan 4), 7.25% (on Jun 29), and 3.41%, respectively; for daily production levels in February, the min, max and mean error rates are 0.65% (on Feb 11), 5.41% (on Feb 20), and 3.25%, respectively; for daily production levels in March, the min, max and mean error rates are 0.61% (on Mar 13), 6.44% (on Mar 5), and 3.28%, respectively; for daily production levels in April, the min, max and mean error rates are 0.13% (on Apr 21), 5.12% (on Apr 28), and 3.48%, respectively; for daily production levels in May, the min, max and mean error rates are 1.03% (on May 7), 4.73% (on May 21), and 2.48%, respectively; for daily production levels in June, the min,

max and mean error rates are 1.22% (on Jun 3), 5.64% (on Jun 23), and 2.91%, respectively; for daily production levels in July, the min, max and mean error rates are 0.58% (on Jul 6), 9.13% (on Jul 20), and 4.90%, respectively; and for daily production levels in August, the min, max and mean error rates are determined as 0.18% (on Aug 7), 3.16% (on Aug 16), and 1.36%, respectively. The error rates of daily production levels for first eight months of 2021 are given in Table 4.

**Table 4.** Error rates by months

Months	Min (%)	Max (%)	Mean (%)
Jan	0.41	7.25	3.41
Feb	0.65	5.41	3.25
Mar	0.61	6.44	3.28
Apr	0.13	5.12	3.48
May	1.03	4.73	2.48
Jun	1.22	5.64	2.91
Jul	0.58	9.13	4.90
Aug	0.18	3.16	1.36

The statistical values for ANN output of each network for training and test data are shown in Table 5. When MAPE values are considered, the ninth network has the highest

MAPE values, while the tenth network has the lowest MAPE values. On the other hand, MAPE values of the networks with one hidden layer are usually close to each other and are observed to be in 5-6 range. When RMS,  $R^2$  and MAPE values are observed in Table 5, the tenth network is found to be the best network. It is clearly indicated in Table 5 that the accurate statistical values of the process represent the tenth ANN model, and these values may predict daily production levels of ANN.

In addition, five different algorithms apart from the LM algorithm are selected in the Matlab environment, and the training and test results were compared with the same data set. These algorithms are BFG (BFGS Quasi-Newton), RP (Resilient Backpropagation), SCG (Scaled Conjugate Gradient), CGB (Conjugate Gradient with Powell/Beale Restarts), GDX (Variable Learning Rate Backpropagation). The results obtained are given in Table 6. It is clearly seen that the best results among these algorithms are obtained from the LM algorithm. The results in the table show the best results from 30 different trials using different random initial weights in each trial. The statistical values for ANN output of each algorithm for training and test data are shown in Table 7.

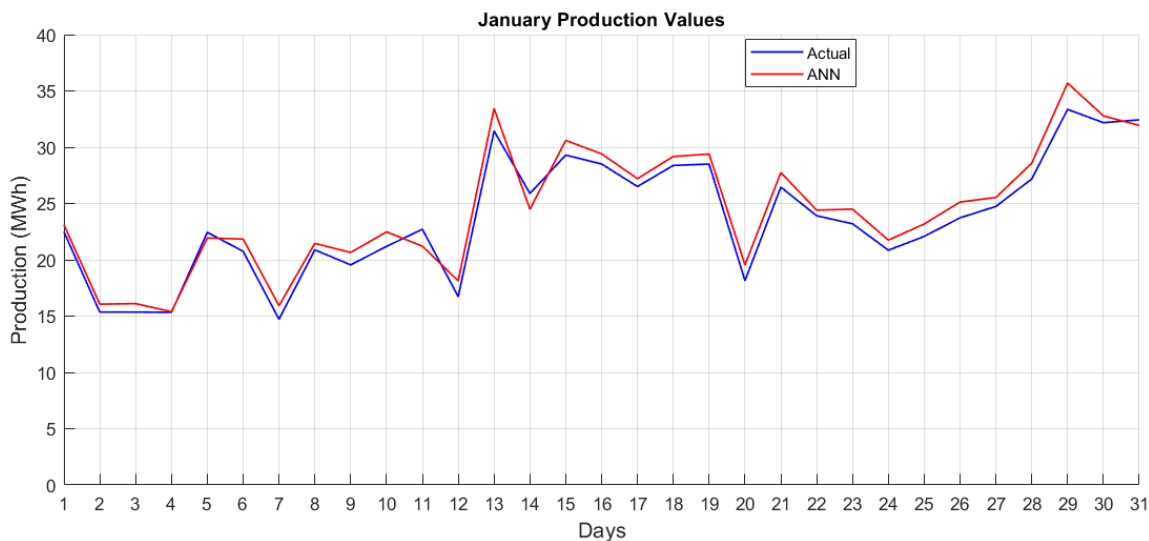


**Figure 7.** Daily production levels of Jan 2021.

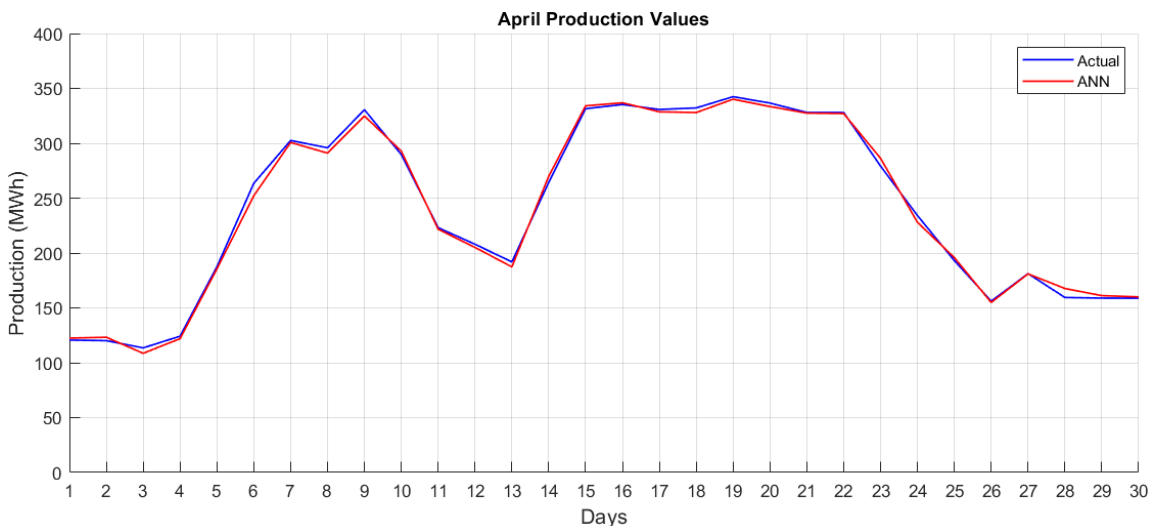


**Figure 8.** Daily production levels of Apr 2021.

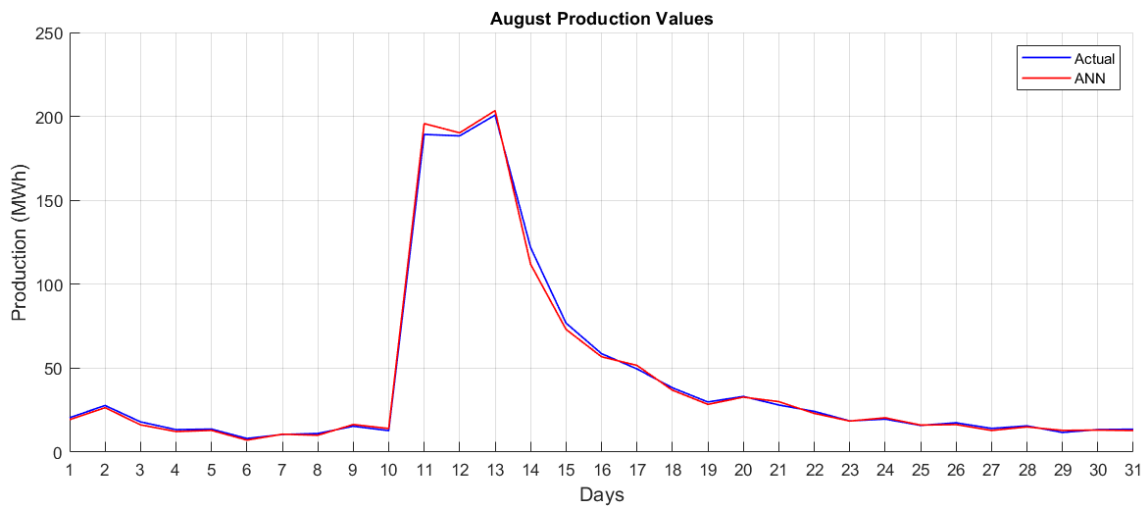


**Figure 9.** Daily production levels of Aug 2021.

**Table 5.** Statistical values of the networks

Networks	RMS training	R <sup>2</sup> training	MAPE training (%)	RMS test	R <sup>2</sup> test	MAPE test (%)
Network 1	0.030271	0.994243	5.781309	0.066026	0.987400	9.095667
Network 2	0.033671	0.992582	5.811954	0.049437	0.992936	5.891360
Network 3	0.036420	0.991917	6.659378	0.046493	0.993752	6.165773
Network 4	0.025555	0.995609	5.886150	0.053759	0.991647	6.117854
Network 5	0.032906	0.993328	5.644807	0.055559	0.991078	6.733954
Network 6	0.024699	0.996333	5.538720	0.050675	0.992578	6.432624
Network 7	0.035923	0.992301	6.317151	0.052849	0.991928	5.794437
Network 8	0.081876	0.960463	10.387326	0.070208	0.985754	6.404879
Network 9	0.137353	0.931282	20.617585	0.162874	0.915841	23.893251
Network 10	0.009243	0.999946	2.873423	0.011517	0.999546	3.217632

**Table 6.** The algorithms regression results

Algorithm	Training	Validation	Test	All
LM (Levenberg-Marquardt)	R=0.99368	R=0.99116	R=0.99247	R=0.99309
BFG (BFGS Quasi-Newton)	R=0.98662	R=0.95406	R=0.98945	R=0.98153
RP (Resilient Backpropagation)	R=0.98071	R=0.98521	R=0.98393	R=0.98211
SCG (Scaled Conjugate Gradient)	R=0.98154	R=0.99055	R=0.98066	R=0.98264
CGB (Conjugate Gradient with Powell/Beale Restarts)	R=0.98295	R=0.98473	R=0.9792	R=0.98258
GDX (Variable Learning Rate Backpropagation)	R=0.97293	R=0.98045	R=0.98026	R=0.97539

**Table 7.** Statistical values of the algorithms

Algorithm	RMS training	R <sup>2</sup> training	MAPE training (%)	RMS test	R <sup>2</sup> test	MAPE test (%)
LM	0.009243	0.999946	2.873423	0.011517	0.999546	3.217632
BFG	0.008271	0.999453	3.689555	0.037236	0.992544	3.811289
RP	0.008036	0.999168	3.745125	0.037384	0.992436	3.853741
SCG	0.008145	0.999237	3.692573	0.038136	0.992158	3.872589
CGB	0.008243	0.999316	3.686782	0.038265	0.991768	3.886723
GDX	0.007736	0.998785	4.875891	0.038244	0.991835	3.885692

## 6. CONCLUSION

This study employed Artificial Neural Network (ANN) to estimate the daily production level of a run-of-river HPP based on meteorological data. A comparison of the ANN and the real data indicated that the model provides fairly satisfying results. The minimum error rate was 0.24%, the

maximum error rate was 14.83%, and the mean error rate was 4.15%. The days with the highest error rates were observed for several days after very high daily total precipitation values occurred in Karabük and/or Kastamonu. We believe that these high precipitation days in these provinces were associated with highly variable quantities of water (and water flow), which in turn led to

significant variability in the production levels of power plant.

We hope that the estimation of the daily energy production of a run-of-river hydropower plant based on meteorological data will bring a new approach and perspective. It was observed that ANNs can be successfully implemented in the modelling of complex and non-linear systems. Most hydropower plants are facilities with considerably high initial setup costs. Thus, in countries such as Turkey that make significant investments in run-of-river hydropower plants, the ANN approach could contribute to the conduct of the effective feasibility studies before investment decisions, and also to correct decision-making processes that minimize the loss of time and funds.

In future studies, meta-heuristic algorithms will be used in the training of artificial neural networks. The data will be analyzed with different techniques. Also, we plan to develop a new ANN model that will allow for the estimation of a power plant's efficiency and increase the efficiency of turbines. In this context, we are also planning to develop an on-line hybrid system that will operate in integration with the PID control system. In addition, we will consider performing similar modelling activities with the ANN for run-of-river hydropower plants in other regions, so that we may compare data for different plants, and further test the reliability of the model.

#### ACKNOWLEDGMENT

We, as authors, would like to express our sincere gratitude to the Filyos Energy Yalnızca Power Plant, the General Directorate of Meteorology, the Provincial Meteorology Directorates of Karabük and Kastamonu, and the Karabük State Water Work (DSİ) for providing us with the necessary data and for their invaluable contributions and assistance.

**Author contributions:** Hüseyin Altinkaya: Concept, Literature review, Data collection, Software, Writing-Review & Editing, Analysis of results, Mustafa Yılmaz: Software, Writing-Review & Editing, Analysis of results, Investigation.

**Conflict of Interest:** No conflict of interest was declared by the authors.

**Financial Disclosure:** The authors declared that this study has received no financial support.

#### REFERENCES

- [1] WED, World Energy Data, <https://www.worldenergydata.org/world-electricity-generation/>
- [2] TEİAŞ, Turkish Electricity Transmission Corporation, <https://www.teias.gov.tr/tr-TR/aylik-elektrik-uretim-tuketim-raporlari>
- [3] TEİAŞ, Turkish Electricity Transmission Corporation, <https://www.teias.gov.tr/tr-TR/kurulu-guc-raporlari>
- [4] Fereidoon M., Najimi M., Khorasani, G., Simulation of hydropower systems operation using artificial neural network, *International Journal of Emerging Science and Engineering*, Volume-1, Issue-12, (2013) 86-89.
- [5] Yadav D., Sharma V., Artificial neural network based hydroelectric generation modelling. *International Journal of Applied Engineering Research*, Volume-1, No-3, (2010) 343-359.
- [6] Kuriqi A., Antonio NP., Ward AS., Garrote L., Flow regime aspects in determining environmental flows and maximising energy production at run-of-river hydropower plants, *Applied Energy*, 256 (2019) 113980.
- [7] Brito MA., Rodriguez DA., Junior VLC., Vianna JNS., The climate change potential effects on the run-of-river plant and the environmental and economic dimensions of sustainability, *Renewable and Sustainable Energy Reviews*, 147 (2021) 111238 1-21.
- [8] Gerini F., Vagnoni E., Cherkaoui R., Paolone M., Improving frequency containment reserve provision in run-of-river hydropower plants, *Sustainable Energy, Grids and Networks*, 28 (2021) 100538 1-12.
- [9] Csiki, S.J.C., & Rhoads B.L., Influence of four run-of-river dams on channel morphology sediment characteristics in Illinois, USA. *Geomorphology*, 206, (2014) 215–229.
- [10] Nwobi-Okoyea, C.C., & Igboanugob, A.C., (2013). Predicting water levels at Kainji dam using artificial neural network. *Nigerian Journal of Technology*, 32, 129-136.
- [11] Sharma, H., Singh, J., Run off river plant: Status and prospects, *International Journal of Innovative Technology and Exploring Engineering*, Volume-3, Issue-2, (2013) 210-213.
- [12] Özdemir MS., Dalcı A., Ocak C., Run of river Hydroelectric Power Plants and Turbine-Generators Used in These Power Plants, *Müh. Bil. Ve Araş. Dergisi* 2(2) (2020) 69-75.
- [13] Anagnostopoulos, J.S., Papantonis D.E., Optimal sizing of a run-of-river small hydropower plant, *Energy Conversion and Management*, 48, (2007) 2663–2670.
- [14] Mishra, S., Singal, S.K. & Khatod D.K., Optimal installation of small hydropower plant—A review, *Renewable and Sustainable Energy Reviews*, 15, (2011) 3862-3869.
- [15] Singal, S.K., Saini, R.P., Raghuvanshi C.S., Analysis for cost estimation of low head run-of-river small hydropower schemes, *Energy for Sustainable Development*, 14, (2010) 117-126.
- [16] Ardizzon, G., Cavazzini, G. & Pavesi, G., A new generation of small hydro and pumped-hydro power plants: Advances and future challenges, *Renewable and Sustainable Energy Reviews*, 31, (2014) 746-761.



- [17] Kumar, D. & Katoch, S.S., Sustainability indicators for run of the river (RoR) hydropower projects in hydro rich regions of India, *Renewable and Sustainable Energy Reviews*, 35, (2014) 101-108.
- [18] Molina J.M., Isasi, P., Berlanga, A. & Sanchis A., Hydroelectric power plant management relying on neural networks and expert system integration, *Engineering Applications of Artificial Intelligence*, 13, (2000) 357-369.
- [19] Dumur, D., Libaux A. & Boucher, P., Robust control for a Basse-Isere run-of-river cascaded hydro-electric plants. *Proceedings of the 2001 IEEE International Conference on Control Applications* September 5-7, Mexico City, Mexico, (2001). 1083-1088.
- [20] Kishor, N., Nonlinear predictive control to track deviated power of an identified NNARX model of a hydro plant, *Expert Systems with Applications*, 35 (2008)1741–1751.
- [21] Pérez-Díaz, J.I., Fraile-Ardanuy J., Neural networks for optimal operation of a run-of-river adjustable speed hydro power plant with axial-flow propeller turbine, *16th Mediterranean Conference on Control and Automation* Congress Centre, Ajaccio, France, 25-27 June, (2008) 309-314
- [22] Salhi, I., Doubabi, S., Essounbouli, N. & Hamzaoui, A., Frequency regulation for large load variations on micro-hydro power plants with real-time implementation. *International Journal of Electrical Power & Energy Systems*, 60 (2014) 6-13.
- [23] İnallı, K., Işık, E., Dağtekin, İ., The prediction of efficiency and production parameters in Karakaya hpp using the artificial neural network. *Dicle University Engineering Faculty Journal*, 5 (2014) 59-68.
- [24] Beale, M. H., Hagan, M. T., & Demuth, H. B. (2013). *Neural network toolbox user's guide*. MathWorks, Technical Support.
- [25] Nabiye V.V. (2005). *Artificial Intelligence*. Seckin publishing.
- [26] Öztemel E. (2003). *Artificial Neural Networks*. Seckin publishing.
- [27] <https://www.mathworks.com/help/deeplearning/ug/multilayer-neural-network-architecture.html>
- [28] Altinkaya, H., Orak İ.M. & Esen İ., Artificial neural network application for modeling the rail rolling process, *Expert Systems with Applications*, 41 (2014) 7135–7146.
- [29] Canakci, M., Ozsezen, A.N., Arcaklioglu, E., & Erdil, A. Prediction of performance and exhaust emissions of a diesel engine fuelled with biodiesel produced from waste frying palm oil, *Expert Systems with Applications*, 36 (2009) 9268-9280.
- [30] Koca, A., Oztop, H.F., Varol, Y., & Koca, G.O., Estimation of solar radiation using artificial neural networks with different input parameters for Mediterranean region of Anatolia in Turkey, *Expert Systems with Applications*, 38 (2011) 8756-8762.
- [31] Ozgoren, M., Bilgili, M., & Sahin, B., Estimation of global solar radiation using ANN over Turkey. *Expert Systems with Applications*, 39 (2012) 5043-5051.
- [32] Ekinci F., YSA ve ANFIS Tekniklerine Dayalı Enerji Tüketim Tahmin Yöntemlerinin Karşılaştırılması, *Düzce Üniversitesi Bilim ve Teknoloji Dergisi*, 7 (2019) 1029-1044.
- [33] Gündoğdu A., Çelikel R., ANN-Based MPPT Algorithm for Photovoltaic Systems, *Turkish Journal of Science & Technology* 15(2), (2020)101-110.
- [34] Kocaarslan İ., Akcay M.T., Akgündoğdu A., Tiryaki H., Comparison of ANN and ANFIS Methods for the Voltage-Drop Prediction on an Electric Railway Line, *Electrica* (2018); 18(1): 26-35.
- [35] Işık H., Şeker M., Yapay Sinir Ağı (YSA) Kullanarak Farklı Kaynaklardan Türkiye’de Elektrik Enerjisi Üretim Potansiyelinin Tahmini, *Journal of Computer Science*. (2021) pp. 304-311, <http://doi.org/10.53070/bbd.991039>
- [36] Uzlu E., Estimates of hydroelectric energy generation in Turkey with Jaya algorithm-optimized artificial neural networks, *GU J Sci, Part C*, 9(3): 446-462 (2021).
- [37] Mustafa Şeker. Yapay Sinir Ağı (YSA) Kullanılarak Meteorolojik Verilere Dayalı Solar Radyasyon Tahmini, *DEÜ FMD* 23(69), 923-935, (2021).
- [38] İlaboya, I.R and Igbinedion O. E. Performance of Multiple Linear Regression (MLR) and Artificial Neural Network (ANN) for the Prediction of Monthly Maximum Rainfall in Benin City, Nigeria, *International Journal of Engineering Science and Application*, Vol. 3, No. 1, (2019).
- [39] Haykin, S.: *Neural Networks: A Comprehensive Foundation*. Prentice Hall PTR, Upper Saddle River (1999).
- [40] Eker, E., Kayri, M., Ekinci, S., İzci, D., A New Fusion of ASO with SA Algorithm and Its Applications to MLP Training and DC Motor Speed Control, *Arabian Journal for Science and Engineering*, 46, (2021) 3889–3911.
- [41] Gülcü, Ş., Training of the feed forward artificial neural networks using dragonfly algorithm, *Applied Soft Computing*, *Applied Soft Computing*, 124, (2022) 109023.
- [42] Kulluk, S., Ozbakir, L., Baykasoglu, A., Training neural networks with harmony search algorithms for classification problems, *Eng. Appl. Artif. Intell.* 25 (2012) 11–19.
- [43] Valian, E., Mohanna, S., Tavakoli, S., Improved cuckoo search algorithm for feedforward neural network training, *Int. J. Artif. Intell. Appl.* 2 (2011) 36–43.
- [44] Faris, H., Aljarah, I., Mirjalili, S., Improved monarch butterfly optimization for unconstrained global search and neural network training, *Appl. Intell.* 48 (2018) 445–464.

- [45] Erdoğan, F., Gülcü, S., Training of artificial neural networks using meta heuristic algorithms, in: The International Aluminium-Themed Engineering and Natural Sciences Conference (IATENS19), Konya, Turkey, (2019), 124–128.
- [46] Xu, J., Yan, F., Hybrid Nelder–Mead algorithm and dragonfly algorithm for function optimization and the training of a multilayer perceptron. *Arab. J. Sci. Eng.* 44, (2019) 3473–3487.
- [47] Mirjalili, S., How effective is the grey wolf optimizer in training multi-layer perceptrons, *Appl. Intell.* 43 (2015) 150–161.
- [48] Zhang, X., Wang, X., Chen, H., Wang, D., Fu, Z., Improved GWO for large-scale function optimization and MLP optimization in cancer identification. *Neural Comput. Appl.* 32, (2020) 1305–1325.
- [49] Tang, R., Fong, S., Deb, S., Vasilakos, A.V., Millham, R.C., Dynamic group optimisation algorithm for training feed-forward neural networks, *Neurocomputing* 314 (2018) 1–19.
- [50] Heidari, A.A.; Faris, H.; Mirjalili, S.; Aljarah, I.; Mafarja, M.: Ant lion optimizer: theory, literature review, and application in multi-layer perceptron neural networks. In: Mirjalili, S., Song Dong, J., Lewis, A. (eds.) *Studies in computational intelligence*, pp. 23–46. Springer International Publishing, Cham (2020).
- [51] Khishe, M.; Mosavi, M.R., Classification of underwater acoustical dataset using neural network trained by Chimp Optimization Algorithm. *Appl. Acoust.* 157, (2020) 107005.
- [52] Heidari, A.A., Faris, H., Aljarah, I., Mirjalili, S., An efficient hybrid multilayer perceptron neural network with grasshopper optimization. *Soft. Comput.* 23, (2019) 7941–7958.
- [53] Khishe, M., Mohammadi, H., Passive sonar target classification using multi-layer perceptron trained by salp swarm algorithm. *Ocean Eng.* 181, (2019) 98–108.
- [54] Ghanem, W.A.H.M., Jantan, A., Training a neural network for cyberattack classification applications using hybridization of an artificial bee colony and monarch butterfly optimization. *Neural Process. Lett.* 51, (2020) 905–946.
- [55] Huang, G. B., Babri, H. A., Upper bounds on the number of hidden neurons in feed forward networks with arbitrary bounded nonlinear activation functions. *IEEE Transactions on Neural Networks*, 9(1) (1998).
- [56] Huang, S. C., Huang, Y. F. Bounds on the number of hidden neurons in multilayer perceptrons, *IEEE Transactions on Neural Networks*, 2(1), (1991) 47–55.
- [57] Karsoliya, S., Approximating number of hidden layer neurons in multiple hidden layer BPNN architecture. *International Journal of Engineering Trends and Technology*, 3(6), 714–717. ISSN: 2231-5381 (2012).
- [58] Khaw, J. F. C., Lim, B. S., & Lim, L. E. N., Optimal design of neural networks using the Taguchi method. *Neurocomputing*, 7 (1994) 225–245.
- [59] Panchal, G., Ganatra, A., Kosta, Y. P., & Panchal, D., Behaviour Analysis of Multilayer Perceptrons with Multiple Hidden Neurons and Hidden Layers, *International Journal of Computer Theory and Engineering* 3(2). ISSN: 1793-8201 (2011).

# A Proposed Approach to Evaluate Digital Business Model Selection for SuperApps using Interval Valued Spherical Fuzzy AHP

\*<sup>1</sup>Murat Levent DEMİRCAN

<sup>1</sup>Department of Industrial Engineering, Galatasaray University, İstanbul, Türkiye, [Idemircan@gsu.edu.tr](mailto:Idemircan@gsu.edu.tr) 

## Abstract

Various users have used SuperApps due to the rapid development of digital platforms. Due to their fast market entry by technical rivals and significant growth potential, SuperApps have become enterprises' preferred business method. SuperApps are the correct business, but senior managers must be careful when choosing which digital business models to employ. By classifying the digital management elements of SuperApps and comparing them to potential alternatives based on the preferences of eight digital leaders, we aimed to propose a method for choosing a suitable digital business model. Interval Valued Spherical Fuzzy Analytic Hierarchy Process (IVSF AHP) helps by giving decision-makers access to a broad range of preference domains. According to the rule, Spherical Fuzzy Sets adhere to the squared sum of the membership, non-membership, and hesitation degrees should fall within the range  $[0, 1]$ . Each element is distinct since it has an independent assignment within the same range. The IVSF AHP approach favored due to the complexity of the features of the digital business model and their transitional structure, is applied. The chosen digital business model may alter not only the managerial dynamics but also the revenue model of SuperApps depending on the sort of structural interaction of their platform network, according to the numerical application's results.

**Keywords:** Analytic Hierarchy Process; Digital Business Model; Multi-criteria Decision Making; Interval-valued Spherical Fuzzy Sets; SuperApps

## 1. INTRODUCTION

Business professionals have used the term SuperApp frequently for the last 5-6 years. WeChat, AliPay, GoJek, Grab, Momo, ZaloPay, and many other SuperApps, which the features and strategies they implement will be detailed in the following sections, are extensively discussed in the current digital economy world, thanks to the considerable volume of their massive digital network and the incredible size of their turnover and income. It attracted the attention of not only chronic enthusiasts, entrepreneurs, senior professionals, and investors but also an extensive user network.

The term SuperApp, which has been discussed frequently recently, and the problems it brings are among the problems faced by the current digital business ecosystem. In today's digital business ecosystem, where more than 90 percent of the projects and applications offered in digital economies fail, choosing and implementing an adequate business model in digital investments is of vital importance for managers and investors. This study evaluated how to choose a business model in SuperApp applications by a decision-maker team

consisting of a digital leader staff of eight people using IVSF AHP.

In the literature and methodology section of the study, the aim of the study and references related to the subject are given. The following part presents detailed information about what SuperApps are and their elements. In the next chapter, the features of SuperApps were evaluated, and the structure design that will form the basis for the AHP method was designed. In the methodology section, the steps of the IVSF AHP methodology are presented, and in the last part, the results are presented by discussion and wishes for future studies in the same field are mentioned.

## 2. LITERATURE

As it is known, the AHP methodology is created by weighing the importance of specific alternatives, certain criteria, and sub-criteria with respect to each other. The alternatives, criteria, and sub-criteria addressed in business problems where the classical AHP methodology is applied consist of more specific and defined options. This situation causes the problem of decision-makers needing to be able to decide certain levels of importance or be able to choose between

levels of importance. This problem is overcome with fuzzy decision-making. However, AHP methodologies that use fuzzy logic, which is used in the classical sense, are primarily focused on decision-makers' indecisiveness and the problem of being stuck between choices. Another critical problem encountered is the types and diversity of alternatives. Business problems trying to be solved; The results of traditional fuzzy logic AHP methods satisfy researchers and decision-makers when it consists of a problem such as choosing a warehouse location, an investment decision, a technical equipment purchase problem, etc.

However, the problems encountered in today's digital business world are far beyond the traditional and fundamental problems mentioned above, intangible, far from being defined and specific, and variable from the customer's point of view, such as experiences and expectations. The choice of business model to be preferred and to be implemented in digital platforms and SuperApp strategies creates an undefined set of alternatives based on user experience and expectations. To overcome this problem, it is the IVSF AHP method, uses fuzzy; however, it differs from traditional fuzzy AHP methods while evaluating the alternatives among each other in terms of criteria and sub-criteria, which creates a broader and more possible decision set.

A powerful idea for dealing with uncertainty is the spherical fuzzy sets (SFs), which present a larger region for making decisions and can detect hesitation. SFs, one of these recent advancements, help achieve this goal by providing decision-makers with a wide range of preference domains. The rule SFs follow states that the squared total of membership, non-membership and hesitation degrees should be within  $[0, 1]$ . At the same time, each element is independently assigned within the same range, which makes it unique.

SFs and IVSF AHP methods are vastly used in the fuzzy decision-making domain: To manage both types of problems concurrently, Szabolcs et al. introduce IVSF AHP, which considers hesitant scoring and uses mathematics to synthesize the views of various stakeholder groups. Interval-valued spherical fuzzy sets outperform the previous extensions because their membership function can be characterized in a wider range of ways. For adding decision makers' opinions about the membership functions of a fuzzy set into the model with an interval rather than a single point, interval-valued spherical fuzzy sets are used. Their paper uses the IVSF AHP approach to address the issue of public transportation [1].

Dogan's work proposes a fuzzy MDCM technique to handle the problem of process mining technology selection under uncertain and ambiguous settings. Their approach is based on spherical fuzzy AHP. Then, one-at-a-time sensitivity analysis is used to lessen the subjectivity of the decision-makers [2].

The AHP is expanded in Sharaf's study by SFs. SFs are employed in the suggested method to build the pairwise comparison matrices. A spherical fuzzy preference scale is therefore presented. To guarantee that a reasonable solution is obtained, the consistency of the spherical fuzzy pairwise

comparison matrices is then verified. To do this, the spherical fuzzy pairwise comparison matrices are transformed into crisp matrices, and the consistency is then checked using Saaty's eigenvalue approach [3].

Under the SFs' dimensions, Sangwan has presented a comprehensive framework that combines the AHP and TOPSIS methodologies. SF AHP is used to determine the criteria weights, which are subsequently utilized in IVSF TOPSIS to determine where the cloud service providers rank. The study considers six contradictory benchmarks set by three decision-makers and five possible solutions. A sensitivity analysis is also carried out to show how trustworthy the suggested method is [4].

Tepe's research focused on the issue of choosing an electric vehicle and included a case study with six criteria and 10 possibilities. The suggested decision model combines interval-valued spherical fuzzy sets with the AHP and ELECTRE methodologies. This study is interesting since it is the first to assess the performance of electric vehicles using IVSF, AHP, ELECTRE and make appropriate choices [5].

To assess farmers' perceptions of Agriculture 4.0 technologies and conduct a prioritization research based on how these technologies are perceived to be used, Erdogan suggests a decision-making framework. To address all qualitative and quantitative decision-making elements, multicriteria decision analysis is also used. Interval-valued spherical fuzzy numbers are utilized in the context of this study to best model the ambiguity in the process and to be able to reflect the uncertainty caused by the use of linguistic variables in the decision process [6].

The goal of Gundogdu and Kahraman is to extend the traditional AHP to the SF AHP approach and to demonstrate its application and validity through a case study involving the selection of a renewable energy source and a comparison of neutrosophic AHP and SF AHP [7].

Gundogdu and Kahraman utilized their proposed method to compare the service performances of various hospitals, and their study expands upon the IVSF AHP method. The approach has been created with this objective in mind, and it analyzes service quality in the healthcare sector using SERVQUAL dimensions [8].

Although there are various articles in the literature about SuperApps and their economic effects, this article on the choice of business model to be applied in SuperApps will be the first article in the literature.

### 3. SUPERAPPS AND THEIR FEATURES

This imposing and inaccessible SuperApp business model raises many questions, such as: Is the concept of "SuperApp" the strategy we should implement, or is the "SuperApp Strategy" a phenomenon that needs to be worked on at a focused level? To answer the questions that arise the definition of SuperApps and their features should be outlined.

SuperApps are digital platforms that offer services and applications to users at the same time, such as food ordering

and delivery, taxi calling, shared driving services, digital payment, sales of bus, plane, or movie tickets, car rental, courier services, insurance services, social networking applications, essential health services, repair, and concierge services. The two main results can be deducted from this definition: SuperApps have a broad user network and business relationships with business partners that provide their services. (If a SuperApp does not carry out all the business processes, it provides other services and applications by establishing cooperations, except for the services that almost all are experts and debut) [9]. The definition outlined above may be biased if we perceive SuperApps as Double-Sided Online Marketplaces. While the supplier cluster has the same characteristics in applications such as AppStore, OpenSea, AliBaba, Delivery Hero that work with the Double or Multi-Sided Online Marketplace business model, the suppliers differ in every aspect.

For example, in Delivery Hero, all suppliers are only food suppliers such as restaurants, buffets, and fast-food restaurants, while in SuperApps, those who are positioned on the supplier side, for instance, the characteristics of the car rental business partner and the movie theater operator business partner are entirely different from each other. For this reason, in marketplaces such as Delivery Hero, it is possible to reach a high number of business partners due to the specific and rapid operation of the management processes on the business partner's side, as well as creating a competitive environment between the marketplace business partners, additional income models can be created through business partners, or the service offered by the business partner below a certain quality. The relevant business partner can be quickly dismissed or sanctioned when detected. On the contrary, the situation is quite different with SuperApps. SuperApps select their business partners through a much more rigorous process (refer to Table 1).

As mentioned above, SuperApps have an extensive user network, and the business partner is expected to have the capacity and service management ability to serve this vast user network. If SuperApp includes limited-service management capability business partners serving at a local level (geographically) among the services it offers, in this case, it will make its users dissatisfied.

**Table 1.** Characteristics of the SuperApp partner candidate

	SuperApp	Online Marketplace
Size of Partner:	Corporate	SME
Management Process:	Common Agreement	Central
Partner Competition:	Non	Extensive and promoted
Human Resources:	Expertise	Best practice based
Number and Variety:	Less	Huge
Relevance and Weight:	Very	Negligible

Since SuperApps need to cooperate with large corporate structures as business partners, they face negotiating with the same business partner it deals with. In this case, it would be challenging to conclude the negotiation terms with satisfying results for both sides. However, if the size of the user network owned by SuperApp appeals to the business partner, the parties can conclude the terms by a successful agreement. If the business partner is already a sub-company of a large

"conglomerate," the possibility of forming a basis for a deal is very slim. In such a case, the candidate partner company would see that most of the user network they discuss intersects with the leading "conglomerate" company and would think such a business partnership would be meaningless [10]. The strategically suitable partner candidate for a SuperApp should have the following three characteristics:

- Specializing in a specific vertical business area,
- Not belonging to a large conglomerate or not having access to a network where it can coincide with the network of the relevant SuperApp,
- To provide active services in a wide area geographically (or preferably digitally).

Finding business partner candidate(s) with these background features may also vary for SuperApps depending on the economies in which they operate. To contribute to this perspective mentioned above, the effect of the economic size of the region or country where the SuperApp operates should be elaborated: As an example, we can compare the economies of the United States and Turkey from a valuation perspective: While the total value of NYSE and Nasdaq was approximately 45 Trillion USD in May 2022, we know that the total value of BIST in the same period was about 170 Billion USD. In large economies, SuperApps would have the opportunity to find business partner candidates or even candidates with ease. This opportunity would be slim in shallow economies. The economy in which SuperApp operates and wants to grow may also lead to changes in the SuperApp strategy. So, what should be the partner acquisition strategy of SuperApps operating in narrower and limited economies?

To overcome this deadlock, SuperApps should focus on early startups which provide services with digital business models in vertical markets. Early startups should deliberately be chosen because they still have time to reach their maturity period. Since an early startup has yet to prove itself, it will likely be overwhelmed by the demands flowing to it from the SuperApp. On the other hand, a startup that has already entered the maturity period would lead to "refine stage" in its internal organization (investors want to maximize the valuation for a possible exit). However, SuperApp would not want to feel the pressure of the "refine stage" strategies the mature startup applies regarding the service it will commission with the business partnership.

### 3.1. SuperApp Business Model Alignment

We also mentioned above that the type of startup that SuperApp should focus on should have a digital business model. This feature is essential in meeting the cascading demands of the SuperApp user base (and naturally, we are referring to the scaling of the partner). Otherwise, it would be an unnecessary managerial risk for SuperApp to bear the potential burden of the startup trying to open a playground for itself in the physical world. If we exemplify this situation with the mobility industry, the most suitable partner candidate for a SuperApp will not be a startup that puts its vehicle fleet into service with an innovative business model

but a startup that markets the uses of other people's vehicles without having a physical vehicle fleet [11].

Although this business partnership strategy is compatible, another critical point to be considered is what the investors of both parties expect from the future of the business partnership. Although the collaborative profile built continues in harmony, the SuperApp has a high probability of acquiring and completely swallowing the small startup in this symbiotic collaboration. For this reason, the fact that the parties clearly state their expectations of each other and the cooperation they established at the very beginning of the road eliminates many potential problems before they arise.

### 3.2. Network Interaction

The importance of the user base of SuperApp was mentioned earlier. The network is essential because the digital platform income arises from the interaction of the network's sides. Thus, it is concluded that in digital platforms and naturally in SuperApps, the network, and interaction are as meaningful as the network. What should be expressed about interaction is the characteristics of interactions. These interactions are not sourced from a single interaction type; instead, they form a set of interactions. It is recommended for SuperApps that the user harmoniously perceives these interactions and that they are "complementary" and "integrated" interactions as much as possible. To exemplify this situation, we can focus on shared driving experiences in the mobility sector: It is expected that the first steps in the journey of an application that started with a shared driving experience service to evolve into a SuperApp will be services that complement this initial point of departure—for example, enriching the application with examples from the mobility sector, such as selling plane, train and bus tickets. Suppose this example of the SuperApp candidate is to provide digital payment systems service in the following steps. In that case, it should do so in an integrated manner, integrate this digital payment service with the sales of plane, train, and bus tickets it offers, and let its users experience it.

The main reason for this binding is the value proposition we deliver to our user network at the beginning of our journey. However, it would be fitting to diversify the services after commissioning several complementary services. We can exemplify this case for an online food ordering service: Providing grocery, water orders, or similar cargo delivery services for users does not cause a jolt in the perceived value proposition from the customer's point of view. On the contrary, it would be welcomed positively. However, suppose an application that started by offering a food order service that suddenly tries to sell insurance to its users. In that case, it may seriously damage the perception of the user base. SuperApps can benefit from "industry similarity indexes" while deciding which service they will deploy next and being inspired by their experiences and opinions. It may also be a very realistic approach to conduct analytical studies that predict which additional services users can request after performing machine learning studies with the "big data" held by SuperApps that have reached maturity [12].

### 3.3. User Audience

Thanks to a single application, the comfort and pleasure of accessing dozens of services the user may need within seconds seem very attractive. SuperApps are expected to require fewer clicks than the "standalone app"; this provides serious comfort to the user. Thus, the user cannot download separate applications for daily activities. Users who can access many services together will keep the SuperApp application on their mobile phones and use it whenever needed.

However, another area that needs to be managed against SuperApps arises in this case. The essential feature of SuperApps, called "Process Excellence" or "flawless," is a concept with an inter-service binding for SuperApps. The fact that a SuperApp serving in, e.g., ten main business lines include nine perfectly functioning business lines and one service line that creates dissatisfaction, unfortunately, binds SuperApp itself due to all its other services. Entire customer processes should be digitally delivered to avoid this disadvantage.

### 3.4. Building the Strategy

Considering the factors mentioned earlier, it is easy to conclude that the SuperApp business model itself is not a strategy. Still, different methods should be implemented considering the relationships with business partners, the depth of the economy in which it operates, and the internal dynamics and maturity level of the SuperApp.

However, it is reasonable to divide the strategies that would be implemented for the SuperApp into phases according to the lifecycle phases of the platform and to establish different but mutually supportive strategies in each phase.

To elaborate on this issue, the life cycle of a SuperApp platform can be evaluated into three periods: development, growth, and maturity (see Figure 1).

The development period is an expansion or a network building for SuperApps. This period is where managers set out with the business line they know best, not potential collaborations, strengthen their value proposition, expand the user pool as much as possible, listen to the customer, and revise the value proposition frequently with feedback. During this period, managers are still determining if they have solved the user base's basic needs and problems. No platform sells products or services. The meta they sell needs to include the missing item of the user vast. The user needs meta, emotion, or experience they are missing. If managers cannot accurately define what they are selling, they will have difficulty establishing and reinforcing the value proposition, thus building collaborations in the later stages of the SuperApp. What are they selling? Time? Comfort? Accessibility?

DEVELOPMENT	GROWTH	MATURITY
Network Building Customer Feedback Focus on Main Expertise	Cooperation Building Contract Management Technical Integration Data Consolidation	Profitability Process Excellence Productivity Cost Cutting

**Figure 1.** Phases of a SuperApp digital platform

### 3.5. Aligning Value Proposition with Business Processes

It is just as essential to embed the value proposition into business processes as it is to identify it. The value proposition should be embedded in an almost corporate DNA format, not only in end-user processes but also in other internal organizational processes. Users interact with the platform not just as a customer but often as an employee, suppliers, or in different forms. The user who takes on these roles should also feel and experience the traces of the value proposition in business processes that touch these roles.

At this stage, the SuperApp candidate will risk significant losses (promotion and marketing budget, i.e., customer acquisition cost "CAC") to grow its network audience. Although this first period is the phase of reaching the user base, which may create a total loss at the bottom line, the application must generate revenue to prove itself. Interaction channels will naturally be established to generate income at this establishment stage. At this point, digital leaders should think and design the interaction channels multidimensionally, not one-dimensional.

### 3.6. Income and Loyalty-Building Interactions

As stated earlier, the interaction between the parties would create revenue. However, more than this one-dimensional interaction is needed. To build user loyalty, i.e., commitment, interaction should be established between and within the parties. Loyalty only depends on the user's interaction with himself and another user. In Table 2, examples of interactions that generate revenue and commitment by the platform in different business lines are listed.

SuperApp candidates, who have passed the infancy stages and reached the growth stage, will find new management areas such as contract management, integration, and data consolidation under the title of collaborations in this stage. Companies that will take part in the SuperApp will have the opportunity to reach a ready and wide network, as well as get rid of software development costs with a technological effort only at the level of integration with the relevant SuperApp and find the opportunity to focus on their own business and service excellence. Although this is a significant gain for the business partner, it also requires pre-calculation of what steps to take if the SuperApp it works with is in any problematic situation.

**Table 2.** Revenue and loyalty creating interactions based on different sectors

<b>Business Line</b>	<b>Revenue based Interactions</b>	<b>Loyalty based Interactions</b>
Career:	Placement	Training Tools, Search and Filter Options
Food Order:	Online Order	Gamification
Online Marketplace:	Product Order	Price Comparison, Comments and Scoring
Messaging:	Online Payment, Money Transfer	Messaging, Facetime Calls

As well as the value proposition of being a solution to the user problems raised earlier, SuperApps should also answer the following question: "Can the problems of collaborating partners be solved?". The response of business partners to finding solutions to each other's needs and problems is the first step in making progress in the "digital innovation" approach.

The platform, which has passed the growth phase, is now taking firm steps towards becoming a great SuperApp. Its partnership structure has changed with the investments and funds it has received until this maturity period. New faces from different backgrounds and experiences have taken their place in senior management. In parallel with the changing partnership structure, the partners will press the top management about the company's valuation to create new funding or different financial opportunities and expect profitability from the company. The SuperApp, which has entered the maturity period, should carry out efficiency studies to reduce costs in the face of these demands and produce diversified and customized offers according to customer segments with analytical studies based on big data.

The possibility of encountering the need to make some arrangements or revisions about the business partners may come to the fore, according to the functional harmony of the business partners in the SuperApp and the users' feedback. Since the harmony with business partners should become more automatic and robotic during the maturity period, it becomes necessary to focus on technical integration studies at this level, in other words, to create a "toolbox effect." The SuperApp may stop working with some partners during this period [13, 14].

At this point, an interesting question may arise: Although standalone apps such as YouTube, Instagram, and Google Maps have more users than SuperApps, why don't they turn their business model into a SuperApp business model and use this massive network in their hands? The answer to this question lies in the business model difference between standalone apps and SuperApps.

In SuperApps, the product is the value arising from interaction; In individual applications such as YouTube and Instagram, the product is the interaction itself.

## 4. DIGITAL PLATFORM FEATURES

### 4.1. SuperApp Platform Building Features

Successful digital platforms have similar features (refer to Figure 2). Almost all of them are built on the model of bringing together buyer and seller groups. Apart from this model, there are, of course, other business models that have been and can be successful. Skype and PayPal cases may be exemplified: Why do users utilize these apps? Would a user utilize Skype if there was no other user to talk to? If a user cannot find a business that accepts PayPal payments, is there any point in using it? The same is true for the online marketplace model, which set out to bring together a massive group of buyers and sellers. The challenge is not just about the number of networks targeted to be managed but also about their diversity. If a marketplace has only one product

line range, its usage frequency would drop dramatically. So, not only the amount but also the diversity of the network is significant [15].

What should managers pay attention to when setting up a digital platform? What should be the strategy that they need to construct and operate? A structural framework can be presented by asking five questions regarding the following digital platform strategy features:

#### 4.1.1. Network Building

The first of five basic questions: Can a user base be attracted to the digital platform? Entering a large user base on a digital platform and being able to register, log in, and use the platform is the first essential step to digitally scaling the platform. To create this, managers must meet the requirements of at least 1 of the 2 cases: The first one is that the business already has a ready-made user base that it addresses and can direct to the platform. The Google AdSense case may exemplify this situation: Google AdSense first opened its service to already existing Google AdWords users. The second case is the strategy of making available data that already exists. Zillow, a real estate search website, used this strategy. First, it collected all the data about the real estate sector, which it could obtain free of charge over the net or from government institutions, and converted this data mass into a format that users could search, list, and turn into a benefit with easy use. In short, it packaged the data it had beautifully and presented it to the users. New data was added to the existing data by the users' use of this data. Zillow presented this new data back to its users. This strategy consists of 3 steps: (1) Organize and pack the existing data and present it as usable, (2) import users and create new data or transaction data, and (3) sell users' data back. This strategy must have brought Google to mind immediately. Did Google follow the Zillow Steps too? In the simplest sense, Google uses web crawlers to reach servers worldwide and store publicly available data. It presents this data as usable with the sorting algorithm it has developed. This time, it sells the search and click data created by the users to those who want to advertise. In other words, the Zillow steps mentioned are also valid for Google. This strategy is used successfully by Google and many digital platforms, even if users do not feel it. This is the first point that online marketplaces use and start for their exit strategy [16, 17].

#### 4.1.2. Value Proposition Building

If managers cannot reach large user groups, they should answer the second question: Can they offer a value proposition if the platform cannot get mass users? This case may be exemplified by a historical videotape boom of the 1980s illustration: Video players are devices that allow users to watch tapes on television. Consider the time when video players and video cassettes first hit the market. Since there needed to be more video players, the movie industry naturally wanted to avoid printing and reproducing their films on videotape. Likewise, end users did not buy video players because they needed more movie cassettes to watch, like the Skype and PayPal example given earlier. Cinema producers do not produce tapes because there is not enough audience potential, and the potential audience does not buy

video players because there need to be more film tapes. This is a very frustrating paradox for video producers. Manufacturers circumvent this dilemma by introducing a new value proposition, adding a "record feature" to video players. End users quickly accepted this value proposition, and with the increasing use of video players, the motion picture industry acted immediately to print their films on videocassettes.

There are two basic strategies managers can implement to offer users value propositions: The first is to focus on a narrow niche market early. Yelp, the city guide that shares information and reviews about hundreds of thousands of places worldwide, was a website that listed only Far Eastern cuisine restaurants in a single city, San Francisco, and shared information and comments about products and user experiences. It took a little while for Yelp to add other towns and places to its portfolio, along with the potential for use.

The other strategy is to make the digital platform available to a limited social group or create an environment where users can socialize. For example, in the past, Zynga company gave an excellent example of a social game design by allowing users to help each other in Farmville. At the time Farmville was popular, the number of daily active users was 35 million unique users. The Clubhouse application, available only to iPhone users, also successfully implements this strategy at an early stage [18].

#### 4.1.3. Trust-based Relationship Building

Another question that should be answered is how to gain users' trust—creating champions for the best experience platform that managers would get on this topic and see the results quickly. Managers can think of the champions of the platform as their paid users. Whatever the platform's subject, promoting and advertising should be considered with well-known champions in the relevant industry, having a high number of followers on social media channels, and will drag other potential users behind them. Managers may have heard that most of the "Gamers" with a high number of followers on social media channels share their gaming experiences with their followers as part of a promotional campaign [19].

#### 1. Platform Building Features

1. Network Building
2. Value Proposition Building
3. Trust based Relationship Building
4. Revenue Model Building
5. Legacy Advantage

#### 2. Interaction Effect Features

1. Matchmaking Effect
2. Magnet Effect
3. Toolbox Effect

#### 3. Network Features

1. Network Effect
2. Cluster Effect
3. Risk of Disintermediation
4. Multi-homing
5. Multiple Network Access

**Figure 2.** Criteria and Sub-criteria



#### 4.1.4. Revenue Model Building

The fourth question is how and how much users should pay for the digital platform. The digital platform needs users, so managers must keep users in the network as much as possible. Users should be reassured about the financial aspect of the business model. Since products and services are in a digital environment, managers can apply many different and creative offers and pricing strategies that they cannot offer offline. They can try various models, such as:

- Pay-as-you-go
- Different payment options according to different feature packs
- Creation of user-specific offers

If the platform has a two-sided marketplace model, managers must offer these applications to the end user, the buyer, and the service provider, the seller. They should develop multiple pricing and revenue turnstile models that will put the network stakeholders at ease and stay on the digital platform, no matter which side they are on. For instance, Uber provides additional rewards to drivers who respond positively to five consecutive calls to avoid the "risk of multi-homing." Thus, it both increases the loyalty of the drivers and offers passengers more driver options when they enter the application [20].

#### 4.1.5. Legacy Advantage

The last question is more relevant for businesses that are already running but want to present their existing customers with a new digital model. One of the fastest and most robust ways to create users for the digital platform is to target current customers. As mentioned earlier, if investors still have an ongoing business, attracting their existing customers to the digital platform will be a fast and very low-cost solution.

#### 4.2. Interaction Characteristics

Today, business professionals can count the most important reasons why digital platforms come to the fore intensively as (1) the transformation of competition as the commercial competition starts to take place over platforms rather than products, and (2) the process of creating shared value that allows interaction to increase in line with end-user expectations [21]. With the shift of competition and customer interaction onto digital platforms, it has become crucial for businesses to recognize and understand the platform features. A digital platform builds on three primary features: (1) Cloud, (2) Mobile, and (3) Social.

The Cloud feature qualifies for the platform's time independence, while the Mobile feature qualifies for the platform's spatial autonomy. The third feature, the social feature, qualifies the human dimension of the platform, that is, the end user dimension, i.e., the customer. With the change of generations, the demand for end users to interact with digital systems is increasing. Responding to this demand on the business side requires a bold and highly motivated management approach as well as technological and organizational means and capacity. Because the

interaction with the end users takes place in social media and similar public environments, or even if this is not the case, this interaction may be made public by the end user positively or negatively. Business processes and policies that support this commercial courage and motivation can be put forward through strategic management. Strategic management also requires visionary leadership. It would not be wrong to describe the digital platforms that we give the basic features of as Cloud, Mobile, and Social as the "Globally Accessible Networks," that is, networks that can be accessed globally, with network management independent of time and location [22].

When digital platforms are defined as networks that can be accessed globally, three essential business elements sustain and feed this structure. These, respectively, are "Connection," which can be understood as the ease of integrating and transacting for users, "Attraction" which can be described as the attractiveness of including users and stakeholders; and "Flow," which can be defined as the convenience of the steps followed in creating interaction and shared value. Business professionals can support these three essential business elements with business elements only after they complete the processes of transforming the big data they have into information and then into managerial decisions. Before moving on to the business elements that support these business elements, the importance of Big Data should be emphasized. The journey of data science, which ends with the transformation of raw data into manageable data, the analysis and modeling of this data using suitable analysis methods, and the entry of the analyzed and modeled data into decision-making processes, is a business layer that is an inseparable part of the items mentioned earlier [23].

##### 4.2.1. The Matchmaking Effect

Managers can supplement the first item of work, "Connection," with Matchmaking, the "Matchmaker Effect." In the digital platform, managers will use data, which is the essential element for the correct matching of the parties. Set up advanced search options on the platform so parties can find their counterparty. Encourage the support of content with data and images.

##### 4.2.2. The Magnet Effect

Managers will use the Magnet, the "Magnet Effect," to support the "Attraction" element. For users to transact, shop, swap, and interact on the digital platform, they need to be able to find parties. Promotions, campaigns, and revenue models should be designed to attract every user group to interact.

##### 4.2.3. The Toolbox Effect

"Tool Effect" is the last element to support the "Flow" item. Managers can create a tool effect only with the technological opportunities and resources they will provide to users. To give an example of the tool effect created by digital platforms, we can cite the following examples: The code libraries provided by Apple to programmers, the hosting opportunities offered by YouTube to content creators, and the collaborative content creation feature provided by

Wikipedia to authors. If other global examples are observed, Amazon gives more importance to Toolbox when we look at the AWS platform. Digital platforms such as eBay and Airbnb have strengthened the influence elements of Matchmaker and Magnet to increase their network interaction. On the other hand, what can managers say about the Facebook platform if they evaluate it in terms of corporate users? Corporate companies that consider Facebook and its group companies as promotional channels are in constant promotional activity on Facebook. While doing this, they use the promotion management interfaces designed in detail. Looking at these comments, Facebook uses Magnet and Tool Effects quite well.

### 4.3. Network Features

In this section, we will focus on five basic platform features that are interesting and that managers should know when operating their digital platforms [24]. Managers who evaluate these five essential features may make pivotal moves to change their digital platform's business model. To better understand the effects and dynamics of these features on digital platforms, the Didi case may be an adequate example.

Didi is the world's largest ride-hailing service company, with 30 million daily transactions. It was established in 2012 in China. It has surpassed Uber in many ways. Didi acquired local competitor Kuaidi in 2015 and Uber China in 2016. In 2016, it reached a daily transaction volume of 25 million. In 2018, Meituan, in the online and offline food market industry, started its ride-sharing service in Shanghai. Meituan began by taking 8% commission from the drivers instead of Didi's 20% commission, and thus thousands of cars were registered to Meituan from Didi. Didi got into the food delivery business in response to Meituan. Companies lost money with mutual promotions and free campaigns, and their profitability decreased considerably. In March 2018, Alibaba's online map service, Gaode Map, started to provide a shared-driving service and accepted other players to its platform using the "opening the doors to others" scenario. On the other hand, Ctrip, an Online Travel Agency, an online tourism agency, also entered the same sector.

As can be seen, the technological possibilities available to digital players have seriously reduced the barriers to entry into different sectors [25]. Based on the size of the market, it is inevitable that the competition will shift from products to digital platforms, as pointed out earlier. So, what is Didi doing now in an intense digital competition environment? Didi continues its operations in China. It started operations in Russia in 2020. However, it still needed to eliminate Alibaba and other competitors from the Chinese market. In short, it continues its activities by expanding and losing a significant market share. So why does this occur? Why are digital platforms subject to such intense competition? What should a digital platform do when faced with such open competition? To answer these questions, it is necessary to understand the Network on which the digital platform runs.

The success factors of traditional and digital companies are different; for this reason, who manages the digital operational processes implemented on digital platforms and

who provides the product and service is crucial. Competitive advantage is not created at the product, service, or company level but during the interaction of the Network and the platform. The success of a platform, that is, the success of digital network management, is possible if a healthy, robust, and dominant ecosystem is established. The soundness of a digital platform means its scalability potential; its robustness means its profitability, and its dominance means its sustainability.

If we pay attention to the example of Didi, we see that it is much easier to scale the platform than to maintain it. Didi needs help becoming a market dominator due to the intense competition environment. Here are the five crucial digital network features to understand why such situations occur:

#### 4.3.1. Network Effect

The first feature is the Network Effect. The network effect brings many advantages to the digital platform; It includes existing users to get more users to the platform, and the growing user presence attracts suppliers; on the contrary, the increasing diversity with the number of suppliers attracts more users, the decrease in promotion, marketing, and sales costs with the content creation of the stakeholders on the platform, and the increased interaction with the shared value creation factor [26].

#### 4.3.2. Clustering Effect

The network's structure is the most significant factor in maintaining the platform's scale. The more types and features of the network structure in small sections, the more fragile and competitive the platform is. For instance, taxi drivers in Istanbul are looking for passengers in Istanbul. Likewise, the passengers need to look for cabs in Istanbul as well. A person who wants to go home after work in Istanbul does not call a taxi from Antalya. In this case, competing with an application like BiTaksi in İzmir, Ankara, or any other geography is straightforward, with the precondition of a definite commercial focus on the relevant region. In the example of Didi, for the same reason, Didi had to compete with dozens of digital players in different cities, despite being the first in the market due to the large geographical structure and large population of China. This effect is called the Clustering Effect. At this point, we can cite Airbnb next to the Didi case. How many ways can we cluster customers when we think about Airbnb? Or conversely, how many other groups can a customer divide the houses in the city he or she will be traveling to? In this case, Airbnb's network cluster is almost homogeneous, i.e., very similar. Therefore, emerging as a competitor to Airbnb requires global competitiveness. However, competing in a narrow area with platforms with a business model open to clustering effects like Didi is possible [27, 28].

#### 4.3.3. Risk of Disintermediation

Another network feature managers may encounter in digital platform management is the Risk of Disintermediation. This feature arises because the parties can continue their commercial relations and interactions without the platform's services after they find their counterpart using the digital

platform. Consider a platform that provides an "Armut" like service and meets users who want to receive assistance. If a user is satisfied with a cleaning worker, he or she met through such a digital platform, would he or she reach that person later on the same platform? Or does the same cleaner use the same platform again when he or she gets enough customers through the platform? Digital platforms with business models at risk of disintermediation can be likened to leaky buckets. Still, they continue to exist and grow due to the tremendous and continuous mutual demand between the network parties.

#### 4.3.4. Multi-Homing

The multi-homing vulnerability occurs when users are simultaneously on multiple competing platforms. To reduce the risk of multi-homing exposure, solutions such as target number of transactions, rewards for turnover, or loyalty systems can be implemented on the platform. Uber rewarding drivers who accept requests five times in a row can be an example. However, the prevention of this risk may vary from business to business. We can give campaign-based platform examples such as "Groupon" or "Şehir Fırsatı." Some of them had prevented their merchants from being on another platform, but customers started using more than one website in this case. In other words, even if multi-homing was blocked on one side of the network, it could occur on another platform [29, 30].

#### 4.3.5. Multiple Network Access Effect

The final network feature is the "multiple network access effect." AliBaba; provides access to different networks with its AliPay application. The strategy of reaching various networks lies behind the fact that digital ecosystems such as Amazon offer multiple services simultaneously [31, 32]. Recall the Didi case. Unfortunately, in the example of Didi, this can only be possible through purchases or differentiation of services.

Many digital platform features should be considered by managers when designing a SuperApp business model. Since these features are transitive both within and between each other, a bundle of strategies that are difficult to manage for managers in different fields and specialties occurs. To manage this complexity and variability, each of the senior executives from different fields, such as marketing, sales, information technologies, finance, and human resources, must evaluate the digital business model to be selected from their perspective. However, a decision that this senior executive team will make jointly, and a digital vision digital platform business model should be chosen. One of the most suitable methodologies for this decision-making process is the "Fuzzy AHP" methodology. "Fuzzy AHP," which enables decision makers to evaluate alternatives from different perspectives and look at the selection problem with a holistic approach, will be used to evaluate all these criteria and sub-criteria mentioned above. Spherical Fuzzy Sets (SFSs), which offer a wider preference domain to decision-makers, would be the right choice when using the fuzzy AHP method.

## 5. METHODOLOGY

### 5.1. Interval-Valued Spherical Fuzzy Sets (IVSFSs): Preliminaries

SFSs are used by decision makers to determine membership degrees within the ranges determined for criteria and sub-criteria. SFSs can have a maximum square sum of 1.0. Thus, decision makers' "hesitancy" can be easily identified in an SFS domain. For example, let the fuzzy numerical value of a verbal preference be (0.6, 0.4, 0.5). The sums are greater than 1, but the sum of the squares is less than 1. SFSs were developed by Gündoğdu and Kahraman [33, 7, 34, 35] based on Pythagorean Fuzzy Sets. The definition of SFSs is given as follows:

**Definition a.** In a universal set of  $U$ , a single-valued SFS  $A_G$  is described as,

$$\tilde{A}_G = \{u, (\mu_{\tilde{A}_G}(u), \nu_{\tilde{A}_G}(u), \pi_{\tilde{A}_G}(u)) | u \in U\} \quad (1)$$

where

$$\begin{aligned} \mu_{\tilde{A}_G}: U &\rightarrow [0,1], \\ \nu_{\tilde{A}_G}: U &\rightarrow [0,1], \\ \pi_{\tilde{A}_G}: U &\rightarrow [0,1], \\ 0 &\leq \mu_{\tilde{A}_G}^2(u) + \nu_{\tilde{A}_G}^2(u) + \pi_{\tilde{A}_G}^2(u) \leq 1 \quad \forall u \in U. \end{aligned}$$

For each  $u$ , the numbers  $\mu_{\tilde{A}_G}(u)$  is degree of membership and  $\nu_{\tilde{A}_G}(u)$  is non-membership. Finally,  $\pi_{\tilde{A}_G}(u)$  is the hesitancy of  $u$  to  $\tilde{A}_G$ .

Gundogdu and Kahraman [8] describe the arithmetic calculation of IVSFSs. They also present the formulas to defuzzify and aggregate IVSFSs.

**Definition b.** An IVSFS  $\tilde{A}_G$  of the universal set  $U$  is defined as in Eq. (2).

$$\tilde{A}_G = \left\{ u, \left( \begin{array}{l} [\mu_{\tilde{A}_G}^L(u), \mu_{\tilde{A}_G}^U(u)], \\ [\nu_{\tilde{A}_G}^L(u), \nu_{\tilde{A}_G}^U(u)], \\ [\pi_{\tilde{A}_G}^L(u), \pi_{\tilde{A}_G}^U(u)] \end{array} \right) | u \in U \right\} \quad (2)$$

where

$$\begin{aligned} 0 &\leq \mu_{\tilde{A}_G}^L(u) \leq \mu_{\tilde{A}_G}^U(u) \leq 1, \\ 0 &\leq \nu_{\tilde{A}_G}^L(u) \leq \nu_{\tilde{A}_G}^U(u) \leq 1, \\ 0 &\leq \left( \mu_{\tilde{A}_G}^U(u) \right)^2 + \left( \nu_{\tilde{A}_G}^U(u) \right)^2 + \left( \pi_{\tilde{A}_G}^U(u) \right)^2 \leq 1. \end{aligned}$$

For each  $u \in U$ ,  $\mu_{\tilde{A}_G}^U(u)$  is the upper degrees of membership and  $\nu_{\tilde{A}_G}^U(u)$  is non-membership. Finally,  $\pi_{\tilde{A}_G}^U(u)$  is the hesitancy of  $u$  to  $\tilde{A}_G$ . For an IVSFS  $\tilde{A}_G$ , an interval-valued spherical fuzzy number is defined as;

$$\langle [\mu_{\tilde{A}_G}^L(u), \mu_{\tilde{A}_G}^U(u)], [\nu_{\tilde{A}_G}^L(u), \nu_{\tilde{A}_G}^U(u)], [\pi_{\tilde{A}_G}^L(u), \pi_{\tilde{A}_G}^U(u)] \rangle$$

For convenience, the pair;

$$\langle [\mu_{\tilde{A}_G}^L(u), \mu_{\tilde{A}_G}^U(u)], [v_{\tilde{A}_G}^L(u), v_{\tilde{A}_G}^U(u)], [\pi_{\tilde{A}_G}^L(u), \pi_{\tilde{A}_G}^U(u)] \rangle$$

is denoted by

$$\tilde{\alpha} = \langle [a, b], [c, d], [e, f] \rangle$$

where

$$\begin{aligned} [a, b] &\subset [0, 1], \\ [c, d] &\subset [0, 1], \\ [e, f] &\subset [0, 1], \\ b^2 + d^2 + f^2 &\leq 1. \end{aligned}$$

## 5.2. Extension of Spherical Fuzzy AHP (SFAHP)

SFAHP comprises the phases below;

**Level 1.** First, we develop a 3-layer model for use within AHP. These model layers are alternatives, main criteria and sub-criteria, respectively.

**Table 3.** Linguistic expressions for SFSs [8]

Linguistic terms $\tilde{\alpha} = \langle [a, b], [c, d], [e, f] \rangle$	Score Index
Definitely Extreme Relevance (DER) ([0.85,0.95], [0.10,0.15], [0.05,0.15])	9
High Extreme Relevance (HER) ([0.75,0.85], [0.15,0.20], [0.15,0.20])	7
Extreme Relevance (EXR) ([0.65,0.75], [0.20,0.25], [0.20,0.25])	5
Slightly More Relevance (SMR) ([0.55,0.65], [0.25,0.30], [0.25,0.30])	3
Equally Relevance (ER) ([0.50,0.55], [0.45,0.55], [0.30,0.40])	1
Slightly Small Relevance (SSR) ([0.25,0.30], [0.55,0.65], [0.25,0.30])	1/3
Small Relevance (SR) ([0.20,0.25],[0.65,0.75], [0.20,0.25])	1/5
Very Small Relevance (VSR) ([0.15,0.20], [0.75,0.85], [0.15,0.20])	1/7
Definitely Small Relevance (DSR) ([0.10,0.15], [0.85,0.95], [0.05,0.15])	1/9

**Level 2.** In this step, we will use Table 3 to reduce the verbal preferences of decision makers to numerical expressions. We will use this measurement reference to compare criteria and sub-criteria pairs when evaluating alternatives.

**Level 3.** We are at the step where we will measure whether the decision makers' comparisons are consistent. For this we must ensure that the CR levels we will measure for each assessment are below 10%. If we do not reach the desired numbers of CR levels, we will revise the consistency of the evaluations of the decision makers.

For instance, the dual-cross comparison matrix

$$J = \begin{matrix} C_1 & ER & SSR & ER \\ C_2 & SMRI & ER & HER \\ C_3 & SR & VSR & ER \end{matrix}$$

is converted to

$$J = \begin{matrix} C_1 & 1 & 1/3 & 5 \\ C_2 & 3 & 1 & 7 \\ C_3 & 1/5 & 1/7 & 1 \end{matrix}$$

and the CR is figured as 0.047, meaning the dual-cross comparison matrix ensures consistency.

**Level 4.** The decision-maker's preferences are taken into account to understand the numeric relevance of IVSFSs. We will calculate weightings based on the Eq. (6) of IVSWAM.

$$IVSWAM_{\omega}(\tilde{\alpha}_1, \tilde{\alpha}_2, \dots, \tilde{\alpha}_k) = \omega_1 \cdot \tilde{\alpha}_1 \otimes \omega_2 \cdot \tilde{\alpha}_2 \otimes \dots \otimes \omega_k \cdot \tilde{\alpha}_k$$

where

$$w = 1/n \text{ (Eq. 6).}$$

**Level 5.** We build the structure of the created hierarchy to calculate the global weights. We calculate the score ranks for each level of the hierarchy based on the preference importance of the IVSFSs. We use the full and partial IVSFAHP methods, see Eqs. (3-6) and Eqs. (7, 8), respectively, and the weights of the criteria are defuzzified.

$$Score(\tilde{\omega}_j^G) = S(\tilde{\omega}_j^G) = \frac{a^2 + b^2 - c^2 - d^2 - (e/2)^2 - (f/2)^2}{2} + 1 \quad (3)$$

Eq. (4) normalizes the criteria weights:

$$\bar{\omega}_j^G = \frac{G(\tilde{\omega}_j^G)}{\sum_{j=1}^n G(\tilde{\omega}_j^G)} \quad (4)$$

Eq. (5) is used for weighting the decision matrix where  $\tilde{\alpha}_{G_{ij}} = \bar{\omega}_j^G \cdot \tilde{\alpha}_{G_i}$ ,

$$\tilde{\alpha}_{G_{ij}} = \left\{ \begin{aligned} &\left[ \left( (1 - (1 - \alpha_{G_i}^2)^{\bar{\omega}_j^G})^{\frac{1}{2}}, (1 - (1 - b_{G_i}^2)^{\bar{\omega}_j^G})^{\frac{1}{2}} \right), \right. \\ &\quad \left. [c_{G_i}^{\bar{\omega}_j^G}, d_{G_i}^{\bar{\omega}_j^G}] \right], \\ &\left[ \left( (1 - \alpha_{G_i}^2)^{\bar{\omega}_j^G} - (1 - \alpha_{G_i}^2 - e_{G_i}^2)^{\bar{\omega}_j^G} \right)^{\frac{1}{2}}, \right. \\ &\quad \left. \left[ \left( (1 - b_{G_i}^2)^{\bar{\omega}_j^G} - (1 - b_{G_i}^2 - f_{G_i}^2)^{\bar{\omega}_j^G} \right)^{1/2} \right] \right] \end{aligned} \right\} \quad (5)$$

Finally, the SFAHP scores are computed based on Eq. (7) fuzzy arithmetics for feasible alternatives to consider their preference relevancies. We can also use Eq. (8) to defuzzify the results as an other way of calculation.

**Level 6.** This is the level where the defuzzification of each digital model alternatives are computed.

**Level 7.** This final level of the methodology, where we sort the final weightings of alternatives.

$$IVSWAM_{\omega} = \left\{ \left[ (1 - \prod_{j=1}^k (1 - a_j^2)^{\omega_j})^{1/2}, (1 - \prod_{j=1}^k (1 - b_j^2)^{\omega_j})^{1/2} \right], [\prod_{j=1}^k c_j^{\omega_j}, \prod_{j=1}^k d_j^{\omega_j}], \left[ (\prod_{j=1}^k (1 - a_j^2)^{\omega_j} - \prod_{j=1}^k (1 - a_j^2 - e_j^2)^{\omega_j})^{1/2}, (\prod_{j=1}^k (1 - b_j^2)^{\omega_j} - \prod_{j=1}^k (1 - b_j^2 - f_j^2)^{\omega_j})^{1/2} \right] \right\} \quad (6)$$

$$\tilde{F} = \sum_{j=1}^n \tilde{\alpha}_{G_{ij}} = \tilde{\alpha}_{G_{i1}} \otimes \tilde{\alpha}_{G_{i2}} \dots \otimes \tilde{\alpha}_{G_{in}} \quad \forall i$$

$$i. e. \tilde{\alpha}_{G_{i1}} \otimes \tilde{\alpha}_{G_{i2}} = \left\{ \left[ \left( (a_{\tilde{\alpha}_{G_{i1}}}^2 + a_{\tilde{\alpha}_{G_{i2}}}^2 - (a_{\tilde{\alpha}_{G_{i1}}} a_{\tilde{\alpha}_{G_{i2}}})^2)^{\frac{1}{2}}, \left[ c_{\tilde{\alpha}_{G_{i1}}} c_2, d_{\tilde{\alpha}_{G_{i1}}} d_2 \right], \left( (b_{\tilde{\alpha}_{G_{i1}}}^2 + b_{\tilde{\alpha}_{G_{i2}}}^2 - (b_{\tilde{\alpha}_{G_{i1}}} b_{\tilde{\alpha}_{G_{i2}}})^2)^{\frac{1}{2}} \right) \right], \left[ \left( (1 - (a_{\tilde{\alpha}_{G_{i2}}}^2) (e_{\tilde{\alpha}_{G_{i1}}}^2) + (1 - (a_{\tilde{\alpha}_{G_{i1}}}^2) (e_{\tilde{\alpha}_{G_{i2}}}^2) - (e_{\tilde{\alpha}_{G_{i1}}} e_{\tilde{\alpha}_{G_{i2}}})^2)^{\frac{1}{2}} \right), \left[ \left( (1 - (b_{\tilde{\alpha}_{G_{i2}}}^2) (f_{\tilde{\alpha}_{G_{i1}}}^2) + (1 - (b_{\tilde{\alpha}_{G_{i1}}}^2) (f_{\tilde{\alpha}_{G_{i2}}}^2) - (f_{\tilde{\alpha}_{G_{i1}}} f_{\tilde{\alpha}_{G_{i2}}})^2)^{\frac{1}{2}} \right) \right] \right\} \quad (7)$$

$$\prod_{j=1}^n \tilde{\alpha}_{G_{ij}} = \tilde{\alpha}_{G_{i1}} \otimes \tilde{\alpha}_{G_{i2}} \dots \otimes \tilde{\alpha}_{G_{in}} \quad \forall i$$

$$i. e. \tilde{\alpha}_{G_{i1}} \otimes \tilde{\alpha}_{G_{i2}} = \left\{ \left[ a_{\tilde{\alpha}_{G_{i1}}} a_2, b_{\tilde{\alpha}_{G_{i1}}} b_2 \right], \left[ \left( (c_{\tilde{\alpha}_{G_{i1}}}^2 + c_{\tilde{\alpha}_{G_{i2}}}^2 - (c_{\tilde{\alpha}_{G_{i1}}} c_{\tilde{\alpha}_{G_{i2}}})^2)^{\frac{1}{2}}, \left[ \left( (1 - (c_{\tilde{\alpha}_{G_{i2}}}^2) (e_{\tilde{\alpha}_{G_{i1}}}^2) + (1 - (c_{\tilde{\alpha}_{G_{i1}}}^2) (e_{\tilde{\alpha}_{G_{i2}}}^2) - (e_{\tilde{\alpha}_{G_{i1}}} e_{\tilde{\alpha}_{G_{i2}}})^2)^{\frac{1}{2}} \right), \left[ \left( (1 - (d_{\tilde{\alpha}_{G_{i2}}}^2) (f_{\tilde{\alpha}_{G_{i1}}}^2) + (1 - (d_{\tilde{\alpha}_{G_{i1}}}^2) (f_{\tilde{\alpha}_{G_{i2}}}^2) - (f_{\tilde{\alpha}_{G_{i1}}} f_{\tilde{\alpha}_{G_{i2}}})^2)^{\frac{1}{2}} \right) \right] \right\} \quad (8)$$

## 6. CONSISTENCY, RESULTS AND CONCLUSION

In our digital application, eight senior managers in sales, marketing, information technologies, finance and human resources departments in different sectors were determined as decision makers. According to the digital business model criteria and sub-criteria listed above, each decision maker has evaluated the following SuperApp digital platform business models; (A) Digital Ecosystem, (B) Multi-Digital Platform, and (C) Service Provider Models.

A "consistency index" is also provided by the traditional AHP approach of Saaty to assess the consistency of a pairwise comparison matrix. The process is encapsulated for a pairwise comparison matrix, the consistency index (CI) and consistency ratio (CR) can be calculated as follows:

$$CI = \frac{(\lambda_{max} - n)}{(n-1)} \quad (9)$$

$$CR = CI / RI(n) \quad (10)$$

In a pairwise comparison matrix of size n,  $\lambda_{max}$  is the maximum eigenvalue, and RI(n) is a random index that depends on n. Random index values are 0.00 for n=1 and n=2, 0.58 for n=3, 0.90 for n=4, 1.12 for n=5, 1.24 for n=6,

1.32 for n=7, 1.41 for n=8, 1.45 for n=9 and 1.49 for n=10. Consistency Ratio (CR) should be less than 0.10 for each pairwise comparison to ensure the accuracy of the results.

**Table 4.** Overall pairwise comparison

	C <sub>1</sub>	C <sub>2</sub>	C <sub>3</sub>	$\tilde{w}_S$	$w_S$
C <sub>1</sub>	ER	SR	ER	[(0.91, 0.89), [0.77, 0.82], [0.87, 0.81]]	0.283
C <sub>2</sub>	EXR	ER	EXR	[(0.83, 0.76), [0.58, 0.63], [0.81, 0.72]]	0.433
C <sub>3</sub>	ER	SR	ER	[(0.91, 0.89), [0.77, 0.82], [0.87, 0.81]]	0.283

CR=0.077

**Table 5.** Dual-cross comparison of the main criteria: Platform Building

	C <sub>11</sub>	C <sub>12</sub>	C <sub>13</sub>	C <sub>14</sub>	$\tilde{w}_S$	$w_S$
C <sub>11</sub>	ER	HER	HER	HER	[(0.75,0.85],[0.17,0.23],[0.16,0.22]]	0.293
C <sub>12</sub>	ASR	ER	SR	SSR	[(0.42,0.49],[0.49,0.58],[0.22,0.30]]	0.167
C <sub>13</sub>	VSR	EXR	ER	ER	[(0.54,0.62],[0.36,0.44],[0.24,0.31]]	0.213
C <sub>14</sub>	VSR	SMR	ER	ER	[(0.55,0.64],[0.36,0.43],[0.24,0.31]]	0.217
C <sub>15</sub>	VSR	SR	SR	VSR	[(0.28,0.33],[0.64,0.74],[0.22,0.29]]	0.110

CR=0.067

**Table 6.** Dual-cross comparison of the main criteria: Interaction Effects

	C <sub>21</sub>	C <sub>22</sub>	C <sub>23</sub>	$\tilde{w}_S$	$w_S$
C <sub>21</sub>	ER	ER	SR	([0.43,0.48],[0.51,0.61],[0.28,0.37])	0.283
C <sub>22</sub>	ER	ER	SR	([0.43,0.48],[0.51,0.61],[0.28,0.37])	0.283
C <sub>23</sub>	EXR	EXR	ER	([0.61,0.70],[0.26,0.33],[0.23,0.30])	0.433

CR=0.027

**Table 7.** Dual-cross comparison of the main criteria: Network Features

	C <sub>31</sub>	C <sub>32</sub>	C <sub>33</sub>	C <sub>34</sub>	C <sub>35</sub>	$\tilde{w}_S$	$w_S$
C <sub>31</sub>	ER	SR	SSR	ER	HER	([0.51,0.59],[0.40,0.49],[0.24,0.32])	0.213
C <sub>32</sub>	EXR	ER	SMR	EXR	EXR	([0.61,0.70],[0.25,0.30],[0.23,0.29])	0.263
C <sub>33</sub>	SMR	SSR	ER	SMR	EXR	([0.53,0.62],[0.31,0.38],[0.25,0.31])	0.233
C <sub>34</sub>	ER	SR	SSR	ER	HER	([0.51,0.59],[0.40,0.49],[0.24,0.32])	0.213
C <sub>35</sub>	VSR	SR	SR	VSR	E	([0.16,0.20],[0.75,0.84],[0.16,0.20])	0.078

CR=0.015

**Table 8.** Dual-cross comparison of models for the criterion: C<sub>11</sub>

	A	B	C	$\tilde{w}_S$	$w_S$
A	ER	SMR	HER	([0.61,0.70],[0.25,0.31],[0.22,0.28])	0.429
B	SSR	ER	EXR	([0.50,0.58],[0.36,0.44],[0.24,0.31])	0.354
C	VSR	SR	ER	([0.32,0.37],[0.59,0.70],[0.23,0.31])	0.214

CR=0.055

**Table 9.** Dual-cross comparison of models for the criterion: C<sub>12</sub>

	A	B	C	$\tilde{w}_S$	$w_S$
A	ER	SMR	HER	([0.61,0.71],[0.27,0.33],[0.22,0.28])	0.429
B	SSR	ER	EXR	([0.50,0.60],[0.38,0.46],[0.26,0.33])	0.356
C	VSR	SR	ER	([0.32,0.37],[0.59,0.70],[0.23,0.31])	0.214

CR=0.055

**Table 10.** Dual-cross comparison of models for the criterion: C<sub>13</sub>

	A	B	C	$\tilde{w}_S$	$w_S$
A	ER	HER	HER	([0.77,0.89],[0.16,0.22],[0.13,0.20])	0.501
B	ASR	ER	SMR	([0.43,0.51],[0.45,0.53],[0.23,0.31])	0.289
C	ASR	SSR	ER	([0.33,0.37],[0.58,0.69],[0.23,0.31])	0.207

CR=0.055

**Table 11.** Dual-cross comparison of models for the criterion: C<sub>14</sub>

	A	B	C	$\tilde{w}_S$	$w_S$
A	ER	SMR	EXR	([0.56,0.65],[0.27,0.34],[0.24,0.30])	0.412
B	SSR	ER	SMR	([0.45,0.52],[0.39,0.47],[0.26,0.33])	0.337
C	SR	SSR	ER	([0.34,0.39],[0.53,0.63],[0.25,0.33])	0.248

CR=0.031

**Table 12.** Dual-cross comparison of models for the criterion: C<sub>15</sub>

	A	B	C	$\tilde{w}_S$	$w_S$
A	ER	EXR	HER	([0.65,0.75],[0.24,0.30],[0.22,0.28])	0.448
B	SR	ER	SMR	([0.45,0.53],[0.42,0.50],[0.26,0.33])	0.321
C	VSR	SSR	ER	([0.34,0.39],[0.57,0.67],[0.25,0.33])	0.231

CR=0.056

**Table 13.** Dual-cross comparison of models for the criterion: C<sub>21</sub>

	A	B	C	$\tilde{w}_S$	$w_S$
A	ER	ER	SSR	([0.44,0.49],[0.48,0.58],[0.29,0.38])	0.300
B	ER	ER	SSR	([0.44,0.49],[0.48,0.58],[0.29,0.38])	0.300
C	SMR	SMR	ER	([0.53,0.62],[0.30,0.37],[0.27,0.33])	0.399

CR=0.031

**Table 14.** Dual-cross comparison of models for the criterion: C<sub>22</sub>

	A	B	C	$\tilde{w}_S$	$w_S$
A	ER	SMR	SSR	([0.45,0.52],[0.39,0.47],[0.26,0.33])	0.337
B	SSR	ER	SR	([0.34,0.39],[0.53,0.63],[0.25,0.33])	0.248
C	SMR	EXR	ER	([0.56,0.65],[0.27,0.34],[0.24,0.30])	0.412

CR=0.031

**Table 15.** Dual-cross comparison of models for the criterion: C<sub>23</sub>

	A	B	C	$\tilde{w}_S$	$w_S$
A	ER	SMR	ER	([0.51,0.58],[0.36,0.44],[0.27,0.36])	0.362
B	SSR	ER	SR	([0.34,0.39],[0.53,0.63],[0.25,0.33])	0.248
C	ER	EXR	ER	([0.55,0.62],[0.33,0.41],[0.26,0.34])	0.387

CR=0.024

**Table 16.** Dual-cross comparison of models for the criterion: C<sub>31</sub>

	A	B	C	$\tilde{w}_S$	$w_S$
A	ER	SMR	HER	([0.61,0.71],[0.25,0.31],[0.22,0.28])	0.429
B	SSR	ER	EXR	([0.50,0.58],[0.36,0.44],[0.24,0.31])	0.354
C	VSR	SR	ER	([0.32,0.37],[0.59,0.70],[0.23,0.31])	0.214

CR=0.055

**Table 17.** Dual-cross comparison of models for the criterion: C<sub>32</sub>

	A	B	C	$\tilde{w}_S$	$w_S$
A	ER	SMR	SMR	([0.52,0.61],[0.29,0.36],[0.26,0.32])	0.394
B	SSR	ER	SMR	([0.45,0.52],[0.39,0.47],[0.26,0.33])	0.339
C	SSR	SSR	ER	([0.35,0.40],[0.50,0.60],[0.26,0.34])	0.264

CR=0.055

**Table 18.** Dual-cross comparison of models for the criterion: C<sub>33</sub>

	A	B	C	$\tilde{w}_S$	$w_S$
A	ER	ER	SSR	([0.44,0.49],[0.48,0.58],[0.29,0.38])	0.300
B	ER	ER	SSR	([0.44,0.49],[0.48,0.58],[0.29,0.38])	0.300
C	SMR	SMR	ER	([0.53,0.62],[0.30,0.37],[0.27,0.33])	0.399

CR=0.055

**Table 19.** Dual-cross comparison of models for the criterion: C<sub>34</sub>

	A	B	C	$\tilde{w}_S$	$w_S$
A	ER	SMR	EXR	([0.56,0.65],[0.27,0.34],[0.24,0.30])	0.412
B	SSR	ER	SMR	([0.45,0.52],[0.39,0.47],[0.26,0.33])	0.337
C	SR	SSR	ER	([0.34,0.39],[0.53,0.63],[0.25,0.33])	0.248

CR=0.031

**Table 20.** Dual-cross comparison of models for the criterion: C<sub>35</sub>

	A	B	C	$\tilde{w}_S$	$w_S$
A	ER	EXR	HER	([0.64,0.74],[0.23,0.29],[0.21,0.27])	0.447
B	SR	ER	SMR	([0.44,0.52],[0.41,0.49],[0.25,0.32])	0.320
C	VSR	SSR	ER	([0.33,0.38],[0.56,0.66],[0.24,0.32])	0.229

CR=0.032

**Table 21.** Final spherical fuzzy global priority weights

	C <sub>11</sub>	C <sub>12</sub>	C <sub>13</sub>	C <sub>14</sub>	C <sub>15</sub>	C <sub>21</sub>	C <sub>22</sub>	C <sub>23</sub>	C <sub>31</sub>	C <sub>32</sub>	C <sub>33</sub>	C <sub>34</sub>	C <sub>35</sub>
<b>A</b>	[(0.40, 0.47), [0.62, 0.67], [0.16, 0.23]]	[(0.26, 0.32), [0.82, 0.85], [0.11, 0.16]]	[(0.42, 0.54), [0.69, 0.74], [0.09, 0.19]]	[(0.28, 0.34), [0.76, 0.80], [0.14, 0.19]]	[(0.33, 0.40), [0.74, 0.78], [0.13, 0.18]]	[(0.23, 0.26), [0.82, 0.87], [0.16, 0.22]]	[(0.25, 0.29), [0.78, 0.82], [0.15, 0.20]]	[(0.37, 0.43), [0.62, 0.68], [0.22, 0.29]]	[(0.31, 0.37), [0.76, 0.79], [0.13, 0.18]]	[(0.31, 0.36), [0.71, 0.75], [0.17, 0.22]]	[(0.23, 0.25), [0.84, 0.88], [0.16, 0.22]]	[(0.28, 0.33), [0.77, 0.81], [0.13, 0.19]]	[(0.33, 0.39), [0.75, 0.78], [0.12, 0.18]]
<b>B</b>	[(0.31, 0.37), [0.71, 0.76], [0.17, 0.22]]	[(0.21, 0.25), [0.86, 0.89], [0.11, 0.15]]	[(0.21, 0.25), [0.85, 0.88], [0.12, 0.17]]	[(0.22, 0.26), [0.82, 0.85], [0.14, 0.19]]	[(0.22, 0.26), [0.83, 0.86], [0.13, 0.18]]	[(0.23, 0.26), [0.82, 0.87], [0.16, 0.22]]	[(0.18, 0.21), [0.85, 0.89], [0.14, 0.19]]	[(0.25, 0.28), [0.75, 0.81], [0.19, 0.25]]	[(0.24, 0.29), [0.76, 0.80], [0.13, 0.18]]	[(0.26, 0.31), [0.76, 0.80], [0.16, 0.21]]	[(0.23, 0.25), [0.84, 0.88], [0.16, 0.22]]	[(0.22, 0.26), [0.83, 0.86], [0.14, 0.18]]	[(0.21, 0.25), [0.84, 0.87], [0.13, 0.18]]
<b>C</b>	[(0.20, 0.23), [0.84, 0.89], [0.15, 0.20]]	[(0.13, 0.15), [0.93, 0.95], [0.10, 0.13]]	[(0.16, 0.18), [0.90, 0.93], [0.12, 0.16]]	[(0.17, 0.19), [0.88, 0.91], [0.13, 0.17]]	[(0.16, 0.19), [0.89, 0.92], [0.12, 0.17]]	[(0.29, 0.35), [0.73, 0.77], [0.16, 0.21]]	[(0.32, 0.38), [0.72, 0.76], [0.15, 0.21]]	[(0.40, 0.47), [0.60, 0.67], [0.21, 0.28]]	[(0.15, 0.18), [0.90, 0.93], [0.11, 0.15]]	[(0.20, 0.23), [0.82, 0.87], [0.16, 0.21]]	[(0.28, 0.33), [0.75, 0.78], [0.15, 0.21]]	[(0.16, 0.19), [0.88, 0.92], [0.12, 0.17]]	[(0.16, 0.18), [0.89, 0.92], [0.12, 0.16]]

**Table 22.** Resulting values and weights of alternatives

Digital Models	Scores	Ranks
<i>A</i>	0.3695	1
<i>B</i>	0.3162	2
<i>C</i>	0.3143	3

To compare the results found with other widely used fuzzy AHP methods, alternative and criterion evaluations taken from decision-makers were also processed with Neutrosophic Fuzzy AHP and Interval Valued Type-2 (IVT2) Fuzzy AHP methods. The results of these other two fuzzy AHP and their comparison with IVSF AHP are given in Table 23. As can be seen, the scores of the Neutrosophic Fuzzy AHP and IVT2 Fuzzy AHP methods are calculated closer to the first alternative for the second alternative. However, the rankings of the alternatives are the same. This result can be interpreted as the IVSF AHP methodology highlighting the chosen alternative more precisely while giving results. On the other hand, from an opposing point of view, it can direct decision-makers evaluations toward the prominent alternative.

**Table 23.** Result comparison

Digital Models	Neutrosophic	IVT2
<i>A</i>	0.3469	0.3523
<i>B</i>	0.3382	0.3258
<i>C</i>	0.3149	0.3219

We recommend that researchers increase and diversify the criteria and sub-criteria numerically in future studies on the business model selection of SuperApps. Since this study is based on the managerial strategy perspective, financial figures and investment information can be added to the criteria in prospect studies. According to the evaluations made by the decision makers, the most weighted business model among the 3 different digital business models is the digital ecosystem. The other 2 digital business models are similar in weight to each other, but less weighted than the digital ecosystem model. We can evaluate that the result will be a digital ecosystem business model for a SuperApp application, because in digital ecosystems, an income is created not only by the interaction of supply and demanders on a network, but also by the interaction of business partners, competing users and other parties. So, this would be a very critical reflection of the result. The business model chosen will also directly determine which dimension of interaction the SuperApp's revenue model stems from.

**Conflict of Interest:** No conflict of interest was declared by the authors.

**Financial Disclosure:** The authors declared that this study has received no financial support.

## REFERENCES

- [1] Duleba Szabolcs, Fatma Kutlu Gündoğdu, and Sarbast Moslem. "Interval-valued spherical fuzzy analytic hierarchy process method to evaluate public transportation development." *Informatica* 32, no. 4 (2021): 661-686.
- [2] Dogan, Onur. "Process mining technology selection with spherical fuzzy AHP and sensitivity analysis." *Expert Systems with Applications* 178 (2021): 114999
- [3] Sharaf, Iman Mohamad. "Global supplier selection with spherical fuzzy analytic hierarchy process." *Decision Making with Spherical Fuzzy Sets: Theory and Applications* (2021): 323-348.
- [4] Sangwan, Om Prakash. "A framework for evaluating cloud computing services using AHP and TOPSIS approaches with interval valued spherical fuzzy sets." *Cluster Computing* 25, no. 6 (2022): 4383-4396.
- [5] Serap, Tepe. "The Interval-Valued Spherical Fuzzy Based Methodology and its Application to Electric Car Selection." *Düzce Üniversitesi Bilim ve Teknoloji Dergisi* 9, no. 5 (2021): 1970-1983.
- [6] Erdoğan, Melike. "Assessing farmers' perception to Agriculture 4.0 technologies: A new interval-valued spherical fuzzy sets-based approach." *International Journal of Intelligent Systems* 37, no. 2 (2022): 1751-1801.
- [7] F. Kutlu Gündoğdu and C. Kahraman. "A novel spherical fuzzy analytic hierarchy process and its renewable energy application." *Soft Computing* 24, no. 6 (2020): 4607-4621.
- [8] F. Kutlu Gündoğdu and C. Kahraman. "Hospital performance assessment using interval-valued spherical fuzzy analytic hierarchy process." In *Decision Making with Spherical Fuzzy Sets*, pp. 349-373. Springer, Cham, 2021.
- [9] Y. Huang, W. Miao, "Re-domesticating social media when it becomes disruptive: Evidence from China's "super app" WeChat". *Mobile Media & Communication*. 2021 May;9(2): pp.177-94.

- [10] K. S. Momaya, "Breakthrough innovation and platform leadership: a case of super app from India.", *International Journal of Global Business and Competitiveness*. 2022 Dec;17(2): pp. 229-38.
- [11] A. S. Nurqamarani, R. Jonathan, E. Gaffar, A. Indrawati, "The Effects of Mobile Service Qualities on Customer Reuse Intention of Gojek Super App.", *Humanities and Social Sciences Reviews*. 2020;8(4): pp. 1134-46.
- [12] R. Chai, P. Amaral, "Is Grab, the Asian Superapp, Leveraging Digital Innovation for Good?.", In *SAGE Business Cases 2022*. SAGE Publications: SAGE Business Cases Originals.
- [13] B. Tabrizi, E. Lam, K. Girard, V. Irvin, "Digital transformation is not about technology.", *Harvard business review*. 2019 Mar 13;13(March): pp. 1-6.
- [14] T. M. Siebel, "Why digital transformation is now on the CEO's shoulders", *MKQ*. 2017 Dec;4(3):pp.1-7.
- [15] M. Zaharee, L. B. Abad, P. Chandra, C. Krautkramer, S. Mehlman, J. Schall, K. T. Taylor, "How Companies Can Benefit from Brilliant Failures: Despite the stigma surrounding failure, companies can use failure to learn, pivot, and achieve success—thus failing "brilliantly."", *Research-Technology Management*. 2021 Jan 23;64(2): pp. 31-8.
- [16] A. Pande, C. Schrey, "Five questions boards should ask about IT in a digital world.", *McKinsey & Company*. 2016 Jul.
- [17] P. C. Verhoef, T. Broekhuizen, Y. Bart, A. Bhattacharya, J. Q. Dong, N. Fabian, M. Haenlein, "Digital transformation: A multidisciplinary reflection and research agenda.", *Journal of Business Research*. 2021 Jan 1;122: pp. 889-901.
- [18] D. Romero, M. Flores, M. Herrera, H. Resendez, "Five management pillars for digital transformation integrating the lean thinking philosophy.", *IEEE International conference on Engineering, technology and Innovation (ICE/ITMC) 2019 Jun 17 (pp. 1-8)*.
- [19] J. Bughin, T. Catlin, "What successful digital transformations have in common." *Harvard business review*. 2017 Dec;19.
- [20] T. Chamorro-Premuzic, "The essential components of digital transformation.", *Harvard Business Review*. 2021 Nov 23.
- [21] M. W. Van Alstyne, G. G. Parker, "Digital transformation changes how companies create value.", *Harvard Business Review*. 2021 Dec 17.
- [22] V. Hermelingmeier, T. von Wirth, "The nexus of business sustainability and organizational learning: A systematic literature review to identify key learning principles for business transformation.", *Business Strategy and the Environment*. 2021 May;30(4): pp. 1839-51.
- [23] C. Shahi, M. Sinha, "Digital transformation: challenges faced by organizations and their potential solutions.", *International Journal of Innovation Science*. 2020 Dec 23.
- [24] F. Vermeulen, "What so many strategists get wrong about digital disruption.", *HBR*. 2017 Jan;3.
- [25] F. Brunetti, D. T. Matt, A. Bonfanti, A. De Longhi, G. Pedrini, G. Orzes, "Digital transformation challenges: strategies emerging from a multi-stakeholder approach." *The TQM Journal*. 2020 Apr 25;32(4): pp. 697-724.
- [26] G. Vial, "Understanding digital transformation: A review and a research agenda.", *Managing Digital Transformation*. 2021 May 26: pp. 13-66.
- [27] I. M. Sebastian, J. W. Ross, C. Beath, M. Mocker, K. G. Moloney, N. O. Fonstad, "How big old companies navigate digital transformation.", In *Strategic information management 2020 Apr 8 (pp. 133-150)*. Routledge.
- [28] S. Yamamoto, "A strategic map for digital transformation.", *Procedia Computer Science*. 2020 Jan 1;176: pp. 1374-81.
- [29] C. Gong, V. Ribiere, "Developing a unified definition of digital transformation.", *Technovation*. 2021 Apr 1;102:102217.
- [30] D. Bonnet, G. Westerman, "The new elements of digital transformation.", *MIT Sloan Management Review*. 2021;62(2): pp. 82-9.
- [31] A. Singh, T. Hess, "How chief digital officers promote the digital transformation of their companies.", In *Strategic Information Management 2020 Apr 8 (pp. 202-220)*. Routledge.
- [32] F. Li, "Leading digital transformation: three emerging approaches for managing the transition.", *IJO & Production Management*. 2020 Jul 23.
- [33] F. K. Gündoğdu and C. Kahraman. "Spherical fuzzy sets and spherical fuzzy TOPSIS method." *Journal of I&FS* 36, no. 1, 2019, pp. 337-352.
- [34] F. Kutlu Gündoğdu and C. Kahraman. "A novel VIKOR method using spherical fuzzy sets and its application to warehouse site selection." *Journal of I&FS*, 37, no. 1 (2019): 1197-1211.
- [35] F. Kutlu Gündoğdu and C. Kahraman. "Spherical fuzzy analytic hierarchy process (AHP) and its application to industrial robot selection." In *International Conference on Intelligent and Fuzzy Systems*, pp. 988-996. Springer, Cham, 2019.



# Prediction of Unconfined Compressive Strength of Microfine Cement Injected Sands Using Fuzzy Logic Method

\*<sup>1</sup>Eray YILDIRIM, <sup>2</sup>Eyübhan AVCI, <sup>3</sup>Nurten AKGÜN TANBAY

<sup>1</sup> Department of Civil Engineering, Bursa Technical University, Bursa, Türkiye, [eray.yildirim@btu.edu.tr](mailto:eray.yildirim@btu.edu.tr) 

<sup>2</sup> Department of Civil Engineering, Bursa Technical University, Bursa, Türkiye, [eyubhan.avci@btu.edu.tr](mailto:eyubhan.avci@btu.edu.tr) 

<sup>3</sup> Department of Civil Engineering, Bursa Technical University, Bursa, Türkiye, [nurten.akgun@btu.edu.tr](mailto:nurten.akgun@btu.edu.tr) 

## Abstract

In this study, unconfined compressive strength values of sand soil injected with microfine cement were predicted using fuzzy logic method. Mamdani and Sugeno methods were applied in the fuzzy logic models. In addition, a regression analysis was carried out in order to compare these two methods. In the models, water/cement ratio and injection pressure were the input variables, and unconfined compressive strength was the output variable. The dataset includes 427 samples, which were experimentally injected with microfine cement. Predictions for unconfined compressive strength were obtained by creating membership functions and rule base for each input (predictive) parameter in fuzzy logic models. The coefficient of determination ( $R^2$ ) and Mean Square Error (MSE) were used as criteria for evaluating the performance of the developed models. The results suggested that the three applied models (i.e., Mamdani, Sugeno and regression) provided statistically significant results, and these methods could be used in the future prediction-based studies. The results showed that Sugeno model provided the best performance for predicting unconfined compressive strength. It was followed by Mamdani and Regression models, respectively. This study has suggested that the fuzzy logic method can be an alternative to the regression method which traditionally has been used in prediction process.

**Keywords:** Fuzzy Logic; Mamdani; Sugeno; Unconfined Compressive Strength

## 1. INTRODUCTION

Many techniques are used in geotechnical engineering to improve the geotechnical properties of soils. In the commonly used injection technique, a suspension or solution type material is injected into the voids of soil and/or rock under pressure [1]. Permeation injection is the most widely used technique and it is the process of injecting material into voids in the soil under low pressures without causing any displacement and/or hydraulic fracture. Following injection, some engineering properties of the soil, such as strength and permeability, improve.

Portland cement is widely used in permeation injection applications. Due to the large particle size of Portland cement ( $D_{100} = 100 \mu\text{m}$ ), its injectability is limited to coarse sands. Chemical injection materials emerged with the motivation to find materials that could be penetrated into small particle size soils. The application areas of chemical injection materials are limited due to their high cost, low strength, and toxic effect. The search for injection materials with smaller particle sizes, which can be an alternative to chemical injection materials, and the reduction of the particle size of Portland cement led to the emergence of microfine

cements. Cements with a particle size less than  $15 \mu\text{m}$  are defined as microfine cements by American Concrete Institute [2]. Several types of microfine cements are produced in different names. The most widely known of these cements are Allofix MS, MC-100, Microdur RX, Micromix, Finosol X, Microcem B, Superfine L, Ultrafine 12 and Spinor A12. Özocak, İncecik and Özocak performed grouting on sand and sand/gravel mixture soil samples under different relative densities and vertical stresses using micro-cement (with plasticizer) and Ordinary Portland Cement (OPC) (with bentonite and plasticizer) [3,4]. The compressive strength values and modulus of elasticity of the injected samples were determined after 7 and 28 days of curing. According to their study, the relative density and the water/cement ratio affect the compressive strength, and that micro-cements showed more successful grouting results than OPC on sandy soils. Gökdemir and Yıldız applied the injection process with micro-cement to soil samples consisting of sand and gravel in different proportions. It has been observed that the finer the cement, the more successful the injection process [5]. Regarding the experiments carried out by Tekin [6], microfine cement suspension provided very good rheological properties. Zebovitz et al. [7], Karol [1] and Warner [8] stated that grouting could be performed easily for

materials ranging from microfine cements to fine sands. Christodoulou et al. [9], Markou and Droudakis [10], Hashimoto et al. [11] observed that the strength of the sands increased after microfine cement was injected. Schwarz and Krizek [12] and Avcı [13] suggested that the permeability coefficients of sands decreased after injecting microfine cement.

Artificial intelligence is a system in which a computer or computer-controlled robot is expected to fulfill the characteristics of human intelligence. Artificial intelligence makes our lives easier with many applications today. It is seen that these applications are used in many fields, such as education, health, security, e-commerce, and engineering. It is foreseen by many people and institutions that the use of artificial intelligence will increase considerably in the future. Fuzzy logic is a technique in artificial intelligence, and it is widely applied to various areas of science and engineering. This technique is also used for the solution of various problems of geotechnical engineering. Chuang [14] used fuzzy logic method to evaluate the shear strength of soils. The study aimed to obtain more consistent results between shear strength parameters measured in field and laboratory environments. In this context, fuzzy sets were formed by expressing the anisotropy of the soils, the effect of loading rate and sampling. The shear strength of soils was predicted by using the input parameters. Huang and Siller [15] developed a fuzzy logic model for geotechnical field characterization using samples collected from drilling studies. In their study, fuzzy sets were created by using the plasticity characteristics for field characterization. Thus, soil profiles could be defined with the developed fuzzy system. Saboya et al. [16] conducted a study on slope stability using fuzzy logic method. Failure potential index was calculated using the data which included slope angle, height, and permeability. Failure index definitions were defined with linguistic terms as very low, low, medium, high and very high in the fuzzy logic method. Reddy et al. [17] carried out a study, which utilized the Mamdani method, on the identification of swellable soils and determination of the swelling potential using the fuzzy logic approach. Liquid limit, swelling index, shrinkage limit, and plasticity index parameters were defined as input parameters while swelling potential was the output parameter. Zorluer et al. [18] used fuzzy logic approach to determine clay dispersibility. The dispersibility of 29 samples were examined using the fuzzy logic technique, and it was found that reliable results were obtained. Yurtçu and Özocak [19] studied on predicting the compression index values of fine grained soils using artificial neural networks and fuzzy logic methods. Çavuş et al. [20] developed a method for determining the liquefaction potential of soils using the fuzzy logic method. The developed fuzzy logic based method was compared with field observations and semi-empirical methods. It was found that the fuzzy logic method has a significant potential for geotechnical engineering problems.

The study in this paper aimed to predict the unconfined compressive strength values of sand soil grouted with microfine cement by using the fuzzy logic methods. Mamdani and Sugeno methods were used in fuzzy models. In addition, regression analysis was conducted in order to make a comparison with the applied fuzzy logic methods. In

all three models, the same inputs and output values were used to make a comparison. Water/cement ratio and injection pressure were predictors and unconfined compressive strength values were the outcome variable.

## 2. EXPERIMENTAL STUDY AND METHODS

### 2.1. Materials Used in Experiments

In the injection experiments, river sand (quartz sand) sample taken from Kızılırmak river was used. The sand sample was divided into two groups by using sieves. The soils between No 10 and No 40 sieves were grouped as medium sand, and the soils between No 40 and No 200 sieve were grouped as fine sand. Then, the grouped samples were mixed in different proportions to obtain 11 different gradations, and injection experiments were performed with these gradations. Table 1 shows the contents and physical properties of the samples used in the experiments.

**Table 1.** Physical properties of the sands used in the experiments [21]

Sample no	Sand content %		Gs	$\rho_{\max}$ (gr/cm <sup>3</sup> )	$\rho_{\min}$ (gr/cm <sup>3</sup> )	$e_{\max}$	$e_{\min}$
	Fine	Medium					
1	100	0	2.70	1.58	1.26	1.14	0.71
2	90	10	2.70	1.57	1.26	1.14	0.71
3	80	20	2.70	1.57	1.27	1.13	0.72
4	70	30	2.70	1.57	1.27	1.13	0.72
5	60	40	2.70	1.56	1.27	1.12	0.73
6	50	50	2.69	1.56	1.28	1.11	0.73
7	40	60	2.69	1.56	1.28	1.11	0.73
8	30	70	2.69	1.55	1.28	1.10	0.74
9	20	80	2.69	1.55	1.29	1.10	0.74
10	10	90	2.69	1.55	1.29	1.09	0.74
11	0	100	2.69	1.54	1.30	1.08	0.75

Two microfine cements with maximum particle sizes of 6  $\mu\text{m}$  and 12  $\mu\text{m}$  were used in the injection experiments. The particle size distributions of the microfine cements used in the experiments are given in Figure 1. The particle size of Spinor A6 used in the study is smaller than Ultrafine 12.

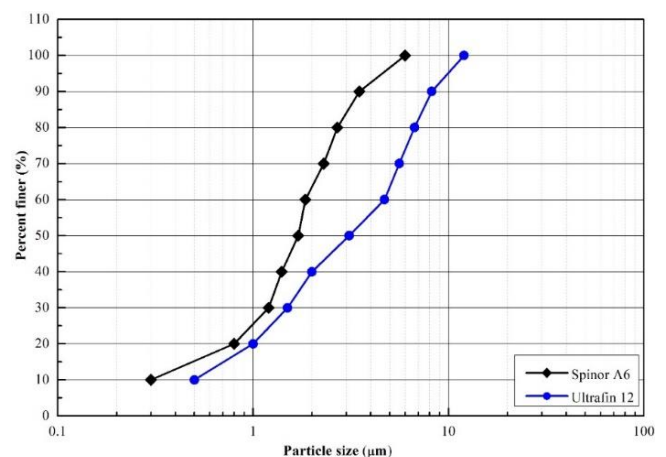


**Figure 1.** Grain size distributions of microfine cements used in the experiments [21,22].

The water/cement ratio was used as 0.8, 1.0, 1.5, 2.0, 2.5, 3.0, and 3.5 in the experiments. While the water/cement ratio increased, the injectability of the samples increased, but the injection pressure values decreased. In injections made with Spinor A6 cement, lower injection pressures were obtained compared to Ultrafine 12. This is because Spinor A6 has a smaller particle size than Ultrafine 12. In the injection experiments, care was taken not to exceed 0.5 MPa in permeation injection pressure values.

## 2.2. Injection and Unconfined Compressive Strength Tests

The experimental setup consists of 40 injection molds, a compressor, an injection tank, a manometer and fittings. The injection mold was made of polypropylene random copolymer material with a diameter of 52 mm and a height of 120 mm, and the upper and lower heads were made of caestamide material. The vibratory hammer was used to adjust the desired relative density for placing the soil into the molds. The injection system included a gear-motor rotating at 100 rpm and pedals connected to the motor. Detachable (pneumatic) pipes were used as fasteners in the injection system. Samples were placed in the mold in three layers with five different relative densities of 30%, 40%, 50%, 60% and 70%. In order to facilitate the removal of the injected sands from the molds, the inner surface of the mold and the heads were lubricated. Sands were placed in the mold, and a filter material made of coarse sand with a thickness of 0.8 cm was placed on the lower and upper head of the mold. Then, the molds were placed in the injection system and injection tests were carried out.

Two microcements, defined as Spinor A6 and Ultrafin 12, were used in the injection process. When all mixing ratios are considered, Spinor A6 cement has a greater injectability than Ultrafin 12 cement. The injectability of Ultrafin 12 cement decreases as the proportion of fine sand in the mixtures increases. In general, as the fineness of the sand in the samples increases, the injection feasibility decreases relatively. Injection experiments were carried out at five different relative density ratios. It was observed that as the relative tightness value increased, its injectability decreased. The samples that were successful in the injection tests were removed from the molds and placed in the curing tank. In the end of the 150th day, the samples, which were kept in curing tank, were tested for determining unconfined compressive strength according to the ASTM D4219-02 standard [23]. Prior to the unconfined pressure tests, a cap made of plaster was constructed for the top and bottom sections of the samples. The Unconfined Compressive Strength values of the microfine cement grouted sands increased with the increase in cement ratio and relative density.

## 2.3. Fuzzy Logic

Artificial intelligence is defined as a system that exhibit behaviours specific to human intelligence. With artificial intelligence, systems perceive problems and also exhibit behaviours such as learning, thinking, making decisions and making predictions. Main methods of artificial intelligence are fuzzy logic, artificial neural networks, adaptive neuro-fuzzy inference systems, genetic algorithms, expert systems

and data mining. These methods have several application areas such as in health, image processing, prediction, planning, and optimization. Regarding the state of the art review, fuzzy logic method was used in this study. The concept and the theory of fuzzy logic were developed in 1965 by Zadeh [24]. Classical logic uses binary values (0-1); while, in fuzzy logic, it is assumed that the variables can have intermediate values (as the glass is half full, the color may be gray). Therefore, the fuzzy logic can provide more flexible predictions. In fuzzy logic, values (information or data) are specified in linguistic terms such as little, big, much, less. The data can take a value between 0 and 1 [24]. In fuzzy logic, calculations are made with rules based on the relationships between linguistic expressions. The mathematical model of fuzzy logic is very suitable for application in systems that are very difficult to construct [25]. Figure 2 shows the processing scheme of the fuzzy inference system.

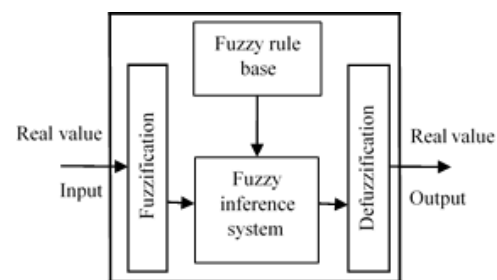


**Figure 2.** The Scheme of Fuzzy Inference System (FIS)

The first step in the fuzzy inference system is fuzzification of the input variables. This is followed by generating the fuzzy rule base. The third stage is to obtain the results of fuzzy input values with the help of the rules. The last step is defuzzification of the results. For a classical A set, if the element  $x$  is a member of the set, it takes the value 1; if it is not, it takes the value 0 (Eq. (1)).

$$\mu_A(x) = \begin{cases} 1, & x \in A \\ 0, & x \notin A \end{cases} \quad (1)$$

Contrary to the classical set, a fuzzy set is defined by the membership function  $\mu_A(x)$ , which can take values between 0 and 1 in space  $U$  (Eqs. (2) and (3)) [26]. Elements in the fuzzy set are expressed linguistically.

$$A = \{x, \mu_A(x) | x \in U\} \quad (2)$$

$$\mu_A(x) = \begin{cases} 1, & \text{if fully included in the fuzzy set} \\ [0,1], & \text{if partially included in fuzzy set} \\ 0, & \text{if not included in the fuzzy set} \end{cases} \quad (3)$$

here,  $\mu_A(x)$  is the membership function.  $X$  values correspond to the membership value in the 0-1 range. Triangle, Gaussian and trapezoidal are the most widely used membership functions in the fuzzy logic. Relationships between fuzzy sets are defined on rule basis. Rules are defined with conditionals. Following the formation of the fuzzy rule base the inference process is started. The most commonly used inference methods in fuzzy logic are Mamdani and Sugeno inference systems. In this study, both inference systems were used. The Mamdani inference system is close to human perception. This system can be created very easily, and its

interpretability is easier than the Sugeno approach. Since the result has a precise value in Sugeno inference system, it is generally preferred in control related problems. The main difference of this method from the Mamdani inference method is that the output values are defined as functions. In Sugeno method, inputs are defined with fuzzy sets, while output calculations are performed in a functional manner.

Defuzzification is the process of converting the results (fuzzy outputs) obtained from fuzzy calculations into numerical values. There are several defuzzification methods available, and in this study, the center of gravity method, which is the most commonly used defuzzification method, is chosen. In this method, the center of gravity of the aggregated fuzzy results of output membership functions is calculated to convert the outputs into numerical values (Eq. (4)) [27].

$$x_{COA}^* = \int \frac{\mu_A(x) \cdot x dx}{\mu_A(x) dx} \quad (4)$$

where,  $\mu_A(x)$  is the membership function.

#### 2.4. Implementation of Models for Prediction of Unconfined Compressive Strength

Fuzzy logic (Mamdani and Sugeno) and regression analysis were carried out using the obtained 427 data. MATLAB was used in the creation of models, operations and analysis. The unconfined compressive strength values of the injected samples were predicted by using created models. In both fuzzy logic and regression analysis, unconfined compressive strength values were used as outcome variables, and water / cement ratio and injection pressure values were used as predictors (See Figure 3).

Membership functions of inputs (water / cement and injection pressure) and outputs (unconfined compressive strength) are shown in Figure 4. Triangular and trapezoidal membership functions were used in creating models, and the degree of membership was normalized between 0-1. Membership functions were defined by using linguistic terms and fuzzy sets were defined by these expressions (VL: Very Low, L: Low, ML: Medium Low, M: Medium, MH: Medium High, H: High, VH: Very High). After creating membership functions and linguistic terms for inputs and outputs, the rules were formed. The number of rules and rule base were determined by expert opinion. Ten rules were formed for the Mamdani method. These rules are presented in Table 2.

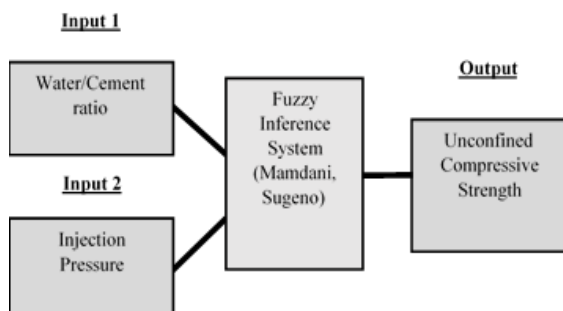


**Figure 3.** The schematic representation of the fuzzy logic models.

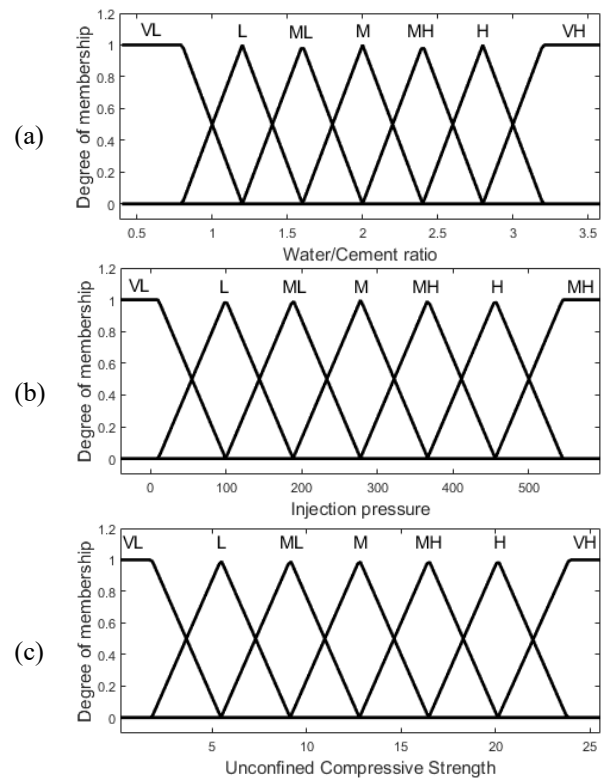


**Figure 4.** Membership functions and degrees of inputs and outputs used in fuzzy logic models, Inputs: (a) Water/Cement ratio and (b) Injection pressures (kPa), Outputs: (c) Unconfined Compressive Strength (UCS) (MPa)

**Table 2.** Rules used for Mamdani fuzzy logic model

No	RULES
1	If (Water/Cement ratio = VH) or (Injection pressure = VL) then (Unconfined Compressive Strength = VL)
2	If (Water/Cement ratio = H) or (Injection pressure = L) then (Unconfined Compressive Strength = L)
3	If (Water/Cement ratio = MH) or (Injection pressure = ML) then (Unconfined Compressive Strength = ML)
4	If (Water/Cement ratio = M) or (Injection pressure = M) then (Unconfined Compressive Strength = M)
5	If (Water/Cement ratio = M) or (Injection pressure = M) then (Unconfined Compressive Strength = ML)
6	If (Water/Cement ratio = M) or (Injection pressure = MH) then (Unconfined Compressive Strength = L)
7	If (Water/Cement ratio = ML) or (Injection pressure = MH) then (Unconfined Compressive Strength = MH)
8	If (Water/Cement ratio = ML) or (Injection pressure = M) then (Unconfined Compressive Strength = M)
9	If (Water/Cement ratio = L) or (Injection pressure = H) then (Unconfined Compressive Strength = H)
10	If (Water/Cement ratio = VL) or (Injection pressure = VH) then (Unconfined Compressive Strength = VH)

For the Sugeno method, the rules were formed by using the linear relationship between input and output variables. Similar to the Mamdani method, ten rules were defined for the Sugeno method. These rules are given in Table 3. The linear relationships shown in Table 3 were obtained from the available data. In this study, in addition to fuzzy logic, regression analysis, which is the most traditionally used approach in prediction problems, was also performed. In regression analysis, relation between output and input variables is expressed by a functional relationship. Multiple

linear regression was utilized. The relationship used for multiple linear regression analysis is;

$$Y = B_0 + B_1X_1 + B_2X_2 + B_3X_3 + \dots + B_kX_k \quad (5)$$

where  $Y$  is the output variable, and  $X_i, i = 1, \dots, k$  indicate the input predictors, and  $B_i, i = 1, \dots, k$  are the prediction coefficients. The unconfined compressive strength was taken as the output variable (i.e., predicted variable), while the water / cement ratio and injection pressure were the input predictors in the regression model.

**Table 3.** Rules used for Sugeno fuzzy logic model

No	RULES
1	If (Water/Cement ratio =VH) or (Injection pressure = VL) then (Unconfined Compressive Strength = -2,3726 (Water/Cement ratio) + 0,01371(Injection pressure) + 10,509)
2	If (Water/Cement ratio =H) or (Injection pressure = L) then (Unconfined Compressive Strength = -2,5927 (Water/Cement ratio) + 0,00695(Injection pressure) + 11,607)
3	If (Water/Cement ratio =MH) or (Injection pressure = ML) then (Unconfined Compressive Strength = -1,7885 (Water/Cement ratio) + 0,0066(Injection pressure) + 10,597)
4	If (Water/Cement ratio =M) or (Injection pressure = M) then (Unconfined Compressive Strength = -2,2 (Water/Cement ratio) + 0,0064(Injection pressure) + 13,177)
5	If (Water/Cement ratio =M) or (Injection pressure = M) then (Unconfined Compressive Strength = -1,7885 (Water/Cement ratio) + 0,0066(Injection pressure) + 10,597)
6	If (Water/Cement ratio =M) or (Injection pressure = MH) then (Unconfined Compressive Strength = -1,2 (Water/Cement ratio) + 0,0064(Injection pressure) + 13,177)
7	If (Water/Cement ratio =ML) or (Injection pressure = MH) then (Unconfined Compressive Strength = -2,6936 (Water/Cement ratio) + 0,0071(Injection pressure) + 17,538)
8	If (Water/Cement ratio =ML) or (Injection pressure = M) then (Unconfined Compressive Strength = -2,1 (Water/Cement ratio) + 0,0064(Injection pressure) + 13,177)
9	If (Water/Cement ratio =L) or (Injection pressure = H) then (Unconfined Compressive Strength = 1,05 (Water/Cement ratio) + 0,010(Injection pressure) + 9,746)
10	If (Water/Cement ratio =VL) or (Injection pressure = VH) then (Unconfined Compressive Strength = 5,0092 (Water/Cement ratio) + 0,02568(Injection pressure) + 7,3092)

### 3. RESULTS AND DISCUSSION

Results for predicting the unconfined compressive strength values were obtained with the Mamdani and Sugeno fuzzy logic methods, and the regression analysis. The results were obtained with rules and the defuzzification processes of Mamdani and Sugeno methods. In Figure 5, a graphical illustration for the calculation of numerical values based on the fuzzy logic models is given where the water / cement ratio as 2.3 and the injection pressure is 145 kPa. According to these input values, the unconfined compressive strength is found to be 8.55 MPa and 7.91 MPa with the Mamdani and Sugeno methods, respectively.

Figure 6 shows the 3D surface viewers of the models used in the study. The graphs in Figure 6 consist of two horizontal ( $X_1$ ;  $X_2$ , injection pressure; water/cement ratio) and one vertical components ( $Y$ , unconfined compressive strength). Figure 6(a) shows the graph obtained from the regression analysis, while Figs. 6(b) and 6(c), show the control surfaces

of Mamdani and Sugeno methods, respectively. A single output value was calculated for certain input values with the fuzzy logic method, and the control surface was formed to observe the values that the output will have against the inputs in the fuzzy inference system.

As can be seen from Figure 6, the surfaces obtained in all three models were similar to each other. Surfaces obtained with fuzzy logic were not linear, but rather wavy or non-linear surfaces. While it was possible to define the surface formed in the regression model mathematically, it was not possible to explain the surface created by fuzzy logic in such manner. In fact, this situation is suitable for problems for which a mathematical relation cannot be expressed explicitly between input and output variables although it is known to exist. The effects of input variables on the unconfined compressive strength values can be seen in all three graphs. It is possible to predict the unconfined compressive strength from the inputs for all the models by using these plots.

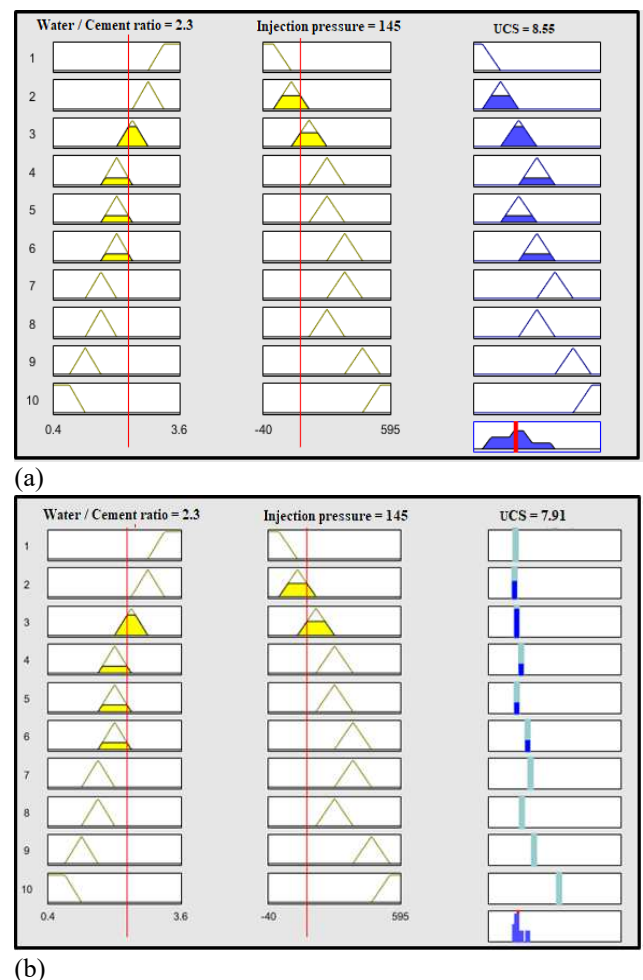


**Figure 5.** Graphic indication of the calculation of outputs in fuzzy logic models (e.g., Water/Cement=2.3 and Injection pressure=145 kPa), (a) Mamdani model, (b) Sugeno model.

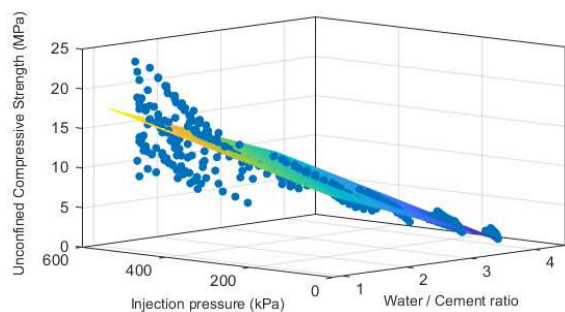
The coefficient of determination and the MSE values were used to measure the performance of the models. First, the predicted unconfined compressive strength values for each input value were calculated. Then, the scatterplot of the measured unconfined compressive strength value was drawn with the predicted unconfined compressive strength as shown in Figure 7. Linear simple regression analysis was

applied to the scatter plots, and the  $R^2$  was determined. The  $R^2$  can have values between 0 and 1. The  $R^2$  value is a criterion that shows the consistency and performance of the relationship between the predicted and measured values. If  $R^2$  is close to 1, there is a strong relationship between input and output variables. On the other hand, a value of  $R^2$  close to 0 indicates a weak relationship. The  $R^2$  values of the models are presented in Figure 7.

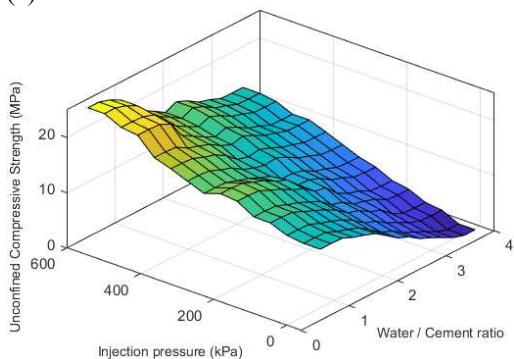
The MSE is defined as;

$$MSE = \frac{1}{n} \sum_{i=1}^n (Y_i - \hat{Y}_t)^2 \quad (6)$$

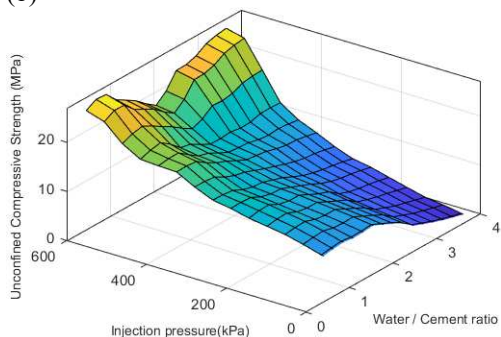
where  $Y$  and  $\hat{Y}$  are the measured and predicted values, respectively. MSE is one of the most widely used criterion to measure the prediction performance of statistical models. A small MSE value indicates that the predicted values are close to the measured ones. The MSEs of the three models are presented in Table 4.



(a)

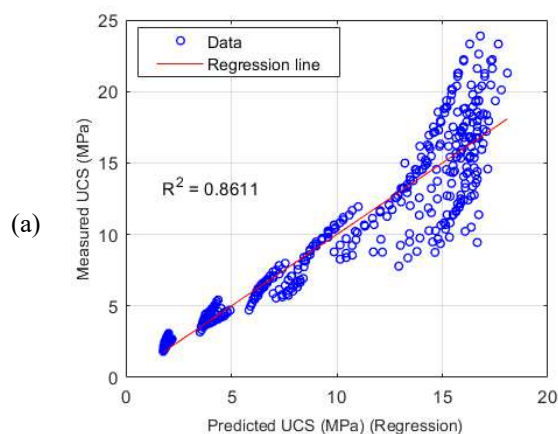


(b)

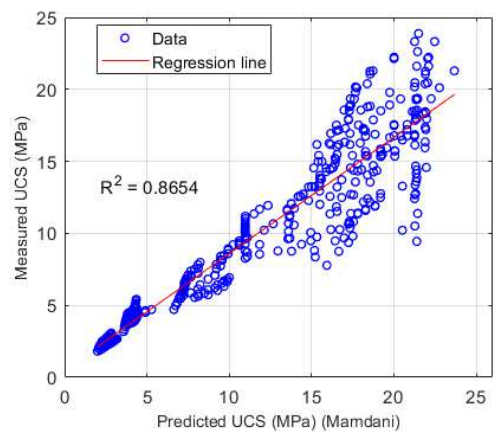


(c)

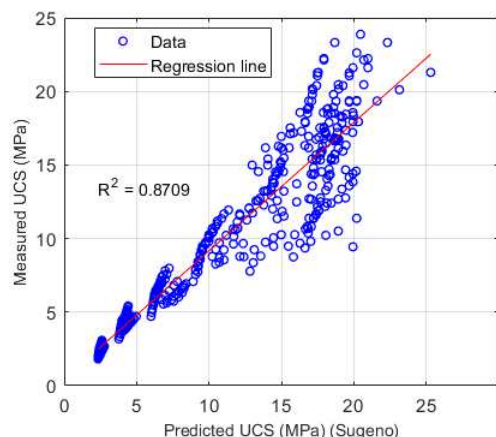
**Figure 6.** Three dimensional graphs of multiple linear regression and fuzzy logic models (Mamdani and Sugeno). Surface viewer (Input: Water / Cement ratio and Injection pressure (kPa) versus Output: Unconfined Compressive Strength (MPa)) of (a) Regression, (b) Mamdani and (c) Sugeno.



(a)



(b)



(c)

**Figure 7.** Comparison of measured and predicted USC (MPa) using (a) Multiple regression modelling, (b) Mamdani fuzzy logic modelling and (c) Sugeno fuzzy logic modelling.

The  $R^2$  values of all models were higher than 0.86, and the MSEs were low (Table 4). It was seen that the models were successful in predicting the unconfined compressive strength value of sand soils injected with microfine cement. The results presented in Table 4 indicated that the prediction performances of the three models were close to each other. The  $R^2$  values of fuzzy logic methods were relatively higher than that of the linear regression, and the MSE of these methods were lower than the regression approach. Hence, it could be stated that the fuzzy logic methods were better than the linear regression for the prediction of unconfined compressive strength of sand soils injected with microfine cement. When fuzzy logic methods were compared among themselves, it was seen that Sugeno method had a higher prediction performance. Figure 8 shows the scatterplot of the measured unconfined pressure strength values together with

the predictions of the three models. For low values of unconfined compressive strength, it was seen that all three models used for prediction gave close results and showed a good prediction performance. On the other hand, in the region, where the unconfined compressive strength was high, the results of the models were different from each other, and it was seen that there was relatively low prediction success compared to the performance exhibited for small values.

**Table 4.** The Coefficient of determination ( $R^2$ ) and Mean Square Error (MSE) values of the models

Model No	Method	Coefficient of determination ( $R^2$ )	Mean Squared Error (MSE)
1	Regression	0,8611	4,7319
2	Mamdani	0,8654	4,5841
3	Sugeno	0,8709	4,3962

As seen in Figure 8, the regression model showed lower performance in predicting high unconfined compressive strength values compared to other models. While the highest measured unconfined pressure strength was 23.88 kPa, the maximum value predicted by regression analysis was 18.08 kPa. In the fuzzy logic model, the difference between the predicted and measured values for both low and high unconfined compressive strength values was low.

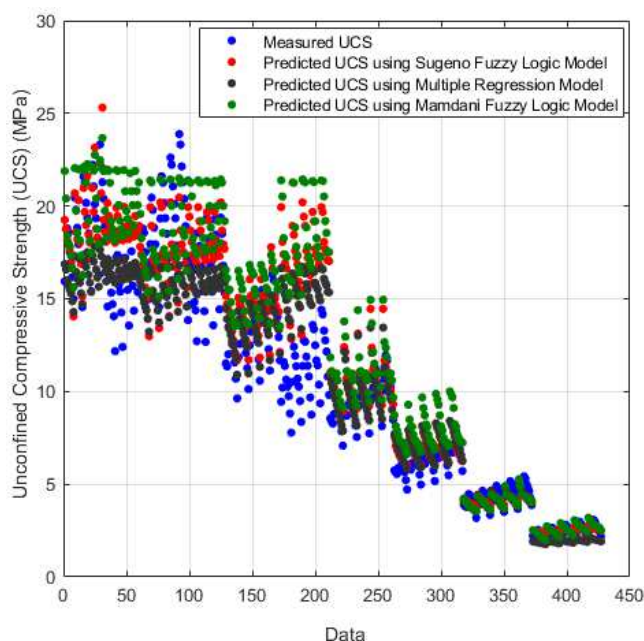


**Figure 8.** Measured and Predicted Unconfined Compressive Strength values (USC) from Multiple Regression, Mamdani and Sugeno Fuzzy Logic Models.

#### 4. CONCLUSIONS

The performance of the developed models (Mamdani method, Sugeno method and Regression analysis) to predict the unconfined compressive strength of sand soils with grouted microfine cement is examined. It is seen that all three give accurate results and they can be used for prediction studies. The  $R^2$  value is 0.8611 for the regression, 0.8654 for the Mamdani and 0.8709 for the Sugeno models. Although these values are close to each other, the Sugeno method

provides relatively better results compared to other models. The mean square error values of the models are calculated as 4.7319 for the regression, 4.5841 for Mamdani and 4.3962 for Sugeno. These values are in line with the values of the coefficient of determination of the models. The compatibility of both MSE and  $R^2$  values show the consistency of the developed models. The prediction performance of all three developed models is high and these approaches can be used in further similar studies. Sugeno model shows the best performance in predicting the unconfined compressive strength of microfine cement grouted sands. This method is followed by Mamdani and Regression models, respectively. This study shows that the fuzzy logic approach is an effective alternative to the traditionally used regression method for prediction problems.

**Author contributions:** Concept – E. Yıldırım, E. Avcı, N. Akgün Tanbay; Data Collection & Processing – E. Avcı; Literature Search – E. Avcı, E. Yıldırım; Writing – E. Yıldırım, E. Avcı, N. Akgün Tanbay

**Conflict of Interest:** No conflict of interest was declared by the authors.

**Financial Disclosure:** The authors declared that this study has received no financial support.

#### REFERENCES

- [1] R. H. Karol, Chemical grouting and soil stabilization. New York: M. Dekker, 2003.
- [2] S. Perret, D. Palardy, G. Ballivy, "Rheological Behavior and Setting Time of Microfine Cement-Based Grouts," *ACI Materials Journal*, vol. 97, no. 4, 2000, doi: 10.14359/7413.
- [3] A. Özocak, "Grouting Model Experiments with Micro-Cement," Yüksek Lisans tezi, Fen Bilimleri Enstitüsü, İstanbul Teknik Üniversitesi, İstanbul, 1994.
- [4] M. İncecik, A. Özocak, "İnce Daneli Çimento Enjeksiyon Model Deneyleri," *Zemin Mekaniği ve Temel Mühendisliği 5. Ulusal Kongresi*, O.D.T.Ü., Ankara, s:486-497. 1994.
- [5] A. Gökdemir, K. Yıldız, "Microcem 525 çimento enjeksiyonunun düşük poroziteli Zeminlerin basınç dayanımına etkisi," *e-Journal of New World Sciences Academy Natural and Applied Sciences*, vol. 2, no.2, A0025, pp. 133-146, 2007.
- [6] E. Tekin, İnce Taneli Çimento (Rheocem 900) Karışımlarının Reolojik Özellikleri, *Gazi Üniversitesi Mühendislik Mimarlık Fakültesi Dergisi*, vol. 26, no. 4, pp.777-785, 2011.
- [7] S. Zebovitz, R. J. Krizek, and D. K. Atmatzidis, "Injection of Fine Sands with Very Fine Cement Grout," *Journal of Geotechnical Engineering*, vol. 115, no. 12, pp. 1717–1733, 1989, doi:10.1061/(asce)0733-9410(1989)115:12(1717).
- [8] J. Warner, Soil solidification with ultrafine cement grout. *Proceedings of the third International Conference, Geotechnical Special Publication*, Reston, ASCE, February 10-12, New Orleans, USA. pp 1360-1371, 2003.

- [9] D. N. Christodoulou, A. I. Droudakis, I. A. Pantazopoulos, I. N. Markou, D. K. Atmatzidis, Groutability and Effectiveness of Microfine Cement Grouts, In: Proceedings of the 17th International Conference on Soil Mechanics and Geotechnical Engineering, Alexandria, Egypt, pp. 2232-2235, 2009, 10.3233/978-1-60750-031-5-2232.
- [10] I. N. Markou and A. I. Droudakis, "Shear strength of microfine cement grouted sands," Proceedings of the Institution of Civil Engineers - Ground Improvement, vol. 166, no. 3, pp. 177-186, 2013, <https://doi.org/10.1680/grim.12.00016>
- [11] K. Hashimoto, S. Nishihara, S. Oji, T. Kanazawa, S. Nishie, I. Seko, et al., Field testing of permeation grouting using microfine cement, Proc. Instit. Civ. Eng.-Ground Improvement, vol. 169 no. 2, pp. 134-142, 2016, <https://doi.org/10.1680/jgrim.15.00030>.
- [12] L. G. Schwarz, R. J. Krizek, Effect of preparation technique on permeability and strength of cement-grouted sand, Geotechnical Testing Journal, vol. 17, no. 4, pp. 434-443, 1994, <https://doi.org/10.1520/GTJ10304J>.
- [13] E. Avci and M. Mollamahmutoğlu, "Syneresis dependent shear strength parameters of sodium silicate grouted sands," Quarterly Journal of Engineering Geology and Hydrogeology, vol. 52, no. 1, pp. 99-109, 2018, <https://doi.org/10.1144/qjgegh2017-080>
- [14] P. H. Chuang, Use of fuzzy sets for evaluating shear strength of soils, Computers and Geotechnics, vol. 17, no. 4, pp. 425-446, 1995, [https://doi.org/10.1016/0266-352X\(95\)94914-C](https://doi.org/10.1016/0266-352X(95)94914-C)
- [15] Y.-T. Huang and T. J. Siller, "Fuzzy representation and reasoning in geotechnical site characterization," Computers and Geotechnics, vol. 21, no. 1, pp. 65-86, Jan. 1997, doi: 10.1016/s0266-352x(95)00013-z.
- [16] F. Saboya, M. da Glória Alves, W. Dias Pinto, "Assessment of failure susceptibility of soil slopes using fuzzy logic," Engineering Geology, vol. 86, no. 4, pp. 211-224, 2006, <https://doi.org/10.1016/j.enggeo.2006.05.001>.
- [17] P. V. S. Reddy, K. M. Rao, C. S. Rani, Identification of expansive soils and assessment of expansion potential by fuzzy approach. Electronic Journal of Geotechnical Engineering, vol. 14, pp. 1-11. 2009.
- [18] I. Zorluer, Y. Icaga, S. Yurtcu, and H. Tosun, "Application of a fuzzy rule-based method for the determination of clay dispersibility," Geoderma, vol. 160, no. 2, pp. 189-196, Dec. 2010, doi: 10.1016/j.geoderma.2010.09.017.
- [19] A. Özocak and Ş. Yurtcu, "İnce Daneli Zeminlerde Sikişma İndisi'nin İstatistiksel ve Yapay Zeka Yöntemleri ile Tahmin Edilmesi," Gazi Üniversitesi Mühendislik-Mimarlık Fakültesi Dergisi, vol. 31, no. 3, 2016, doi: 10.17341/gummfd.95986.
- [20] U. S. Cavus, M. Kilit, İ. Zorluer, and T. B. Edil, "Fuzzy logic-based assessment of seismic soil liquefaction potential and its application to foundations of bridge piers," Journal of Intelligent & Fuzzy Systems, vol. 36, no. 6, pp. 6001-6011, 2019, doi: 10.3233/jifs-181795.
- [21] E. Avcı, E, "Ultra ince taneli (spinor a6) süspansiyon enjeksiyonunun, solüsyon türü kimyasal enjeksiyonlara alternatifliğinin araştırılması," Doktora Tezi, Fen Bilimleri Enstitüsü, Gazi Üniversitesi, Ankara, 2015.
- [22] E. Avcı, "Farklı rölâtif sıklık ve tane dağılımına sahip kum zeminlerde Ultrafin 12 enjeksiyonu permeasyon yetisi", Yüksek Lisans tezi, Fen Bilimleri Enstitüsü, Gazi Üniversitesi, Ankara, 2009.
- [23] ASTM D4219-02, Standard Test Method for Unconfined Compressive Strength Index of Chemical-Grouted Soils, West Conshohocken: ASTM International, 2002.
- [24] L. A. Zadeh, "Fuzzy algorithms," Information and Control, vol. 12, no. 2, pp. 94-102, Feb. 1968, doi: 10.1016/s0019-9958(68)90211-8.
- [25] Ç. Elmas, Bulanık Mantık Denetleyiciler (Kuram, Uygulama, Sinirsel Bulanık Mantık), Seçkin Yayıncılık, 2003.
- [26] M. Monjezi, M. Rezaei, and A. Yazdian Varjani, "Prediction of rock fragmentation due to blasting in Gol-E-Gohar iron mine using fuzzy logic," International Journal of Rock Mechanics and Mining Sciences, vol. 46, no. 8, pp. 1273-1280, 2009, doi: 10.1016/j.ijrmms.2009.05.005.
- [27] G.W. Nurcahyo, S.M. Shamsuddin, R.A. Alias, M.N.M. Sap, Selection of defuzzification method to obtain crisp value for representing uncertain data in a modified sweep algorithm, Journal of Computer Science and Technology, vol. 3, no. 2, pp. 22-28, 2003.